



รายงานวิจัยฉบับสมบูรณ์

โครงการ

“การศึกษาพลวัตปฏิสัมพันธ์ของเซลล์เจ้าบ้านกับไวรัสระหว่างการติดเชื้อ
เพื่อค้นหาเป้าหมายของยาโดยใช้ไวรัสไข้เลือดออกดัดแปลง”

“Elucidation of host-virus interaction dynamics during infection using engineered,
tagged dengue virus to search for drug targets”

โดย ผศ.ดร. ศรินทร์ ฉิมณรงค์

เดือน ปี ที่เสร็จโครงการ

29 พฤษภาคม 2563

รายงานวิจัยฉบับสมบูรณ์

โครงการ

“การศึกษาพลวัตปฏิสัมพันธ์ของเซลล์เจ้าบ้านกับไวรัสระหว่างการติดเชื้อ
เพื่อค้นหาเป้าหมายของยาโดยใช้ไวรัสไข้เลือดออกดัดแปลง”

“Elucidation of host-virus interaction dynamics during infection using engineered,
tagged dengue virus to search for drug targets”

ผศ.ดร. ศรินทร์ ฉิมณรงค์

สถาบันชีววิทยาศาสตร์โมเลกุล มหาวิทยาลัยมหิดล

สนับสนุนโดยสำนักงานกองทุนสนับสนุนการวิจัย

และมหาวิทยาลัยมหิดล

(ความเห็นในรายงานนี้เป็นของผู้วิจัย สกว. และมหาวิทยาลัยมหิดลไม่จำเป็นต้องเห็นด้วยเสมอไป)

Table of contents

	<i>Page</i>
1. Abstract	3
2. Introduction	5
3. Literature review	6
4. References	11
5. Objective	13
6. Materials and Methods	13
7. Results and Discussion	18
8. Output	32
9. ภาคผนวก	35

List of tables

1. GO terms showing enrichment of particular interest	21
2. Summary of DENV RNA and NS5 interactome	22
3. Peptides of DENV proteins identified at 30 and 60 min, and 48 hours after infection	25
4. Host proteins showing differential phosphorylation upon infection	26
5. Host proteins showing differential regulation at 48 hours after infection	27
6. Potential RNA modifications on DDX6 interface	31

List of figures

1. Statistics of dengue diseases in Thailand	5
2. Existing model of viral RNA replication in infected cells	7
3. Our proposed new DENV replication model	8
4. Flow cytometry analysis of etDENV infection in multiple human cell lines	9
5. Isolation of tagged DENV NS5 from infected HuH-7 cells	9
6. List of enriched gene ontology groups of DENV RNA-interacting proteins	10
7. Plaque assay of propagated etDENV	19
8. SDS-PAGE analysis of immunoprecipitation of tagged NS5 from etDENV-infected HuH-7	19
9. Schematic diagram of modified PAR-CLIP in this study	20
10. Interaction map between DENV RNA and human proteome in HuH-7	21
11. Comparison of light, medium, and heavy peptide MS counts	23
12. Typical MS1 spectra, chosen from fraction 6 from the no-enrichment condition	24
13. MS2 spectra of a phosphopeptide found in DENV NS5	26
14. MS2 spectra of a new glutathionylation site found in DENV NS5	28
15. Mutational analysis of DENV A2-A3 RNA elements using yeast three-hybrid (Y3H)	29
16. Mutational analysis of human DDX6 using Y3H	30
17. Potential DDX6-vRNA interaction sites identified by new CL-LC/MS/MS procedure	32

Project Code: RSA6080066

Project title: Elucidation of host-virus interaction dynamics during infection using engineered, tagged dengue virus to search for drug targets

Principal investigator: Asst. Prof. Dr. Sarin Chimnaronk

Address: Laboratory of RNA Biology, Institute of Molecular Biosciences, Mahidol University

25/25 Phutthamonthon 4 Rd., Salaya, Phutthamonthon, Nakhon Pathom, Thailand 73170.

E-mail: sarin.chi@mahidol.ac.th

Telephone: 02-441-9003 ext. 1383; 089-502-8998 (mobile)

Project duration: 3 years

Total budget: 1,500,000 Baht

Abstract: Dengue virus (DENV), an ~10.7-kb positive-sense single-stranded RNA virus, is the most common arthropod-transmitted pathogen in the world. Currently, there is no approved drug for pre- and post-treatment of the diseases. Despite a great number of genetic and biochemical studies have been so far achieved, accurate mechanisms for replication of the virus in infected host still remain poorly understood. In this work, we resolved dynamics in interactions between DENV and human liver cells at multiple stages of infection in a quantitative manner via combining our developed engineered-tagged dengue virus or “*etDENV*”, harboring a tandem tag of octahistidine and FLAG in the NS5 gene, with crosslink immunoprecipitation, protein labeling, and mass spectrometry. Our results revealed that DENV RNA interacts with at least four distinct machinery of RNA processing, ribosome, chaperones, and unexpectedly, MCM complexes. The interactors also comprise several DEAD-box RNA helicases. Of those, we employed Y3H assay and a new MS procedure to demonstrate that the C-terminal RecA of human DDX6 specifically binds to the 3′ hairpin of the A3 RNA element in the 3′-UTR of the DENV genome. Moreover, we also investigate early host responses upon infection through phosphoproteomic analysis. We successfully identified a subset of host proteins with significant changes in phosphorylation levels in a quantitative manner. Interestingly, we also found uncharacterized phosphorylations in the RNA-binding paths on the viral NS5 polymerase. Though roles played by these post-translational modifications (PTMs) in the viral life cycle are not well understood, our work provides the first comprehensive view of human-DENV interactions in a natural infection environment. Given that viral RNA-interacting proteins must play important roles in viral replication, their inhibitions feasibly open a new avenue for the therapeutic approach.

Keywords: Dengue virus, tandem affinity purification (TAP) tag, interactome, viral RNA, co-immunoprecipitation (co-IP), labeling mass spectrometry

รหัสโครงการ: RSA6080066

ชื่อโครงการ: การศึกษาพลวัตปฏิสัมพันธ์ของเซลล์เจ้าบ้านกับไวรัสระหว่างการติดเชื้อเพื่อค้นหาเป้าหมายของยาโดยใช้ไวรัสใช้เลือดออกดัดแปลง

ชื่อนักวิจัย: ผศ. ดร. ศรินทร์ นิมนรงค์

ที่อยู่: สถาบันชีววิทยาศาสตร์โมเลกุล มหาวิทยาลัยมหิดล

25/25 ถนนพุทธมณฑลสาย 4 ศาลายา พุทธมณฑล นครปฐม 73170

อีเมล: sarin.chi@mahidol.ac.th

โทร: 02-441-9003 ext. 1383; 089-502-8998 (mobile)

ระยะเวลาโครงการ: 3 ปี

งบประมาณรวม: 1,500,000 บาท

บทคัดย่อภาษาไทย: ไวรัสใช้เลือดออกเด็งกีเป็นอาร์เอ็นเอไวรัสที่มีสารพันธุกรรมเป็นอาร์เอ็นเอสายบวกขนาดประมาณ 10.7 กิโลเบส (kb) เป็นเชื้อโรคติดต่อผ่านอาร์โทรพอดที่พบได้มากที่สุดในโลก ปัจจุบันยังไม่มียาที่ได้รับการรับรองสำหรับการป้องกันก่อนและรักษาหลังการติดเชื้อ แม้จะมีการศึกษาทางพันธุศาสตร์และชีวเคมีจำนวนมากแต่กลไกระดับโมเลกุลของการจำลองตัวของไวรัสในโฮสต์ที่ติดเชื้อมันยังไม่เป็นที่เข้าใจมากนัก ในโครงการวิจัยนี้คณะผู้วิจัยได้ใช้เทคโนโลยีใหม่ที่พัฒนาขึ้นได้แก่ ไวรัสใช้เลือดออก “etDENV” ที่ถูกดัดแปลงทางพันธุกรรมให้มีฉลากหรือ tag (octahistidine ตามด้วย FLAG) ในยีนของโปรตีน NS5 เทคนิค PAR-CLIP และการติดฉลากโปรตีนกับแมสสเปกโตรมิเตอร์ (MS) มาใช้ศึกษาเชิงปริมาณของพลวัตปฏิสัมพันธ์ของเซลล์กับไวรัสระหว่างการติดเชื้อ จากผลการวิเคราะห์คณะผู้วิจัยได้ค้นพบโปรตีน complexes อย่างน้อย 4 ชนิดที่เกี่ยวข้องกับปฏิสัมพันธ์กับสายอาร์เอ็นเอของไวรัส คือ RNA processing, ไรโบโซม, chaperone และ MCM complex ซึ่งในโปรตีนเหล่านี้ประกอบด้วย DEAD-box helicase หลายชนิด คณะผู้วิจัยได้ใช้เทคนิค Y3H และ MS แบบใหม่ในการค้นพบว่าโดเมน RecA ด้านปลาย C ของโปรตีน DDX6 ของคนมีปฏิสัมพันธ์จำเพาะกับอาร์เอ็นเอ A3 ในบริเวณ 3'-UTR ของจีโนมของไวรัส นอกจากนั้นคณะผู้วิจัยได้ศึกษาการตอบสนองของโฮสต์ต่อการติดเชื้อผ่านการวิเคราะห์ phosphoproteomic และประสบความสำเร็จในการจำแนกโปรตีนของโฮสต์ที่มีการเปลี่ยนแปลงของระดับ phosphorylation อย่างมีนัยสำคัญ ที่น่าสนใจอย่างมากคือการค้นพบ phosphorylation ในบริเวณที่มีปฏิสัมพันธ์กับอาร์เอ็นเอในโปรตีน NS5 ของไวรัสที่ยังไม่มีการรายงานมาก่อน แม้ว่าบทบาทสำคัญของ post-translational modifications (PTMs) ที่ค้นพบนั้นต่อกระบวนการเพิ่มจำนวนไวรัสใช้เลือดออกยังต้องอาศัยการศึกษาเพิ่มเติม แต่โครงการวิจัยนี้ได้สร้างวิธีใหม่ในการศึกษาปฏิสัมพันธ์ของไวรัสภายในเซลล์ รวมถึงแสดงให้เห็นลักษณะโครงสร้างปฏิสัมพันธ์ระหว่างเชื้อโรคและเซลล์เจ้าบ้านในสิ่งแวดล้อมที่เหมือนกับการติดเชื้อจริง เนื่องจากโปรตีนที่มีปฏิสัมพันธ์กับอาร์เอ็นเอของไวรัสต้องมีบทบาทสำคัญในการจำลองตัวของไวรัส จึงอาจจะเป็นเป้าหมายใหม่ในการพัฒนาแนวทางการรักษาต่อโรคใช้เลือดออกได้

คำหลัก: ไวรัสใช้เลือดออกเด็งกี, tandem affinity purification (TAP) tag, interactome, ไวรัสอาร์เอ็นเอ, co-immunoprecipitation (co-IP), labeling mass spectrometry

Executive Summary

ความสำคัญและที่มาของปัญหา (Introduction)

Dengue fever is an infectious tropical disease caused by the dengue virus (DENV), which is transmitted via several species of mosquito within the genus *Aedes*, principally *A. aegypti*. Symptoms range from a mild fever, to incapacitating high fever, with severe headache, pain behind the eyes, muscle and joint pain, and rash. However, complex infection with different circulating dengue serotypes (DENV-1–4) may lead to the life-threatening dengue hemorrhagic fever (DHF), resulting in bleeding, low levels of blood platelets and blood plasma leakage, or to dengue shock syndrome (DSS), where dangerously low blood pressure occurs [1]. Today about 2.5 billion people, or 40% of the world's population, live in areas where there is a risk of dengue transmission according to the World Health Organization (WHO). Dengue is endemic in at least 100 countries in Asia, the Pacific, the Americas, Africa, and the Caribbean. It is estimated that beyond 100 million infections occur yearly, including 500,000 DHF cases and 22,000 deaths, mostly among children [2]. In 2015, the incidence of dengue marked 3.5-fold increase to 142,925 cases over the previous year in Thailand (<http://dhf.ddc.moph.go.th/>). About 0.1% (141 cases) of those infected died. Despite progress in biotechnology, an increasing trend of hospitalized patients is remarkable, with a pandemic in every 2-3 years (Fig. 1). Currently there is no approved antiviral drug available for prevention and post-treatment of DENV infection [3]. Current treatments are mostly symptomatic, and they make use of analgesics for the containment of fever and fluid replacement to address the vascular leakage in DHF and DSS patients. Hence, at present, the only method to control or prevent the transmission of DENV is to combat vector mosquitoes. Moreover, development of a vaccine for DENV has been challenging, principally because of the need to immunize and induce long-lasting protection against all 4 serotypes of DENV simultaneously; an incompletely immunized individual may be sensitized to DHF or DSS. These complications have underscored the importance for development of an effective therapy for DENV and other flavivirus infections.

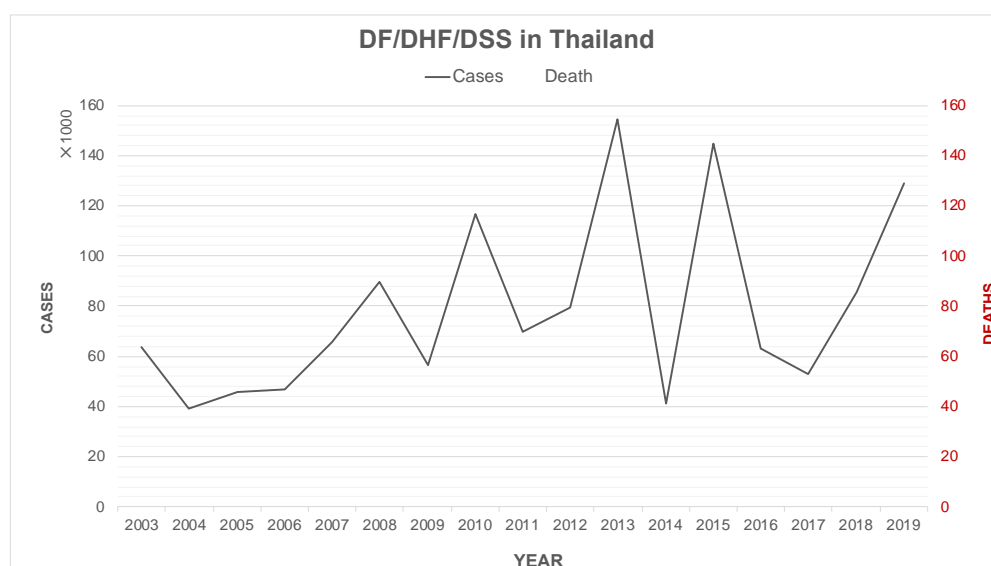


Figure 1. Statistics of dengue diseases in Thailand (as of January 7th, 2020).

Towards discovery of therapeutic compounds against DENV, deep understanding of the whole viral life cycle in infected cells is indispensable. To date, a vast majority of DENV studies in the country and overseas have mainly focused on mechanisms for receptor-mediated cell entry or endocytosis, and broad cellular effects in the late phase of infection such as cell stress, immune response, and cell death or apoptosis. The studies usually investigated a limited number of proteins or a single pathway and were mostly performed via *in vitro* experiments. This gives rise to a knowledge gap in viral life cycle concerning the replication process of viral RNA (vRNA) in host cells. For example, how does viral polymerase initiate vRNA synthesis? how does the translation of vRNA initiate? how does virus regulate the timing of RNA and protein syntheses? How does it switch between positive and negative strand syntheses? and so on. It is surprising how little we precisely know about the replication of DENV in host cells.

In our previous study supported by Mahidol University and TRF (RSA5680054), we have isolated and characterized the DENV NS5 polymerase protein *in vitro* [4] and discovered the consensus RNA promoter sequence, for the first time, in the 3'-untranslated region (UTR) of the DENV RNA genome, which is specifically recognized by the viral NS5 polymerase, and is indispensable for vRNA synthesis in infected cells [5]. Our discovery completely revises the current model of viral replication in which the existence of a 5'-UTR promoter had been believed for a decade (Fig. 2). To understand the virus life cycle and discover targets for antiviral therapy, it is obvious that a global study of host-pathogen interactions at multiple stages of infection should be required. It has been shown that flaviviral RNA genome directly interacts with various host cellular proteins, likely to form the replication complex, so-called “*replicase*”, to stabilize its own genome during replication in cells, to regulate host gene expression, and to modify host immune response. The host-virus interaction networks are complicate and changed upon stages of infection. To date, there is no technology that is capable of visualizing these interaction networks or “*interatome*” inside infected cells in a time-dependent manner. In our recent work supported by TRF (RSA5680054), we have successfully developed an engineered, viable DENV particle that contains an epitope tag inside the viral NS5 polymerase for the first time [6]. We have proven that this engineered, tagged DENV, hereafter designated “*etDENV*”, had comparable infection property to the native virus, and was useful for isolation of protein complexes that interact with DENV RNA and NS5 in infected cell [6]. In order to expand our work to provide more comprehensive understanding of DENV life cycle in human cells, we propose here a deep interactome analysis of human-DENV in a time-resolved scale for the first time, using our artificial *etDENV* and our newly-established RNA technology called modified PAR-CLIP. The knowledge gained from this project will completely renew the model of DENV replication, and provide new avenues for the development of antiviral drugs by inhibiting essential interactions of human factors with vRNA at the earlier stage of infection.

Literature review

Flaviviruses comprise one of the three genera within the *Flaviviridae* family. The Flavivirus genus is divided into three groups based on their ecological characteristics, mosquito-borne, tick-borne, and no-known vector flaviviruses. Among the mosquito-borne flaviviruses, there are important human pathogens such as dengue virus (DENV), yellow fever virus (YFV), West Nile virus (WNV), Saint Luis encephalitis virus (SLEV), and

Japanese encephalitis virus (JEV). Like all flaviviruses, DENV is an enveloped virus possessing an ~10.7-kb, positive-sense, single-stranded RNA genome that is translated as one long polyprotein and proteolytically cleaved into 10 viral proteins: three structural (capsid, C, premembrane, prM; and envelope, E) and seven nonstructural (NS1, NS2A, NS2B, NS3, NS4A, NS4B, and NS5) proteins [7]. DENV circulates as a complex of four antigenically distinct serotypes, DEN1–4. DENV RNA genome contains a type 1 cap (m7GpppAmp) structure at the 5'-end but lack 3' poly(A) tail [8], and its single coding region is flanked by highly structured 5'-untranslated region (UTR) which is about 100 nucleotides (nt) in length, and an ~450-nt 3'-UTR [9].

DENV RNA replication takes place in the cytoplasm following the endocytosis [10], whereby several viral NS and host proteins are believed to constitute the replication complex or “*replicase*”, the proposed replication machinery of flaviviruses [11]. Two key enzymes in the replication process, viral NS3 and NS5, the RNA helicase and the RNA-dependent RNA polymerase (RdRp), respectively, interact together and recruit several human factors to the replicase in the endoplasmic reticulum (ER) membrane. Following successful assembly, the viral replicase then initiates vRNA synthesis from the positive to the negative strand. An only existing model of DENV RNA replication showed that the negative-strand synthesis initiates by the DENV genome cyclization, which is mediated by hybridization between UAR (Upstream AUG Region) and CS (Cyclization Sequence) in both 5'- and 3'-UTRs (**Fig. 2**). In the canonical model, the viral RdRp then binds to a 5' stem-loop (SLA) in 5'-UTR, and by long-range RNA-RNA interactions the polymerase is transferred to the site of initiation at the 3'-end of the genome [12]. The newly synthesized minus strand serves as template for production of the genomic strand [13].

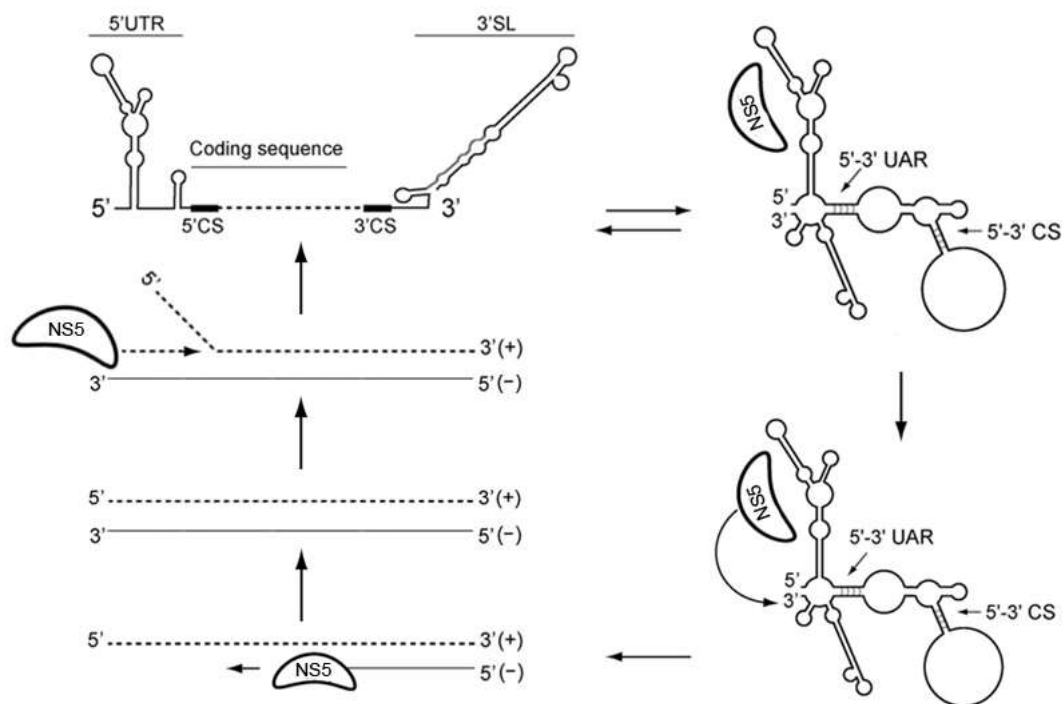


Figure 2. Existing model of viral RNA replication in infected cells.

Recently, we utilized an unbiased genome-wide yeast three-hybrid (Y3H) scan to explore all interaction sites between DENV RNA and NS5 RdRp, and have discovered that the 3' stem-loop (SL), but not the 5' SLA, is the authentic RNA promoter for DENV replication [5]. Our results completely revised the current model of DENV replication (Fig. 3). Moreover, the current model assumes that the DENV genome exists in cells as a naked RNA, which is highly unlikely. Several lines of evidence recently proved that flaviviral vRNAs interact with cellular proteins to stabilize and promote the replication such as eukaryotic initiation factor 1A (eIF1A) [14,15], human La autoantigen (La) [16], poly-pyrimidine tract binding protein (PTB) [17], Y-box binding protein 1 (YB-1) [18], and heterogeneous nuclear ribonucleoproteins (hnRNP A1, hnRNP A2/B1 and hnRNP Q) [19]. It has also been reported that the RNA degradation pathway may play an important role in the quantity control of the vRNA turnover [20]. Moreover, vRNA directly recruits the TRIM25 protein to suppress interferon response [21]. Hence, the accurate mechanism for DENV RNA replication in cells seems to be much more complex and involve more cellular factors than previously thought.

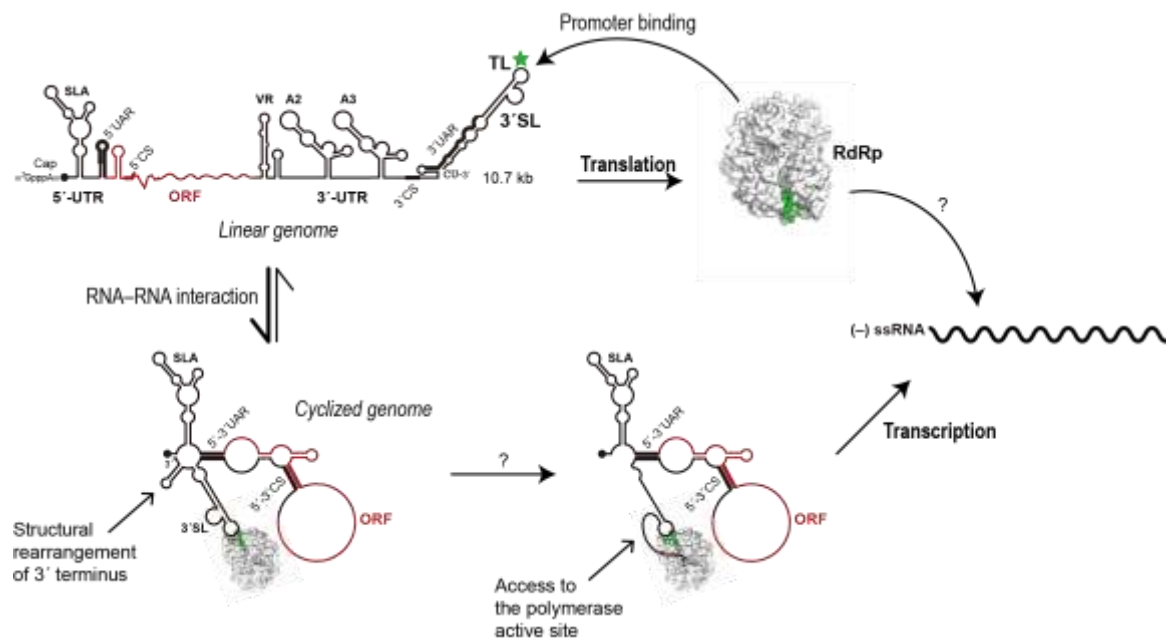


Figure 3. Our proposed new DENV replication model [5].

The search for inhibitors against vRNA replication is a key research in virology field. The idea was corroborated by a success in HIV drug by interrupting viral RNA polymerase to block viral replication in an early state of infection. Since the precise mechanism of DENV replication in human cells still remains enigmatic and the global genome-wide interaction with vRNA inside the cell remains mostly elusive, our initial attempt to address this question was supported by TRF (RSA5680054) to design and create an infectious DENV particle that contains an epitope tag inside the viral NS5 polymerase for interactome study. It has been reported that the insertion of tags into DENV NS3 and NS5 proteins in the context of viable virus was not possible [22]. However, we utilized a rational design of tag insertion and succeeded in engineering DENV to contain a tandem affinity purification (TAP) tag including a polyhistidine and FLAG tags inside the NS5 protein

for the first time [6]. We used our engineered, tagged (et) DENV particle to infect a human liver Huh-7 cell line, and showed that etDENV retained efficient infection comparable to the wild type (WT) DENV (Fig. 4) [6]. We also found that the tag inserted into our etDENV was very stable even after seven passages of viral culture [6]. We further established the procedure to isolate tagged DENV NS5 from infected cells via a two-step affinity against nickel and anti-FLAG resins [Fig. 5]. The results showed that the inserted tags were exposed to solvent and fully functional for purification. The gel also proved that the quality and quantity of NS5 pull-down was sufficient for our further interactome study [Fig. 5].

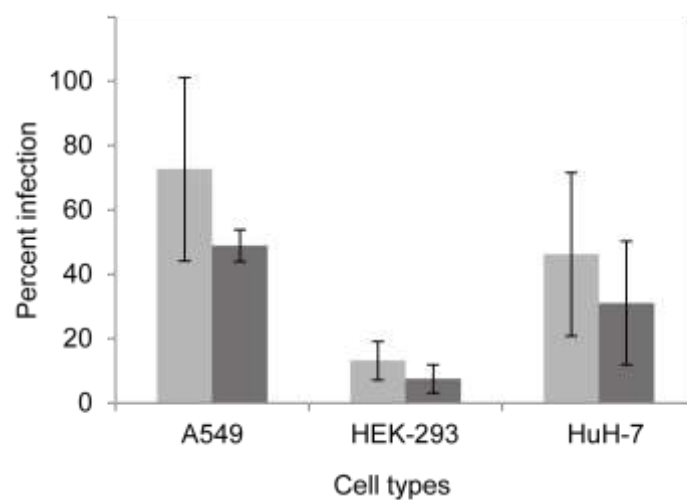


Figure 4. Flow cytometry analysis with anti-E antibody revealed that our developed etDENV could infect several human cell lines comparable to the wild type. Light and dark grey bars represent DENV-2 16681 and etDENV, respectively [6].

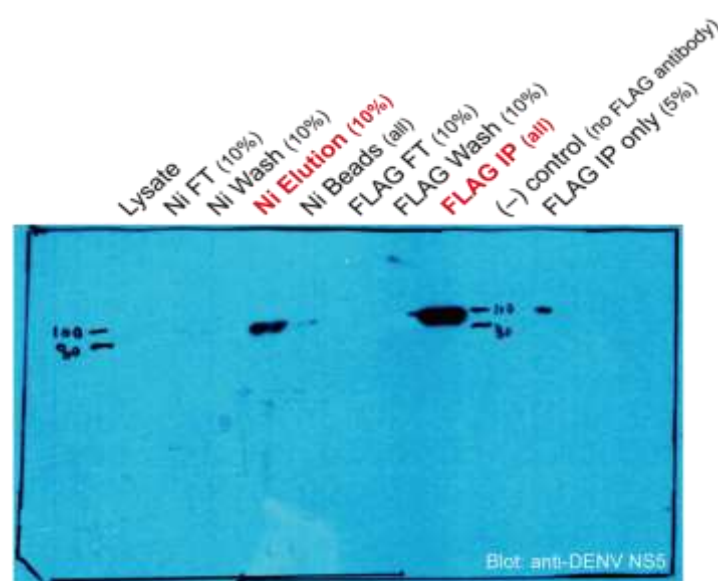


Figure 5. Isolation of tagged DENV NS5 from infected HuH-7 cells at day 2nd post infection by etDENV. The Western blot with anti-NS5 validated immunoprecipitation results.

To this end, we developed a new technological platform called modified PAR-CLIP (Photoactivatable-Ribonucleoside-Enhanced Crosslinking and Immunoprecipitation) [23] as a tool for genome-wide exploration of human proteins that interact with viral RNA (see Methodology and Fig. 9). Our preliminary results revealed that at least four cellular complexes interact with DENV RNA during replication including MCM, RNA processing, ribosome, and protein chaperone (unpublished results). Gene ontology analysis revealed significant dengue vRNA-interacting protein networks in DENV infection (Fig. 6). Altogether, our published and preliminary results clearly suggest that our developed etDENV and PAR-CLIP technology are suitable for system biology study of DENV interactome in infected human cells.

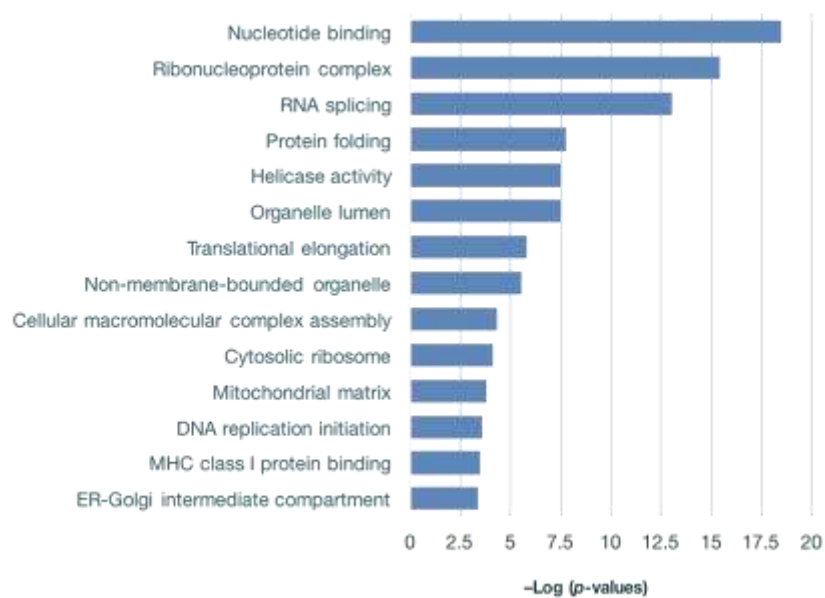


Figure 6. List of enriched gene ontology groups of DENV RNA-interacting proteins (unpublished preliminary data).

In this proposal, we would like to use our established materials and new technology to perform time-resolved host-DENV interactome for the first time. To date, a number of approaches have been used to identify DENV proteins and RNA-interacting partners using the yeast two-hybrid (Y2H), and affinity isolation of ectopically expressed viral proteins [22, 24-25]. However, these approaches did not mimic physiological conditions of viral infection, and usually utilized a very short RNA fragment with uninfected cell lysate; therefore, downplayed a body of work that suggested that viral RNA and proteins are tightly associated from translation to later stages in the viral life cycle. Indeed, these different studies have, thus far, shown a curious lack of overlap in their datasets. For example, Khadka et al. [25] and Le Breton et al. [26] both revealed DENV NS5 interaction network, with no overlapping data! In addition, host-virus interactions are supposed to be more aggressive and dynamic during different infection stages; however, no any earlier study could so far visualize dynamic events of viral replication. We wish to find missing pieces of the jigsaw puzzle of DENV replication, and open new avenues for development of therapeutic agents in the future via our new approach which combines cutting edge techniques of etDENV, PAR-CLIP, protein labeling mass spectrometry, high-content cell imaging, and *in silico* bioinformatics analysis.

References

1. Gubler, D.J. (1998) Dengue and Dengue Hemorrhagic Fever. *Clin Microbiol Rev.* **11**(3), 480-96.
2. WHO. (2010) Dengue: Guidelines for diagnosis treatment prevention and control, World Health Organization (Geneva).
3. Whitehead, S.S., Blaney, J.E., Durbin, A.P., Murphy, B.R. (2007) Prospects for a dengue virus vaccine. *Nat Rev Microbiol.* **5**(7), 518-28.
4. Kamkaew, M., Chimnarong, S. (2015) Characterization of soluble RNA-dependent RNA polymerase from dengue virus serotype 2: The polyhistidine tag compromises the polymerase activity. *Protein Expr Purif.* **112**, 43-9.
5. Hodge K, Tunghirun C, Kamkaew M, Limjindaporn T, Yenchitsomanus PT, Chimnarong S. (2016) Identification of A Conserved RdRp-RNA Interface Required for Flaviviral Replication. *J Biol Chem.* **291**(33), 17437-49.
6. Poyomtip T., Hodge K., Matangkasombut P., Sakuntabhai A., Pisitkun T., Jirawatnotai S., Chimnarong S. (2016) Development of viable TAP-tagged dengue virus for investigation of host-virus interaction in viral replication. *J Gen Virol.* **97**(3), 646-58.
7. Kuno, G., Chang, G.J., Tsuchiya, K.R., Karabatsos, N., Cropp, C.B. (1998) Phylogeny of the genus Flavivirus. *J Virol.* **72**(1), 73-83.
8. Lodeiro, M.F., Filomatori, C.V., Gamarnik, A.V. (2009) Structural and functional studies of the promoter element for dengue virus RNA replication. *J Virol.* **83**(2), 993-1008.
9. Markoff, L. (2003) 5' - and 3' -noncoding regions in flavivirus RNA. *Adv Virus Res.* **59**, 177-228.
10. Modis, Y., Ogata, S., Clements, D., Harrison, S.C. (2004) Structure of the dengue virus envelope protein after membrane fusion. *Nature.* **427**(6972), 313-9.
11. Paranjape, S.M., Harris, E. (2010) Control of dengue virus translation and replication. *Curr Top Microbiol Immunol.* **338**, 15-34.
12. Alvarez, D.E., Lodeiro, M.F., Ludueña, S.J., Pietrasanta, L.I., Gamarnik, A.V. (2005) Long-range RNA-RNA interactions circularize the dengue virus genome. *J Virol.* **79**(11), 6631-43.
13. Villordo, S.M., Gamarnik, A.V. (2009) Genome cyclization as strategy for flavivirus RNA replication. *Virus Res.* **139**(2), 230-9.
14. Davis, W.G., Blackwell, J.L., Shi, P.Y., Brinton, M.A. (2007) Interaction between the cellular protein eEF1A and the 3'-terminal stem-loop of West Nile virus genomic RNA facilitates viral minus-strand RNA synthesis. *Virology.* **81**(18), 10172-87.
15. De Nova-Ocampo, M., Villegas-Sepúlveda, N., del Angel, R.M. (2002) Translation elongation factor-1 α , La, and PTB interact with the 3' untranslated region of dengue 4 virus RNA. *Virology.* **295**(2), 337-47.
16. Vashist, S., Anantpadma, M., Sharma, H., Vrati, S. (2009) La protein binds the predicted loop structures in the 3' non-coding region of Japanese encephalitis virus genome: role in virus replication. *J Gen Virol.* **90**(6), 1343-52.

17. Anwar, A., Leong, K.M., Ng, M.L., Chu, J.J., Garcia-Blanco, M.A. (2009) The polypyrimidine tract-binding protein is required for efficient dengue virus propagation and associates with the viral replication machinery. *J Biol Chem.* **284**(25), 17021-9.
18. Paranjape, S.M., Harris, E. (2007) Y Box-binding protein-1 binds to the dengue virus 3'-untranslated region and mediates antiviral effects. *J Biol Chem.* **282**(42), 30497-508.
19. Noisakran, S., Sengsai, S., Thongboonkerd, V., Kanlaya, R., Sinchaikul, S., Chen, S.T., et al. (2008) Identification of human hnRNP C1/C2 as a dengue virus NS1-interacting protein. *Biochem Biophys Res Commun.* **372**(1), 67-72.
20. Pijlman, G.P., Funk, A., Kondratieva, N., Leung, J., Torres, S., van der Aa, L., Liu, W.J., Palmenberg, A.C., Shi, P.Y., Hall, R.A., Khromykh, A.A. (2008) A highly structured, nuclease-resistant, noncoding RNA produced by flaviviruses is required for pathogenicity. *Cell Host & Microbe* **4**(6), 579-591.
21. Manokaran, G., Finol, E., Wang, C., Gunaratne, J., Bahl, J., Ong, E.Z., Tan, H.C., Sessions, O.M., Ward, A.M., Gubler, D.J., Harris, E., Garcia-Blanco, M.A., Ooi, E.E. (2015) Dengue subgenomic RNA binds TRIM25 to inhibit interferon expression for epidemiological fitness. *Science.* **350**(6257), 217-21.
22. Carpp, L. N., Rogers, R. S., Moritz, R. L., and Aitchison, J. D. (2014) Quantitative proteomic analysis of host-virus interactions reveals a role for Golgi brefeldin A resistance factor 1 (GBF1) in dengue infection, *Mol Cell Proteomics* **13**, 2836-2854.
23. Hafner, M., Landthaler, M., Burger, L., Khorshid, M., Hausser, J., Berninger, P., Rothballer, A., Ascano, M. Jr., Jungkamp, A.C., Munschauer, M., Ulrich, A., Wardle, G.S., Dewell, S., Zavolan, M., Tuschl, T. (2010). Transcriptome-wide identification of RNA-binding protein and microRNA target sites by PAR-CLIP. *Cell* **141**(1), 129-141.
24. Doolittle, J. M., and Gomez, S. M. (2011) Mapping protein interactions between Dengue virus and its human and insect hosts, *PLoS Negl Trop Dis* **5**, e954.
25. Khadka, S., Vangeloff, A. D., Zhang, C., Siddavatam, P., Heaton, N. S., Wang, L., Sengupta, R., Sahasrabudhe, S., Randall, G., Gribskov, M., Kuhn, R. J., Perera, R., and LaCount, D. J. (2011) A physical interaction network of dengue virus and human proteins, *Mol Cell Proteomics* **10**, M111 012187.
26. Le Breton, M., Meyniel-Schicklin, L., Deloire, A., Coutard, B., Canard, B., de Lamballerie, X., Andre, P., Rabourdin-Combe, C., Lotteau, V., and Davoust, N. (2011) Flavivirus NS3 and NS5 proteins interaction network: a high-throughput yeast two-hybrid screen, *BMC Microbiol* **11**, 234.
27. Noppakunmongkolchai W., Poyomtip T., Jittawuttiopoka T., Luplertlop N., Sakuntabhai A., Chimnaronk S., Jirawatnotai S., Tohtong R. (2016) Inhibition of protein kinase C promotes dengue virus replication. *Virology* **13**(1), 35.

วัตถุประสงค์ (Objective)

1. To expand our previous research outcome and apply a new technological platform to address an important question concerning the replication mechanism of DENV in human cells for a search for antiviral drug target.
2. To explore the global interactions between DENV RNA and human proteins in infected human hepatic Huh-7 cells, for the first time, at multiple stages of infection in a quantitative manner.
3. To produce high-motivated, world-class young researchers including Ph.D. and M.Sc. students, and also, publications on high-impacted international scientific journals.

เนื้อหางานวิจัย

Materials and Methods

Virus propagation

Vero cells were cultured at 37°C with 5% CO₂ in minimum essential medium (MEM) supplemented with 10% of fetal bovine serum (FBS) without antibiotic until 100% confluence was obtained. The engineered, tagged dengue virus (etDENV) was filtered through 0.22 µm membranes. Then, cells were infected with the etDENV passage 2, using an MOI (multiplicity of infection) of 0.1 in diluent medium (2% FBS) for 90 min, for virus adsorption. Media were substituted by the virus production serum free medium (VP-SFM) with 1% of L-glutamine. Cytopathic effects (CPE) was investigated, and viruses from cells and supernatant were harvested by freeze-thaw twice when about 90% CPE was observed. The virus titer was determined by the plaque assay. The MK2 cells were seed into 6-well plate at the concentration of 20,000 cells per well and cultured for 7 day for complete adhesion. Then, media were removed, and cells were incubated with 0.2 ml of serial dilutions of virus samples. After 90-min incubation, the minimum essential medium without phenol red supplemented with 10% FBS, 2% penicillin-streptomycin, 1% L-glutamine, 6% neutral red and 1.5% of carboxymethyl cellulose (CMC) was added. After 7 days, plaques were counted, and virus yields were calculated by

$$\frac{PFU}{ml} = \frac{\text{number of plaques}}{\text{dilution} \times \text{volume of diluted virus added to the plate}}$$

PAR-CLIP

We performed our modified PAR-CLIP (Photoactivatable-Ribonucleoside-Enhanced Crosslinking and Immunoprecipitation) by infected human HuH-7 cells (a well differentiated hepatocyte-derived carcinoma cell line) with etDENV at an MOI (multiplicity of infection) of 5 in the presence of 100 µM s⁴U in the culture media. At 48 h after infection, cells were lysed with 3 volumes cell lysis buffer per pellet for 30 minutes on ice with occasional gentle agitation, and its completion was checked under microscopy. The lysate was extracted via centrifugation at 13,000 rpm for 15 min at 4°C. Cleared lysate was directly applied to pre-equilibrated Ni-NTA beads. Best results were obtained with small bed volumes of beads. Currently, lysate corresponding to 10⁷ cells (approximately 1.5 mg lysate protein) was applied to a 10 µl bed volume. The binding was performed

for 1 h at 4°C, and then unbound fraction was removed by centrifugation at 2500 rpm. At least 5 cycles of washing with 100 µl washing buffer for 10 min at 4°C were performed. Elution from Ni-NTA was accomplished with 20 µl elution buffer and repeated at least 4 times. It is important to save appropriate volumes of fractions for possible Western blotting or Bradford assays.

Ni-elution fractions were combined with pre-equilibrated anti-FLAG M2 affinity beads (Sigma-Aldrich). The volumes of bedded beads per estimated protein content were the same as the Ni-NTA step above (10 µl/1.5mg protein). The beads were rotated at 4°C for 1 h before collection of the flow through fraction. Washing with 500 µl TBS buffer (10 mM Tris pH 7.5, 150 mM NaCl) was performed 3 times. Occasionally, we treated the FLAG resin with 100 U/µl RNase T1 (NEB) for 20 minutes at 22°C to release proteins that interacted with DENV RNAs, and then the FLAG resin was further washed twice with TBS to remove RNase T1. Protein-RNA complexes including NS5 that remained on the beads was collected and subjected to SDS-PAGE and LC/MS/MS analyses. Solutions used in PAR-CLIP are described as below.

- i) Lysis buffer: 77.5% basic solution, 5 mM β-mercaptoethanol, 0.3% RNase-free DNase I, 1% NP-40
- ii) Nickel basic solution: 50 mM HEPES-NaOH pH 7.2, 150 mM KCl, 1% Triton X-100, 25 mM imidazole, 10% Glycerol, 50 mM NaCl, 2% RNasin (NEB), 1x protease inhibitor, 1x phosphatase inhibitor
- iii) Ni wash buffer: 77.5% basic solution, 1% NP-40, 5 mM β-mercaptoethanol
- iv) Ni elution buffer: 77.5% basic solution, 22.5% 1 M imidazole

Sample preparation for the mass spectrometry (MS)

Co-IP samples were separated by SDS-PAGE, and the gel was stained with colloidal Coomassie dye, and destained with ddH₂O overnight. Strongly staining bands of interest (e.g. those at the expected NS5 size of 103 kDa) were specifically excised, diced into approximate 1 mm² fragments, and placed in Eppendorf tubes, with non-staining regions being stored in separate tubes. 200 µl of a solution composed of 25 mM ammonium bicarbonate (Ambic) and 50% acetonitrile (ACN) was applied to each sample, vortexed, briefly centrifuged, and allowed to stand for 10 min. Supernatant was then discarded via aspiration. Application and removal of Ambic/ACN was repeated, followed by SpeedVac treatment at medium heat for about 30min. A reduction step followed with application of 100 µl DTT in 25 mM AmBic. The reaction proceeded for 1 hour at 56°C. Alkylation (specifically, blocking of cysteine residues to prevent reformation of disulfide bridges) was conducted by adding 100 µl of 55 mM iodoacetamide (IAA) in 25 mM AmBic to each sample. The reaction occurred in the dark for 45 min at room temperature. The solution was then removed, and the samples were dehydrated with 200 µl of 25 mM Ambic in 50% ACN, vortexed, and allowed to stand for 10 min. This step was repeated once more and then samples were dried via SpeedVac.

Trypsinization was performed with “Trypsin Gold” suspended in 25 mM Ambic. Each sample tube received about 2 µg of trypsin. 75 µl of this solution was applied to each sample for 30 min at 4°C. The solution was then removed, and samples rehydrated with 200 µl of 25 mM Ambic, followed by overnight incubation at 37°C. Peptide extraction and desalting were achieved as follows. 200 µl of 50% ACN and 0.5% formic acid were added to the samples, vortexed, and allowed to stand for 20 min. The supernatant was then transferred to new sample tubes. This extraction process was repeated two more times. The samples

were placed in a SpeedVac and dried at moderate heat. “ZipTips” (200 µl tips containing “solid phase extraction” paper) were treated with wetting and equilibration solution. The ZipTips were inserted into eppendorf tubes with a small hole in the cover and centrifuged at low speed, followed by treatment with washing solution samples are treated with washing solution and centrifugation. Elution solution was then added, followed by centrifugation to isolate the peptides of interest. The desalted peptides were transferred to new tubes and dried in a SpeedVac.

MS analysis of DENV RNA-interacting proteins

Mass spectrometry was performed in Dr. Trairak Pisitkun’s group at Chulalongkorn University on a Thermo-Scientific “Q Exactive plus” platform. Mass spectrometry results were initially analyzed according to the GPM database (future work will include at least one other database, e.g. “Skyline”). Parent mass errors between -10 to 10 ppm were used. The matching proteome was *H. sapiens* male and female. The database was winnowed by excluding common contaminants (e.g. keratin) and, most significantly, by excluding all proteins that were found in both mutant (TAP-tagged virus) and control (wild-type virus). That is, only proteins found exclusively in the mutant samples were considered as potential DENV RNA interactors. Proteins could be ranked by several means. Most simply, unique peptide fragments could be counted. Bias for high-molecular weight proteins could be eliminated or reduced by dividing the unique peptide count by the putative protein’s mass. GPM also generates a number of confidence measures based on the probability of false positives. The presumed DENV RNA interaction network was generated via the STRING 10.0 database (<http://www.string-db.org>) at a confidence mode of 0.4. Gene ontology (GO) groupings were gotten from DAVID (<http://david.abcc.ncifcrf.gov/>). A lab database of known flaviviral interactors was constructed by extensive literature survey; this database could be used, for example, for determining overlap between our results and other results, for selecting promising protein candidates for future study, and more.

Dimethyl Labeling

Following harvest, cells were lysed via sonication in the presence of 5% sodium deoxycholate, with 50 mM TEAB (triethyl ammonium bicarbonate, no pH adjustment) substituting for Tris, as unnecessary compounds with primary amines may interfere with downstream peptide identification. The protein mix was then incubated with a final 10 mM concentration of DTT at room temperature for 30 min. Iodoacetamide (IAA) was added to a final 15 mM and incubated for 30 min, at room temperature, in the dark. IAA was then inhibited by addition of 40 mM DTT and room-temperature incubation for 15 min. TEAB was added to produce a final 25 mM concentration in 1000 µl. Standard trypsin digestion was then performed 14-16 hr at 37°C. Trifluoroacetic acid (TFA) was added to a final 0.5% concentration, with incubation at room temperature for 15 min. Centrifugation was then performed at high speed at 4°C for 15 min, followed by collection of supernatant. “speed vac” at moderate temperature (not high) was performed until dry. 100 µl of 100 mM TEAB was added, followed by addition of 15 µl of 4% formaldehyde isotope (the choice of three isotopes is determined by experimental design) and incubation for one hour. The reaction was quenched by addition of 1% ammonia on ice. Keeping the mix on ice, 15 µl 100% FA was added.

Phosphoproteomic analysis

We desired to examine phosphorylation events at very early stages (30 and 60 min) of infection, as numerous studies have shown dramatic alterations in phosphorylation at early time points [e.g. a 1 min cutoff in a publication by Wojcechowskyj J.A. et al. (2013) Quantitative Phosphoproteomics Reveals Extensive Cellular Reprogramming during HIV-1 Entry, *Cell Host Microbe*. 13(5), 613-23]. A 48-hour time point was also examined; this way, reversion of early phospho-states to the pre-infection state could be examined.

For the early stage experiments, an MOI of 50 was used in order to maximize phosphoproteomic alterations. In all cases, a large (24 cm diameter) dish was used, allowing infection of 15-20 million cells. Following a 30-min infection period, one infected plate and one mock infection plate were harvested. Also, the 60-min condition plates (infected and mock) were washed with PBS and then allowed to incubate with DMEM for another 30 min before a second harvest. Since four conditions with potentially different phospho-states were generated, and our dimethyl reagents only allow three labeling states (though additional reagents could allow up to five labeled states), the experiments were divided into two groups: 30 min test (T1), 30 min mock (M1), and 60 min test (T2) constituted “mix 1”, while “mix 2” included 60 min mock (M2), as well as T1 and T2. At the level of dimethyl labeling, mock always received a medium label, while T1 was labeled light and T2 heavy. Future experiments will seek to minimize complexity, possibly using only two of the three labels. For the 48-hour infection condition, a mock and infected condition were utilized. This time, an MOI of 5 was used. Again, a medium label was used for mock, while light indicated the infected condition. Harvest, lysis, and early preparation for mass spectrometry were performed as previously described.

Phosphoproteomic enrichment

We performed “phospho-enrichment” follows tryptic digest and, if desired, dimethyl labeling. Labeling methods, of which the dimethyl technique is one, allow mixing of samples generated under a variety of conditions, heightening the accuracy of mass spectrometric results. “Label free” methods, whereby mixing is not performed and samples are injected separately into the spectrometer have seen a resurgence but may still not be comparable to labeling-based protocols.

At a suitable timepoint, 5 mg TiO₂ (Titansphere, GL Sciences) was dissolved in 500 µl 100% acetonitrile (ACN), and equilibrated overnight with shaking at 4°C. Following labeling, quenching, and mixing of samples, 10% of the total volumes were set aside and did not undergo phospho-enrichment. Downstream analysis may then be able to ascertain whether, for example, a phospho-peptide is upregulated due to increase abundance of the underlying protein, or due to increased phosphorylation. Following vacuum-centrifugation (speed-vac) drying of mixed samples, the samples were reconstituted in loading buffer (1 M glycolic acid, 80% ACN, 5% trifluoroacetic acid (TFA) and 15% H₂O). A “zip-tip” was prepared by inserting a small portion of C8 filter membrane into a 200 µl pipette tip, followed by addition of 100 µl TiO₂ solution and centrifugation of the tip at RT, 1500g, 5 min. Equilibration of the tip follows, with two cycles of addition of 75 µl loading buffer and centrifugation at 1000g, rt for 3 min. Sample was then loaded, followed by 2 washes under the previous centrifugation conditions. Four cycles of washing with 60 µl wash buffer (prepared as for loading buffer *sans* glycolic acid) under the above centrifugation conditions were performed. Flow-through and wash samples

were, of course, saved. Elution was performed 3x with 60 µl elution buffer (0.5% ammonia; pH 10.5) under the above centrifugation conditions.

Fractionation

Enhanced MS results require fractionation, normally according to hydrophobicity. Both enriched and non-enriched samples undergo fractionation. The current procedure utilizes the Pierce High pH Reversed-Phase Peptide Fractionation Kit (Cat #84868), with increased concentrations of ACN providing the required differentially hydrophobic elution conditions. A number of modifications have been here introduced. In brief, the provided tips (one per sample) were centrifuged at 5000g, 2 min to remove storage solution. They were then equilibrated twice with 300 µl ACN at the above centrifugation conditions. Washing was performed twice, with a solution of 0.5% ammonia (the elution buffer used in phospho-enrichment), centrifugation as above.

In parallel with column preparation, differential elution solutions might be prepared. These consisted of 8 solutions with ACN concentrations increasing from an initial 2.5% to a final 50%, with a 0.1% trimethylamine solution making up the difference. This step-wise increases in ACN content reduced the concentration differentials in the early fractions.

Samples were loaded into the prepared columns, followed by centrifugation (3000g, 2 min), with the eluate saved as “flow through”. The following wash step simply used H₂O, with eluate saved as “wash”. Successive eluate collections used the above-prepared 300 µl elution solutions under the above centrifugation conditions. Following collection, all samples were vacuum-dried in preparation for MS injection.

Analysis of MS raw (m/z) data

We have found MaxQuant software (v1.6.0.16) to be intuitive and practical for analyzing raw m/z data. For phospho-data, the following settings were used. Underlying sequences included the Uniprot human proteome and a six-frame dengue proteome. Carbamidomethylation was included as a global modification. PSM FDR and protein FDR were set to 0.01. Minimum peptide length was set to 7, while maximum mass is 4600 daltons. Dimethyl-labeled lysines are “group-specific” modifications (dimethLys0, dimethLys4, dimethLys8), with Phospho(STY), acetylation, and oxidation also found in this category. Data was arranged according to fraction number, allowing the “matching across fractions” function to be used.

Downstream analysis utilized a combination of Thermo Xcalibur software (visualization of MS1 data), MaxQuant (MS1 and MS2 data), and Perseus (data manipulation, statistics).

MS analysis of Protein–RNA interfaces

To expand our DENV protein–RNA interaction toolbox, we applied an underlying technology based on a previous study of Kramer K et al. [photo-cross-linking and high-resolution mass spectrometry for assignment of RNA-binding sites in RNA-binding proteins (2014) *Nature Methods* 11(10), 1064-70.]. The method is also capable of determining RNA sequences of up to 4 nucleotides that are bound to proteins of interest. In brief,

10 µg purified DDX6 was mixed with equimolar, purified, *in-vitro*-transcribed RNA representing the 180 nt “A2A3” region of the DENV-2 3′-UTR in 10 µl EMSA assay buffer (50 mM Tris-HCl pH 7.5, 10 mM Mg(OAc)₂, 65 mM NH₄OAc, 1 mM EDTA) at room temperature for 15 minutes. Crosslinking was performed at a high intensity UV₂₅₄ on a Spectrolinker (Spectronics Corp). Control samples were not crosslinked. RNA was then digested using a combination of RNase A and RNase T1 at two different concentrations: 0.1 µg/µl and 0.1 U/µl, and 10 µg/µl and 10 U/µl, respectively. The samples were then flash-frozen and prepared for standard label-free mass-spectrometry (with DTT and IAA treatment, trypsinization, and desalting), as described above.

Following generation of mass spectrometric raw data, a specific bioinformatic workflow was followed, as outlined in the aforementioned Methods paper. The underlying concept is simply to compare the control (no cross-linking) and cross-linked samples, remove all shared peptides, and use MS analysis software developed for the purpose of analyzing covalently linked RNA–peptide combinations. Specifically, TOPPAS MS analysis software was utilized, with the “RNPxl” and “RNPxlxic Filter” programs specifically applied to protein–RNA analysis.

Y3H

Molecular cloning and Y3H protocols are available in detail in our previous work [5]. In brief, RBP genes of interest were amplified by RT-PCR with total RNAs from Hela and HuH-7 cells, or YBZ-1 yeast (to obtain *Dhh1*), and cloned into the Y3H protein expression plasmid pACT2. For Y3H RNA expression, a previously generated DENV-2 pIII_A-MS2-2 library was used for screening, while specific RNAs of interest were created via PCR against a DENV-2 (16681) clone [5], followed by cloning into pIII_A-MS2-2. Standard QuikChange (Agilent Technologies) protocols were applied to generate all mutants. Y3H YBZ-1 yeast were co-transformed with the protein and RNA expression plasmids, followed by plating on Leu⁻/Ura⁻/His⁻-deprived agar media, with addition of the histidine metabolism inhibitor 3-AT to concentrations as high as 5 µM. Binding affinities were monitored via β-galactosidase expression assay as described previously.

Results and Discussion

We have produced 1 liter of etDENV with the FFU quantitation of approximately 10⁷ (Fig. 7). We employed Sanger DNA sequencing to verify the tagged virus clone, and the Western blot to verify the intact FLAG tag after infection into human HuH-7 cells.

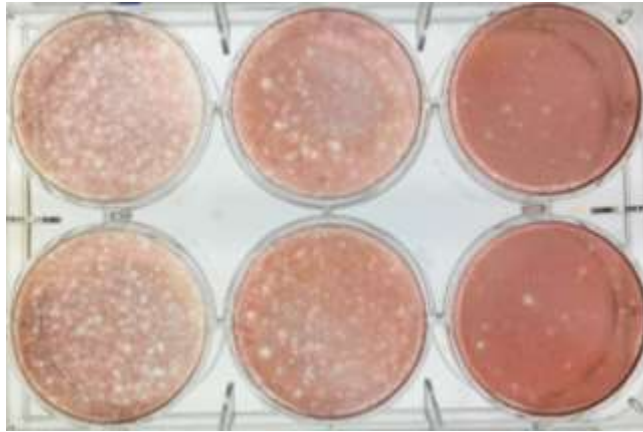


Figure 7. Plaque assay of propagated etDENV

Prior to PAR-CLIP, we validated our PAR-CLIP protocol and estimated the yield of tagged NS5 isolated by IP from etDENV-infected cells. The Western blot analysis revealed that FLAG-IP yielded about 0.05 μg NS5 from 10^6 HuH-7 cells (**Fig. 8**). The SDS-PAGE clearly showed a high purity of NS5 after IP (FLAG beads lane), prompting us to perform PAR-CLIP.

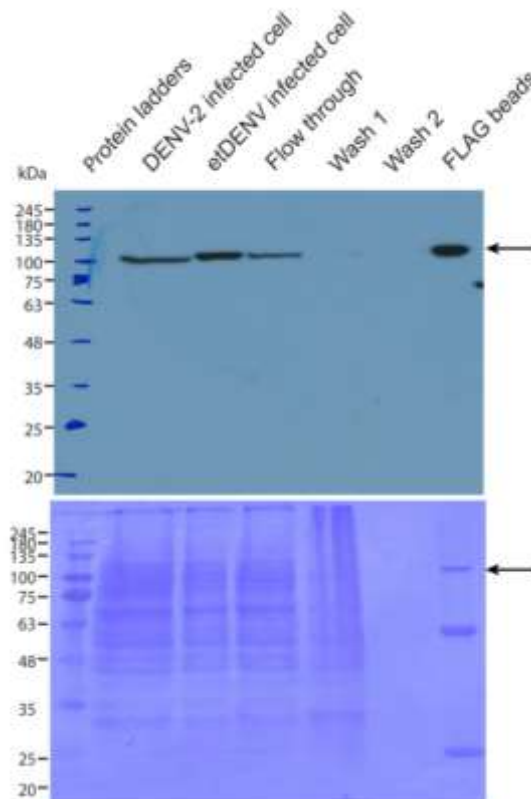


Figure 8. Isolation of tagged NS5 from etDENV-infected HuH-7. Each protein fraction from FLAG-IP was resolved by SDS-PAGE and visualized by the Western blot with anti NS5 polyclonal antibody (top panels) and Coomassie (brilliant blue R-250) staining (bottom panels) and the black arrows indicate tagged NS5 bands (105.7 kDa).

Since we reported that DENV RdRp binds to the 3' SL RNA element in the dengue 3'-UTR with a high binding affinity (K_d) of ~ 3.2 nM [5], We took this advantage of strong affinity of RdRp against the viral genome to explore viral RNA interactions in human cells via modified PAR-CLIP procedure (Fig. 9).

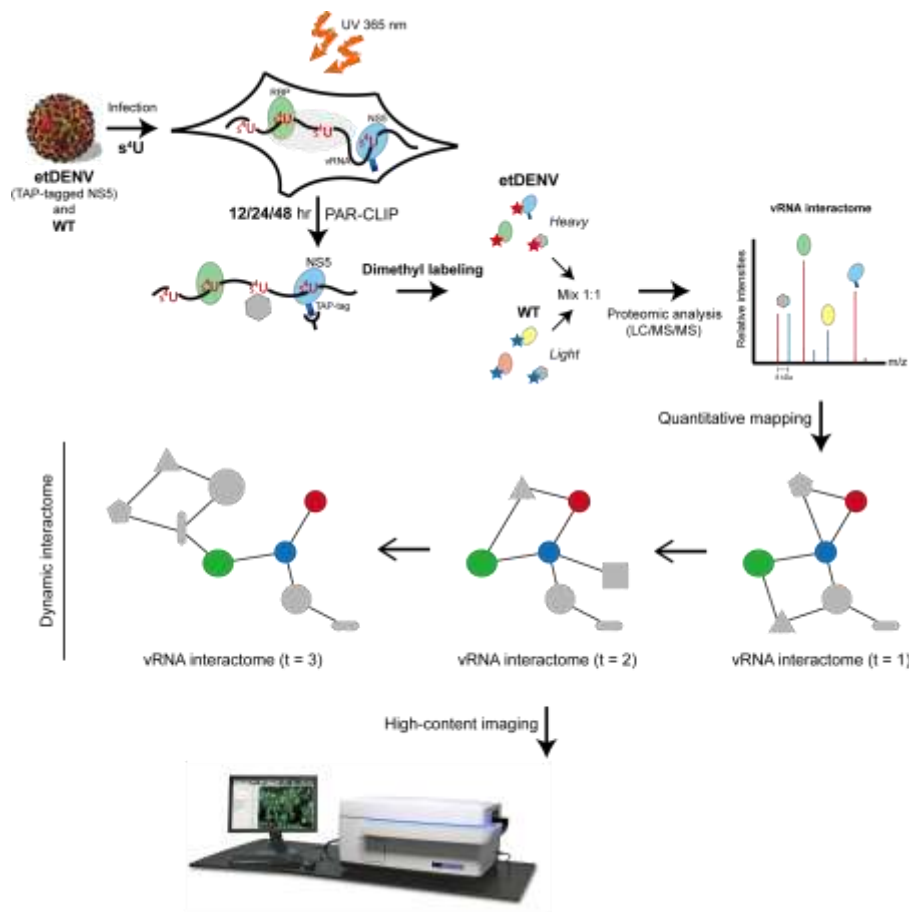


Figure 9. Schematic diagram of modified PAR-CLIP in this study.

We performed PAR-CLIP by infected the human HuH-7 cells with etDENV at MOI 5 in the presence of 100 μ M s⁴U in the media. At 48 h after infection, cells were exposed to UVA to cross-link protein and RNA inside the cell prior to PAR-CLIP via two steps of nickel and FLAG affinity resins. Proteins interacting with viral RNA (vRNA) were eluted from FLAG beads with acidic condition, and subjected to MS analysis. The resulting GPM-based list of 122 proteins found only in tagged NS5 elutions was judged to be highly satisfactory based on several criteria. First, nucleotide and RNA-binding proteins were highly enriched ($p = 6 \times 10^{-16}$, **Table 1**). Secondly, the STRING network showed clear clustering of proteins (**Fig. 10**), suggesting well-defined viral or host strategies. Finally, comparing our protein list against our database of host proteins known to be relevant in flaviviral infections showed that 60% of our proteins were also seen in the database. While our protein list and network conformed well to general expectations, there were a number of surprises. For example, mini-chromosome maintenance (MCM) proteins were prominent in our results, though flaviviral associations with this complex are absent in the literature. Also, proteins associated with mitochondrial lumen were enriched in our results, again with little mention in the literature.

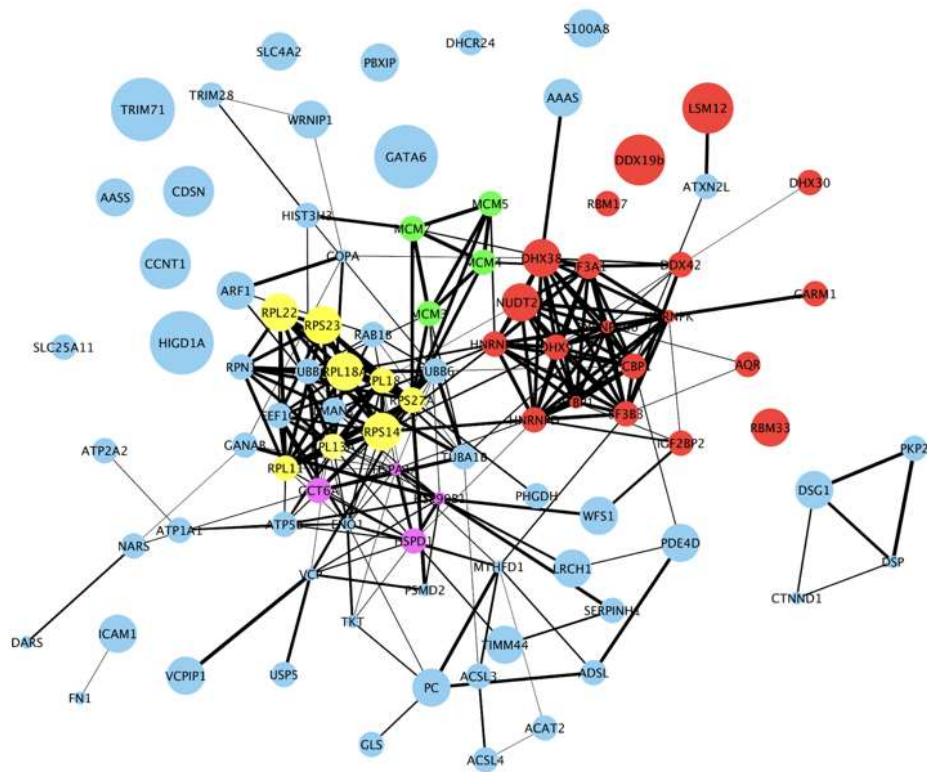


Figure 10. Interaction map between DENV RNA and human proteome in HuH-7 cell at 48 h after infection. At least, we found 4 different human complexes with vRNA, which are RNA processing and RNA helicases (red circles), ribosome (yellow circles), chaperones (pink circles), and unexpectedly, MCM complex (green circles). It is also noted that only a few proteins were found as isolated nodes.

Table 1. GO terms showing enrichment of particular interest.

Groups	<i>P</i> -values (Benjamini-correction)
RNA-binding	6.0×10^{-16}
Chaperones	4.4×10^{-7}
Helicases	5.5×10^{-5}
Organelle lumen	5.7×10^{-6}
Tubulin	6.6×10^{-4}
Mitochondrial matrix	9.5×10^{-4}

To increase fidelity of PAR-CLIP-identified vRNA interactors, we repeated another round of PAR-CLIP and performed bioinformatics analysis of MS results to validate our interactome map. Parallel wild-type and etDENV viruses are used to infect HuH-7 cells in the presence of s^4U . DENV NS5 was linked to vRNA via crosslinking at UV₃₆₅ (causes covalent protein—RNA linkages at higher efficiency as compared to that of standard UV₂₅₄). Only the tagged NS5 in etDENV-infected cells could be pulled down with efficiency, allowing a contrast against background (proteins bound to FLAG beads from DENV-2 infected cells). Proteins found in duplicated PAR-CLIP experiments would be, therefore, considered particularly confident at this point (Table 2).

In parallel, we also performed IP of NS5 in the absence of crosslinking with the aim of generating a list of direct NS5 interactors. These interactors, when seen also in the vRNA interaction list, would be questionable as direct RNA interactors, and could be subtracted out from the RNA interactome list (**Table 2**). While the experiment has also been performed in our previous studies [6], we wished for our interaction list to be generated under conditions that paralleled our RNA-pulldown conditions as closely as possible. The resulting NS5 interactome was deep, with over 400 identifications, 147 of which were identified via 3 or more unique peptides. The largest list strongly intersected with known HCV NS5B interactors with a $p = 10^{-35}$ via Fisher's exact test [Germain MA et al. Elucidating novel hepatitis C virus-host interactions using combined mass spectrometry and functional genomics approaches. (2014) *Mol Cell Proteomics*. 13(1), 184-203.], and DENV-2 interactors with a $p = 10^{-7}$ [De Maio FA et al., The dengue virus NS5 protein intrudes in the cellular spliceosome and modulates splicing. (2016) *PLoS Pathog*. 12(8), e1005841.]. As stated above, the results were used to refine our PAR-CLIP results. In addition to host proteins, we also detected 8 of the 10 viral proteins. NS5 itself was represented by 81 unique peptides, covering greater than 70% of its amino acid sequence. The viral helicase/protease NS3, a known NS5 interactor, was seen via 25 unique peptides. Given capsid's small size (114 aa), it was somewhat surprising to find 3 unique associated peptides.

Table 2. Summary of two rounds of vRNA interactome via PAR-CLIP, and a single round of NS5 interactome.

2 nd PAR-CLIP			Shared with 1 st PAR-CLIP	Functions	Not found in NS5 protein-protein interactome
M6PR	RPL21	VCP	HSPA5	ER, transport	M6PR
HSPA5	STAU1	HSP90B1	RPL18	Ribosome	YBX3
YBX3	RPS10	KATNAL2	PKM2	Glycolysis	U2AF2
RPL18	APOE	RPL13	HSP90AB1	Protein folding	POLDIP3
U2AF2	AMPD3	KRT1	RPL18A	Ribosome	CTSZ
SUGP2	DHX9	GFRA2	HSPA9	Ubiquitination	HNRPUL1
PKM2	CKAP4	TRAPPC12	DHX9	Splicing	ZNF574
RPLP0	RPS6	DDX23	CKAP4	ER, cell structure	H2AFV
HSP90AB1	SLTM	PSMD2	HNRPD	Splicing	PRKAG2
POLDIP3	HNRPD	RAB6A	RPL11	Ribosome	TARS
CTSZ	RPL11	RPLP2	HSPD1	Mitochondrial import	STAU1
RPS16	RPS8	MRPS23	HNRNPU	Splicing	RPS10
FBL	SCCPDH	RUVL2	PBXIP1	Transcription	APOE
HNRNPUL1	MMTAG2	TUBB	RPS14	Ribosome	AMPD3
RPS19	HSPD1	ACTG1	VCP	ER, Golgi	SLTM
RPL18A	RPS3A	KRT6B	HSP90B1	ER, protein folding	SCCPDH
ZNF574	RPL7A	POLR1D	PSMD2	Proteasome	MMTAG2
H2AFV	RPS3	HNRNPUL2	TUBB	Cell structure	ZYX
PRKAG2	HNRNPU	ATP5O			KALRN
RPL19	ZYX	MRPL12			SAFB
GAPDH	KALRN	NEFL			PBXIP1
SFRS3	SAFB				OTOP1
C11orf98	PBXIP1				VCP
HSPA9	OTOP1				KATNAL2
TARS	RPS14				GFRA2

Once we validated our PAR-CLIP procedure and obtained the first complete interactome map of DENV RNA in human cell, we further pursued if vRNA-interactions could be resolved in time-dependent manner, which is a truly challenging issue and there has not so far been reported. To do this, there is a need to

precisely quantitate the peptides after PAR-CLIP, and we decided to use the dimethyl labeling method here. Initial experiments required validation of light, medium, and heavy dimethyl labeling, as inefficient labeling in one condition vs. another could cause significant errors. Labeling efficiency was checked by simply injecting samples into the spectrometer immediately prior to mixing. Ideally, all peptides are labeled. Our actual results showed efficiencies greater than 99.0% in all cases. **Fig. 11** shows another indicator of labeling efficiency, a comparison of peptide counts in six different labeling conditions, which clearly shows (balanced) normal distribution centered around 0. We here have to note and acknowledge that these experiments required a great deal of optimization and were done with a tight collaboration with the Center of Excellence in Systems Biology, leading by Dr. Trairak Pisitkun, at Chulalongkorn University.

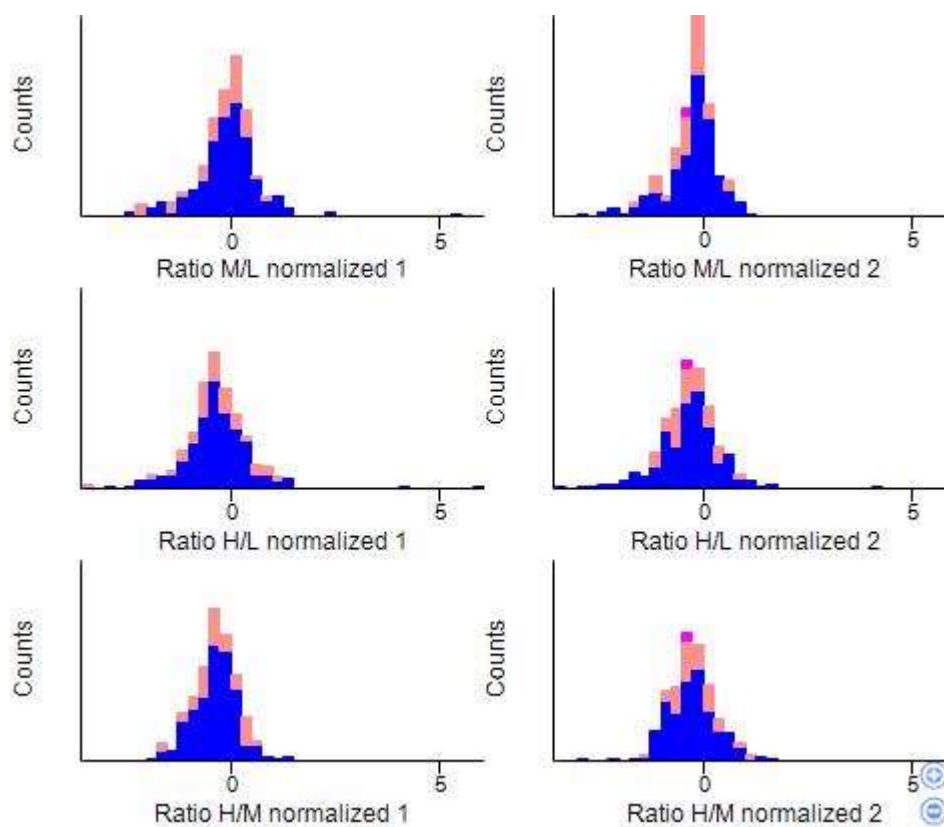


Figure 11. Comparison of light, medium, and heavy peptide counts shows no strong bias (which would be indicated by strong positive or negative skew) toward a particular labeling condition. “Normalized 1” and “normalized 2” refer to the two “mixes” in the 30 and 60 minutes phospho-enrichment.

After several months of optimization of the dimethyl labeling procedure, once established, we decided to utilize this technique for further investigation of different aspects of human-DENV interactions as well. We asked if DENV infection might cause a change in post-transcriptional modification (PTM), in particular “*phosphoproteome*”, of host proteome. Given the fact that no such studies have been performed with DENV, we chose to take advantage of this opportunity.

We infected HuH-7 cells with DENV-2 and collected the cell fractions at two early time points of 30 and 60 mins, and at a late time point of 48 hr after infection. Experimental details in enrichment of

phosphopeptide is described in **Methods** above. Following generation of m/z data (.raw files), MS1 data was examined. Typical output, consisting of fraction 6 from the 48 hr experiment, is shown in **Fig. 12**. A high density of peaks, as well as an even spread of LC-eluted peptides, is considered desirable; in cases where few peaks are seen at initial or late time points, the results suggest an alteration of LC gradient in order to capture more peptides over a “run”.

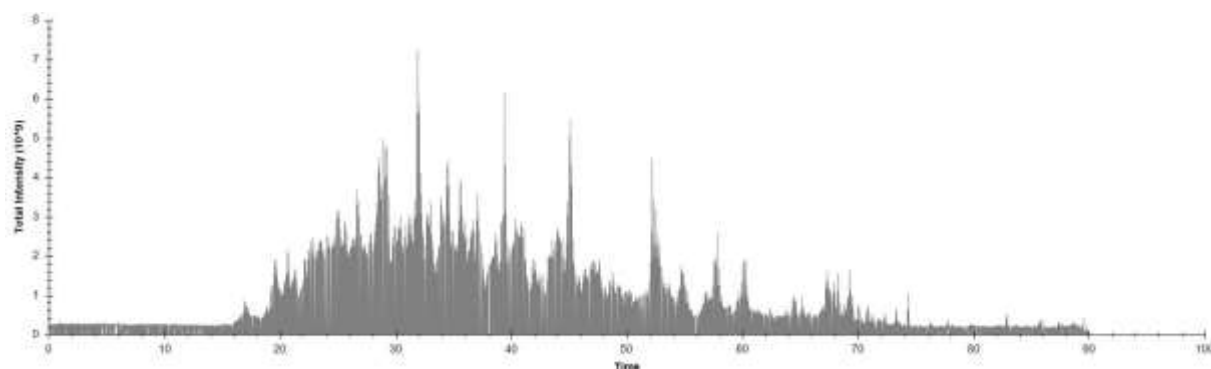


Figure 12. Typical MS1 spectra, chosen from fraction 6 from the no-enrichment condition of the 48 hr experiment (mock vs. infection). The horizontal axis shows retention time in minutes, while the vertical axis shows intensity of samples chosen for MS2 analysis.

Data was further processed at the spreadsheet level (Perseus software). A great many manipulations are possible, with the primary task being the elimination of low-quality data. In the early-phosphorylation studies, a total of 8,341 phosphopeptides (not necessarily unique) were identified at various confidence levels, against a total of 14,031 peptides (59% phosphopeptides) from 2,012 proteins. The most rigorous, final filtration resulted in 124 phosphopeptides that could be identified at high intensity in light, medium, and heavy conditions in all experiments. Obviously, this extreme level of stringency is not necessarily desirable, as DENV proteins would not be identified, since the medium condition would not contain any virus, and any other peptides absent in a particular condition would also be excluded.

Surprisingly, peptides corresponding to DENV proteins could be identified at the 30 min time point. In theory, dengue proteins in the supernatant used to infect cells would be limited to capsid, membrane, and envelope. Though not impossible, we believe it unlikely that other dengue proteins from lysed cells were present in the supernatant at levels detectable by MS, particularly since we washed cells 3x with PBS prior to lysis. Note also that capsid and envelope were not detected at all in our work; these proteins, along with membrane, would be expected to be the dominant viral proteins in the supernatant. Nevertheless, future MS experiments can be conducted on the supernatant to test for levels of viral proteins. **Table 3** details all dengue peptides found in our experiments.

Table 3. All dengue peptides identified at 30 min, 60 min, and 48 hours after infection. In the three cases where phosphosites are seen, an asterisk shows the phosphorylated residue (all serine in this case), with likely kinases shown in the far-right column (identified via biocuckoo.org).

Sequences	Locations	IDs	Experiments	Possible kinases (http://gps.biocuckoo.org)
DFVEGVSGGSWVDIVLEHGSCVTTMAK	M	3,1	60 min, 48 h	
CPTQGEPSLNEEQDKR	M	1	48 h	
AWNSLEVEDYGFVFTTNWLK	NS1	1	48 h	
SVTRLENLMWK	NS1	1	48 h	
NENDQYIYMGEPLENDEDCAHWK	NS3	5	60 min	
RGDLPVWLAYR	NS3	1	48 h	
SGAYVSAIAQTEK	NS3	2	48 h	
SIEDNPEIEDDIFRK	NS3	2	48 h	
SWNSGHEWVTDFK GK	NS3	1	48 h	
GETDHHAVSRG S *AK	NS5 (MT)	2	60 min	bark1, rock, vrk2, prkcb
LNALGKSEFQIYKK	NS5 (MT)	1	48 h	
YKKATYEPDVLGSGTR	NS5 (MT)	1	48 h	
EDQWCG S *LIGLTSR	NS5 (RdRp)	1	30 min	bark1, rock, prkca, grk, vrk2
EN S *LSGVEGEGLHK	NS5 (RdRp)	1,1	30 min, 60 min	plk2, vrk2, ck1, bark1, prkca
DVSKKEGGAMYADDTAGWDTR	NS5 (RdRp)	3	48 h	
SLIGNEEYTDYMPMKR	NS5 (RdRp)	2	48 h	
VLVPCRNQDELIGR	NS5 (RdRp)	2	48 h	

DENV phosphopeptides were detected in three cases, all corresponding to NS5 serines. Oddly, none of these detections were at the 48 hr point. In two cases, phosphorylation events would appear to be capable of altering RNA binding to the polymerase, as the phosphosites are located in known RNA-binding regions. MS2 spectra from one of these cases is shown in **Fig. 13**. Such results point to the possibility of using kinase inhibitors in an experimental or clinical context to alter viral behavior. It should also be noted that, to our knowledge, these phosphosites have not previously been reported for NS5. Further experiments have the potential to generate a complete picture of NS5 phosphorylation at various time points and sub-cellular fractions.

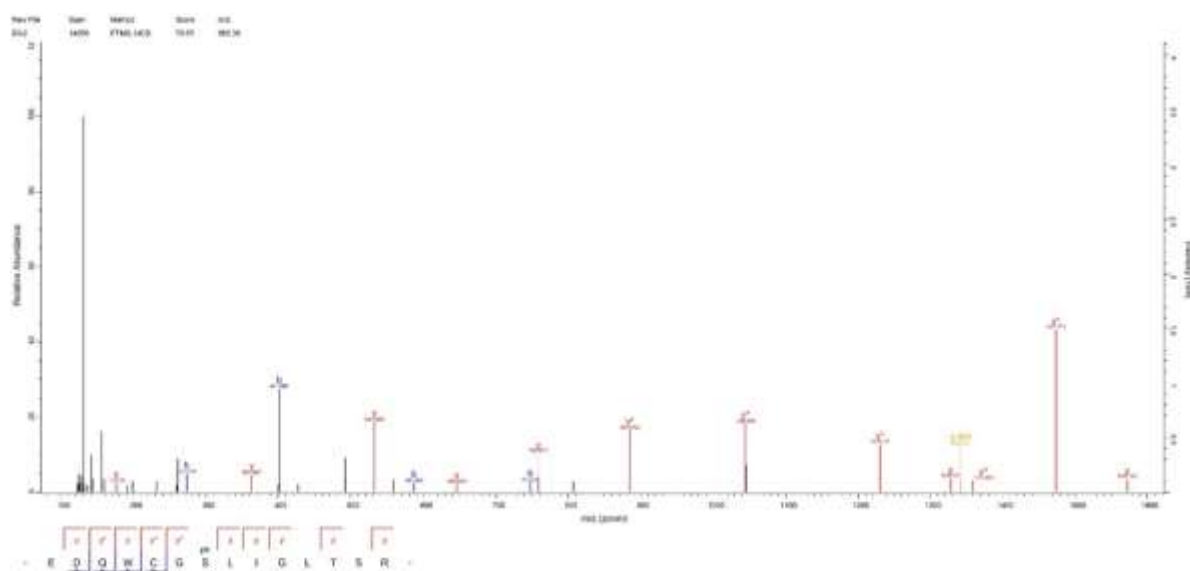


Figure 13. MS2 spectra of a phosphopeptide found in DENV NS5's C-terminal thumb domain. A top 10 list of peptides of interest is automatically selected for MS2 fragmentation following each electrospray event. Though not of high intensity, this peptide is of particular interest, as the phosphorylated serine lies in a region responsible for specific binding to dengue genomic RNA.

Examination of all up-phosphorylated peptides at the 30 and 60 min timepoints show a tendency toward motifs for casein kinase (CSK1), β -adrenergic receptor kinase (BARK1), G protein-coupled receptor kinase 1 (GRK1), as well as GSK-3, ERK1, ERK2 and CDK5 phosphorylation. Phosphorylation events with $|\log_2|$ differentials greater than 2 are shown in **Table 4**. Regardless of phosphorylation status, regulation of protein levels can also be monitored via MS. No alterations would be expected at early time points (though we will perform such an analysis following necessary repeat studies, looking for possible surprises). **Table 5** details such up/down-regulated proteins. Enrichment analysis of the entirety of these results showed a tendency toward alteration in levels of enzymes responsible for post-translational modification ($p = 10^{-5}$).

Table 4. Host proteins showing differential phosphorylation. Care must be taken in interpreting protein-level results, as a particular protein may be simultaneously up-phosphorylated and down-phosphorylated in different

Up-phosphorylated at 30 min	Down-phosphorylated at 30 min	Up-phosphorylated at 60 min	Down-phosphorylated at 60 min	Up-phosphorylated at 48 hours	Down-phosphorylated at 48 hours
CSTF3	EIF3F	CSTF3	TELO2	PURB	TOP2A
KIAA1143		BAZ1B	RB1	NOLC1	HIST1H1B
HNRNPN		SEPT9	EIF3F	DYNC1LI1	UBE2E1
SEPT9		KIAA1211	LMNB1		DAP
PLEC			MTFR1L		RTN4
SPEN					SCFD1
SH2D4A					HMGA2
RHBDF2					PTMAP7
IWS1					

regions.

Table 5. Host proteins showing evidence of differential regulation 48 hpi. Taken as a whole, a trend toward proteins involved in post-translational modification is seen ($p = 10^{-5}$, DAVID).

Up-regulated at 48 hrs	Down-regulated at 48 hrs
PPA1	ACAT2
C19orf60	RPS21
KRT18	COX6B1
KRT8	ACTG1
PGM2	C12orf57
TTC30A	CCDC85C
ACTB	DDX47
PTGES3	CWC15
HSPA5	PPP1CC
H3F3C	SYF2
TAGLN	NUBP2
STX7	ARFIP2
HIST2H2BF	SUPT4H1
CKB	CNN3
PPIA	PRSS23
SAFB	PSME3
HSPH1	TMSB10
RPS17	PKM2
HIST1H4H	FAM107B
CLIC1	NAPA
HIST2H2BF	HIST1H1D
	C1D
	PRIM1
	DNAJB14

When we searched the preceding NS5 interactome MS results for NS5 post-translational modifications in the absence of phospho-enrichment, no new phosphorylation sites were uncovered. However, two new hydroxyproline sites were uncovered, as well as a previously undescribed glutathionylation site. The spectra for this site is shown below (Fig. 14).

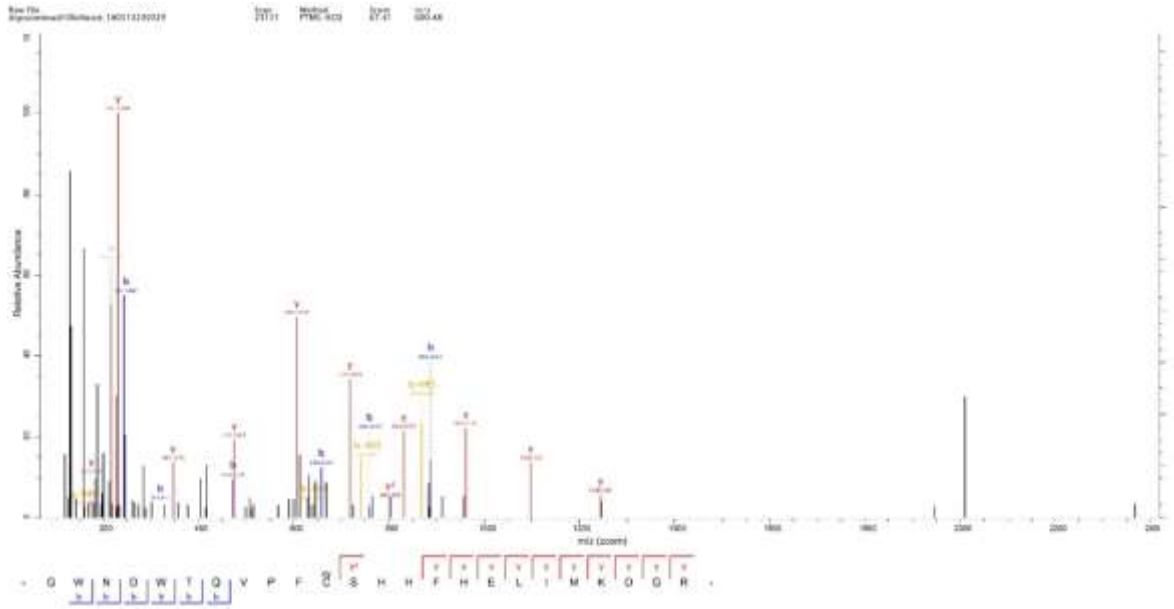


Figure 14. MS2 spectra of a new glutathionylation site found in DENV NS5.

As described above, we have established solid protocols for using the dimethyl labeling and MS analysis to map global host–DENV interactions in many aspects. Though, to this end, we decided to perform deep molecular characterization of DENV RNA interactors to investigate those protein functions in the viral life cycle. According to our PAR-CLIP results in **Table 1**, we paid attention to the GO of helicases ($p = 5.5 \times 10^{-5}$) and asked if human helicase would have important roles in DENV replication in human cells. We utilized Y3H assay as previously describes in our work [5] to screen for RNA elements in DENV genome which interacts with human helicases of interest found in our PAR-CLIP including EF1A, La, PTBP, PABP, DDX6, PCBP1, TUBB4B, ENOA, HSP1, CCT6A, LSM12, DDX19, ATP5A1, DHH1, DDX3, DDX5, DDX10, DDX18, DDX23, DDX28, DDX42, DDX43, DDX52, DDX53, DDX54, DDX56, and EIF4A3. We found the strongest interaction pair being human DDX6 and a 180-nt sequence represented two tandem dumbbell structures, termed A2 and A3, in the DENV 3′-UTR. In order to map the minimal RNA sequences and/or structures required for the DDX6 interaction, we continued to employ Y3H to dissect the DDX6 interaction with a series of A2-A3 RNA variants. The Y3H interaction strength was quantitated using the β -galactosidase assay, which has been demonstrated to correlate with apparent K_d values. None of the A2-A3 variants examined outperformed the wild type A2-A3 construct (**Fig. 15**). A2 alone bound poorly to DDX6, indicating that A3 is a prerequisite for robust DDX6 interaction. Joining A3 in tandem proportionally increased the interaction strength but the difference between duplicated (A3-A3) and triplicated A3 (A3-A3-A3) was moderate (~20%). Reversing the order of the dumbbells (A3-A2) showed comparable binding strength to that of A3-A3, with an approximately 50% drop in signal from the wild type A2-A3. The complementary sequence of A2-A3, (–) A2-A3, showed no affinity with DDX6, and yeast DDX6 homologue, DHH1, showed only subtle binding signals against A2-A3. These data demonstrated that A3 is the predominant binding site for human DDX6, and implied that A2 might have been added during viral evolution to facilitate binding of DDX6 to A3.

We found that minor alterations in stem length, loop purine content, and size of the 3' hairpin of A3 abolished the interaction with DDX6 (M6-M11 in **Fig. 15A**), having more profound influence on the binding than 5' HP1 alterations (M1 and M2) (**Fig. 15B**). Moreover, the middle bulges in A3 were also indispensable (M4 and M5), suggesting that the interaction should not be characterized as canonical, whereby an RNA-binding protein (RBP) recognizes a specific 4-10 nt sequence. Given that A2 and A3 share 67% sequence similarity, it is obscure how DDX6 discriminates these two RNAs, and how A2 enhanced the DDX6-A3 interaction to a level beyond that of a doubled A3-A3 sequence.

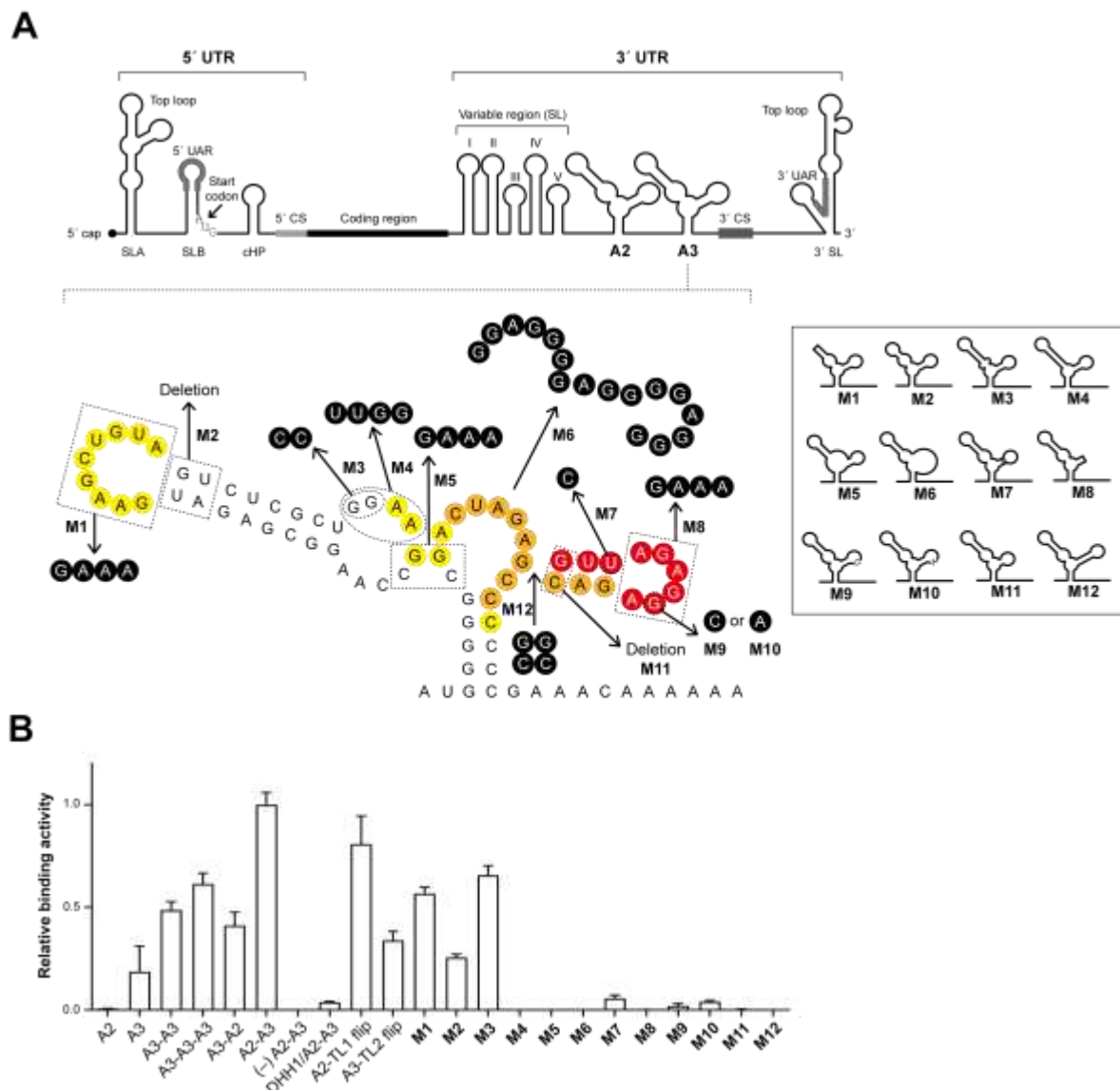


Figure 15. (A) The extent of conservation of elements within the flaviviral A3 element was determined and displayed as color codes depending on sequence similarity. Yellow, orange and red represent perfect conservation in dengue viruses, strong conservation in all mosquito-borne flaviviruses, and conservation that extends into some tick-borne and NKV flaviviruses, respectively. 11 A3 mutations were introduced individually as follows: M1) replacement of the HP1 loop with GAAA, M2) HP1 stem shortening by removal of two initial base pairs, M3) alteration of bulge 1 by replacing GG with CC, M4) HP1 stem extension by replacing GGAA with UUGG, M5) formation of a single large bulge by destroying GG:CC interactions between bulge 1 and 2

with GAAA, M6) substitution of predicted strong G-quadruplex, M7) strengthening the HP2 stem by replacing U with C, M8) HP2 GNRA formation by replacing the HP2 loop with GAAA, M9-M10) substitution of G with either C or A, M11) HP2 stem shortening by removing the GC pair, M12) HP2 stem extension through addition of two GC base pairs. Their possible secondary structures are demonstrated and indicated as M1-M11 on the right panel. **(B)** Specific interactions between DDX6 and minimal RNA sequences were quantified by utilizing β -galactosidase assays. RNA constructs are shown with the following abbreviations: A2 and A3 represent A2 and A3 elements; A3-A3 and A3-A3-A3 represent duplicated and triplicated A3 tandems; A3-A2 and A2-A3 represent reverse and common orders of A2 and A3; (-) A2-A3 represents the negative strand of the A2-A3 element; Dhh1/A2-A3 represents the interaction strength of *S. cerevisiae* DDX6 ortholog DHH1 with the A2-A3 element; A2-TL1 and A3-TL2 flip represent reversed sequences of the TL1 and TL2 regions; A3-HP2-G4 represents a large substitution of HP2 with a sequence designed to form a strong G4 quadruplex; M1-M11 represents A3 variants. The interaction strength of DDX6 with A2-A3 is set to 1. Error bars represent SEM; n = 3.

Next, we also used Y3H to perform mutational analysis of DDX6 to identify residues involved in A3 interaction. In the aforementioned Y3H screen with 15 DDX helicases, which included the yeast DDX6 homolog of Dhh1, only DDX6 evinced specificity against the DENV RNA library. Therefore, we performed amino acid sequence comparison to seek out DDX6 residues that differ from all human RNA helicases tested (i.e. binder versus non-binder). This information was combined with a structural model of DDX6 in the RNA-bound complex form, based on the Vasa structure to select candidate residues for mutagenesis in Y3H (**Fig. 16**). The assays showed that all mutants lowered Y3H signals with A2-A3 to some extent, with K307A and a double K367A/R369A mutant evincing the most dramatic drops (65% and 90%, respectively) (**Fig. 16**). In addition, the deletion of 26 amino acid residues from the unstructured C-terminal extension specific to DDX6 severely impaired A2-A3 binding. These data suggested that bound A2-A3 occupies an extensive interaction surface in the C-terminal domain of DDX, and DENV A3 exclusively recruits DDX6 via interactions with DDX6-unique basic residues.

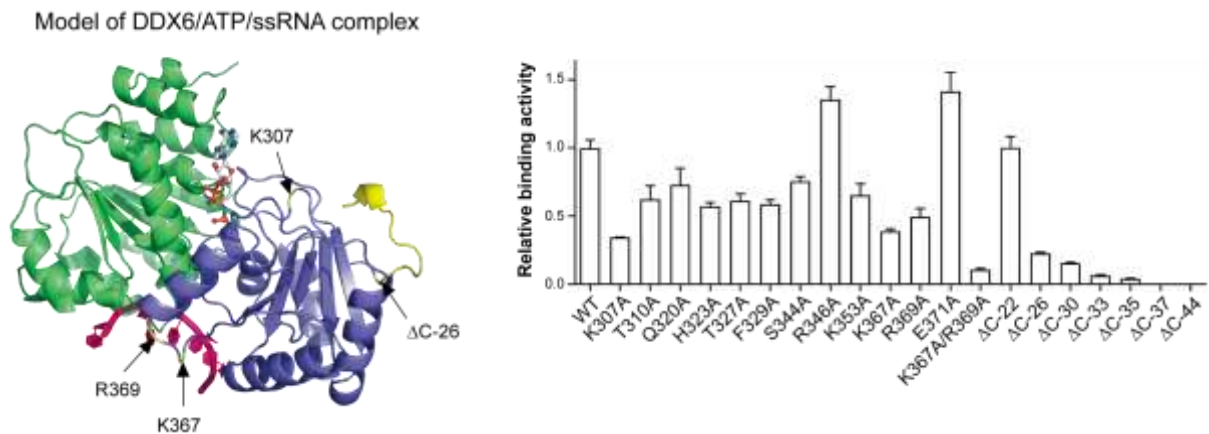


Figure 16. (A) Locations of K307, K367, and R369 residues on a homology model of DDX6 (PDB code: 4CT5) superposed with three-dimensional structure of *D. melanogaster* DEAD-box protein vasa, with RNA substrate and ATP analog (PDB code: 2DB3). Green color indicates N-terminal domain; blue color indicates C-terminal domain; Red color indicates RNA substrate. (B) Specific interactions between A2-A3 element and various DDX6 mutants were strongly quantified by utilizing β -galactosidase assays. Unit of interaction strength with wild-type DDX6 was set to 1. Error bars represent SEM; n = 3.

To enhance our technological platforms for analysis of protein–RNA interaction, we introduced here a new approach to use a new MS pipeline with protein–RNA crosslinking to pinpoint the interfaces of RNA-binding proteins. We applied the system with a human RNA helicase DDX6, which was known to have a strong and specific interaction with a 180 nt sequence in DENV’s 3′-UTR known as “A2A3”, of which the sequence and structure is strongly conserved in mosquito-borne flaviviruses, in our own work, as well as that of others [Ward AM et al., Quantitative mass spectrometry of DENV-2 RNA-interacting proteins reveals that the DEAD-box RNA helicase DDX6 binds the DB1 and DB2 3′ UTR structures. (2011) *RNA Biol.* 8(6), 1173-86.]. **Table 6** reveals the most confident DDX6–A2A3 RNA interactions, and **Fig. 17** places these peptides on the DDX6 crystal structure. While the initial experiment gave interesting results, more important are the lessons learned, allowing us to optimize for future experiments. In particular, we note that considerably more identifications were obtained in the high RNase condition. A high percentage of identified peptides showed missed trypsin cleavage sites, indicating that trypsin levels could be increased during MS prep. We also intend to increase the RNA/protein ratios (currently equimolar), allowing greater RNA occupancy of DDX6 binding sites. Note that the precise residues at which RNA is crosslinked are not indicated; such results may be obtained by manual examination of individual, high-quality spectra. We hope to identify 3 or 4 nt linkages (as opposed to 1 or 2, currently) via the aforementioned improvements, allowing us to specify not only linked peptides, but the linked nucleotides of interest. We believe impressive results are forthcoming, and that the basic methods could be expanded to study protein–RNA interactions from cell extracts in the future.

Table 6. Potential RNA modifications on DDX6, sorted by confidence.

RNA modification	Modified peptides
AA-H2O1-H1O3P1+C4H8O2S2	TLKLPPKDLR
UU-H2O1+H1O3P1	NLVCTDLFTR
A-H2O1-H1O3P1	TENPVIMGLSSQNGQLRGPVK(Carbamyl)PTGGPGGGGPQTQ QQMNQLK(Carbamyl)
U-H2O1-H1O3P1	TENPVIMGLSSQNGQLRGPVKPTGGPGGGGPQTQQMNQLK NTNTINNGTQQQAQSMTTTTIKPGDDWK
AG-H2O1-H1O3P1+C4H8O2S2	NRQILLYSATFPLSVQKFM(Oxidation)NAHLQKPYEINLM(Oxidati on)EELTLK(Carbamyl)
G-H1O3P1+C4H8O2S2	NRQILLYSATFPLSVQK
GU+C4H8O2S2	(Carbamyl)NLVCTDLFTR
G-H1O3P1+C4H8O2S2	NRQILLYSATFPLSVQK
C1H2N3O6	FM(Oxidation)NAHLQK(Carbamyl)PYEINLMEELTLK(Carbamyl) GVTQYYAYVTER
C-H2O1-H1O3P1	TENPVIMGLSSQNGQLRGPVKPTGGPGGGGPQTQQMNQLK NTNTINNGTQQQAQSMTTTTIKPGDDWK
C-H2O1-H1O3P1	TSDVTSTK(Carbamyl)GNEFEDYCLK(Carbamyl)
G+H1O3P1	FNLK(Carbamyl)SIEEQLGTEIK(Carbamyl)PIPSNIDK
U-H1O3P1+C4H8O2S2	FNLK(Carbamyl)SIEEQLGTEIK(Carbamyl)PIPSNIDK(Carbamyl)
CC-H2O1	KDNIQAMVIVPTRELALQVSQICIQVSK
C-H2O1	NRQILLYSATFPLSVQK
CC-H1O3P1	(Carbamyl)NLVCTDLFTRGIDIQAVNVVINFDFPK
CG-H1O3P1	NGTGKSGAYLIPLLR

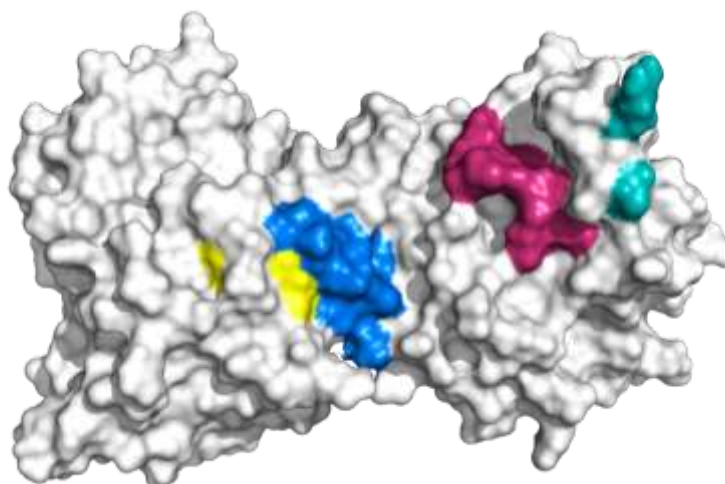


Figure 17. Potential DDX6–vRNA interaction sites identified by new CL-LC/MS/MS procedure. Blue indicates canonical helicase–RNA interaction sites, and yellow for the DEAD-box location. Highest confidence of MS results for interaction site is mapped on the protein surface as deep pink. Cyan reveals 2 amino acid mutations abolished RNA-binding activity of DDX6 in our Y3H results.

Altogether, in this work, we established several experimental procedures such as labeling MS analysis, modified PAR-CLIP, Y3H, and MS analysis of RNP interface. We employed these technologies to investigate host–DENV interaction at different times post infection. We unveiled the interactome map of DENV RNA with human factors, and of those, we demonstrated that DDX6 recognizes the 3′ hairpin in the A3 element in the 3′-UTR of the DENV genome by the DDX6-specific residues in its C-terminal RecA domain for the first time. We also showed that host proteins undergo significantly differential phosphorylation upon DENV infection. Moreover, we identified novel serine phosphosites at the early stage of infection, and one uncharacterized glutathionylation site in DENV NS5. These differential post-translational modifications in NS5 and host proteins await further study of molecular functions in viral life cycle.

Output ที่ได้จากโครงการ

In this study, we have developed various new experimental procedures and obtained a number of significant results. Most importantly, we revealed an interactome map of DENV RNA in human HuH-7 cells using etDENV, and characterized an interaction of DDX6 with DENV RNA. Our system completely mimic environment in human tissue than other studies that use exogeneous expression of viral proteins. We would like to summarize our output from the project as follows.

Technology developed or established in the project

1. Engineered, tagged dengue virus (etDENV): Infectious DENV possessing His–FLAG tag inside NS5 gene.
2. Modified Photoactivatable-Ribonucleoside-Enhanced Crosslinking and Immunoprecipitation (PAR-CLIP) that allows two-dimensional omics analysis.

3. Dimethyl labeling/LC/MS/MS
4. Quantitative phosphoproteomic analysis
5. MS analysis of RNP interface
6. Yeast three-hybrid (Y3H) screen of the viral RNA genome

Novel knowledge

1. DENV RNA interacts with at least four distinct machinery of RNA processing, ribosome, chaperones, and MCM complexes in infected hepatic cells.
2. Human DDX6 RNA helicase specifically binds a short hairpin in the A3 RNA element in the 3'-UTR of the dengue genome through its C-terminal RecA domain.
3. In DENV NS5, three serine residues are phosphorylated and one cysteine accepts S-glutathionylation in infected cells.
4. Host phosphoproteome is differentially altered at different stages of infection.

Education

Three M.Sc. students

1. Mr. Jakkrit Jantiya (will have the defense exam in July 2020)
2. Miss Lakkana Thaveepornkul (will have the defense exam in July 2020)
3. Mr. Veerakorn Narkthong (passed the defense exam on December 12, 2019)

Two Ph.D. students

1. Mr. Opas Choksupmanee (passed the defense exam on April 29, 2020)
2. Mr. Chairat Tunghirun (passed the defense exam on April 29, 2020)

Publications

1. Choksupmanee O., Tangkijthavorn W., Hodge K., Narkthong V., Phornsiricharoenphant W., Tulakarnwong S., Ngamphiw C., Tongsimma S., **Chimnarong S.** (2020) Sequestration of DDX6 by an RNA hairpin in the 3'-UTR of the dengue genome mediates cell cycle arrest and pathogenicity. Submitted.
2. Tunghirun C., Narkthong V., Chaicumpa W., **Chimnarong S.** (2020) Interference of dengue replication by blocking the access of 3' SL RNA to the viral RNA-dependent RNA polymerase. Submitted.
3. Hodge K., Kamkaew M., Pisitkun T., **Chimnarong S.** (2019) Flavors of flaviviral RNA structure: towards an integrated view of RNA function from translation through encapsidation. *Bioessays*. 41(8), e1900003.

Other activities

1. Proceedings
 - 1.1. Chokesaksrikul C. and **Chimnarong S.** (2019) Visualization of viral replication process via fluorescent dengue RNA. Oral presentation and proceeding at the 7th Burapha University International Conference on Interdisciplinary Research, Bangsaen Heritage Hotel, Chonburi, Thailand on November 27-29, 2019.
 - 1.2. Narkthong V., Promptmas C, **Chimnarong S.** (2019) Correlation of dengue severity with cell cycle alteration. Oral presentation and proceeding at the 7th Burapha University International

Conference on Interdisciplinary Research, Bangsaen Heritage Hotel, Chonburi, Thailand on November 27-29, 2019. Best Paper Award.

- 1.3. Jantiya J., Punyahathaikul S., Hodge K., Pisitkun T., and **Chimnarong S.** (2019) Identification of human poly(A)-binding proteins as dengue NS5 interactors in infected cell. Poster presentation and proceeding at the 14th International Symposium for the Protein Society of Thailand (PST), Maruay Garden Hotel, Bangkok, Thailand on July 22-23, 2019.
 - 1.4. Thaveepornkul L., Krittanai C., Puthavathana P., and **Chimnarong S.** (2019) In silico screening of inhibitor specific to dengue non-structural protein 5. Poster presentation and proceeding at the 14th International Symposium for the Protein Society of Thailand (PST), Maruay Garden Hotel, Bangkok, Thailand on July 22-23, 2019.
 - 1.5. Jantiya J., Hodge K., Pisitkun T., and **Chimnarong S.** (2018) Investigation of host–dengue virus interaction via proteomics. Poster presentation and proceeding at the 13th International Symposium for the Protein Society of Thailand (PST), Chulabhorn Conference Center, Bangkok, Thailand on August 7-9, 2018.
2. Oral presentation
- 2.1 Title: “Development of new anti-flaviviral drug by targeting RNA interaction interfaces in viral RNA-dependent RNA polymerase” at the PerkinElmer Seminar Therapeutic discovery: Trends, future & beyond, Room 101, SIMR Building, Faculty of Medicine Siriraj Hospital, Mahidol University on November 21st, 2019.
 - 2.2 Title: “Host–viral RNA interaction may contribute to dengue severity” at the 18th TRF-OHEC Annual Congress (TOAC2019) (นักวิจัยรุ่นใหม่ พบ เมธีวิจัยอาวุโสสกว.), The Regent Chaam Beach Resort, Petchburi on January 10, 2019.
 - 2.3 Title: “Inhibition of promoter-binding site in flaviviral RNA-dependent RNA polymerase” at the 13th International Symposium for the Protein Society of Thailand (PST), Chulabhorn Conference Center, Bangkok, Thailand on August 7-9, 2018.
 - 2.4 Title: “Specific interaction between human DDX6 RNA helicase and the dengue viral RNA genome” at the 5th Asia Pacific Protein Association (APPA) Conference and the 12th International Symposium for the Protein Society of Thailand (PST), The Tide Resort, Bangsaen, Chonburi, Thailand on August 11-14, 2017.

ภาคผนวก



Dear Dr. Chimnaronk,

On April 23, 2020, we received the manuscript "Sequestration of DDX6 by an RNA Hairpin in the 3'-UTR of the Dengue Genome Mediates Cell Cycle Arrest and Pathogenicity" by Opas Choksupmanee, Worapol Tangkijthavorn, Kenneth Hodge, Veerakorn Narkthong, Worawich Phornsirichaoenphanth, Sarun Tulakarnwong, Chumpol Ngamphiw, Sissades Tongsimma, and Sarin Chimnaronk. The submission form indicates that this paper should be processed as a(n) Full-Length Text intended for publication in the section Virus-Cell Interactions.

The manuscript has been assigned the control number JVI00727-20. Take note of this number, and refer to it in any correspondence with the Journals Department or with the editor.

You can check the status of this manuscript by clicking on the link below and selecting Check Status:

<https://jvi.msubmit.net/cgi-bin/main.plex?el=A1GO1BdXZ4A6CPRz6F5A9ftdI2M64gW7qzMxgW7XPZOz7wZ>

Conflicts of Interest: All authors must disclose any commercial affiliations as well as consultancies, stock or equity interests, and patent-licensing arrangements that could be considered to pose a conflict of interest regarding the submitted manuscript. All funding sources for the project, institutional and corporate, and any potentially conflicting interests, such as relationships that might detract from an author's objectivity in presentation of study results, must be acknowledged, both in the Acknowledgments section and on this form. The corresponding author must review this policy with all coauthors.

The author submitting the manuscript must state in the submission form whether or not any of the authors has a conflict of interest. Here is how Dr. Chimnaronk responded:

Conflict of Interest: No conflict of interest.

If you have a conflict of interest that is not disclosed here, please notify the journal staff immediately at jnachman@asmusa.org

To find contact information for the editor handling your manuscript, go to the following URL:

http://www.asm.org/components/com_php/files/editors.php

Editorial Policy: In submitting your manuscript to JVI, the author(s) guarantees that a manuscript with substantially the same content has not been submitted or published elsewhere and that all of the authors are aware of and agree to the submission.

By publishing in the journal, the authors agree that any DNAs, viruses, microbial strains, mutant animal strains, cell lines, antibodies, and similar materials newly described in the article are available from a national collection or will be made available in a timely fashion, at reasonable cost, and in limited quantities to members of the scientific community for noncommercial purposes. The authors guarantee that they have the authority to comply with this policy either directly or by means of material transfer agreements through the owner.

Similarly, the authors agree to make available computer programs, originating in the authors' laboratory, that are the only means of confirming the conclusions reported in the article but that are not available commercially. The program(s) and suitable documentation regarding its (their) use may be provided by any of the following means: (i) as a program transmitted via the Internet, (ii) as an Internet server-based tool, or (iii) as a compiled or assembled form on a suitable medium (e.g., magnetic or optical). It is expected that the material will be provided in a timely fashion and at reasonable cost to members of the scientific community for noncommercial purposes. The authors guarantee that they have the authority to comply with this policy either directly or by means of material transfer agreements through the owner.

If your manuscript is accepted for publication, you will be contacted separately about payment when the proofs are issued; please follow the instructions in that e-mail. Arrangements for payment must be made before your article is published. For a complete list of **Publication Fees**, including supplemental material costs, please visit our [website](#).

Corresponding authors may [join or renew ASM membership](#) to obtain discounts on publication fees. Need to upgrade your membership level? Please contact Customer Service at Service@asmusa.org.

Prepublication Online Posting: For its primary-research journals, ASM posts online PDF versions of manuscripts that have been peer reviewed and accepted but not yet copyedited. This feature is called "JVI Accepts" and is accessible from the Journals website. The manuscripts are published online as soon as possible after acceptance, on a weekly basis, before the copyedited, typeset versions are published. They are posted "As Is" (i.e., as submitted by the authors at the modification stage), and corrections/changes are NOT accepted. Accordingly, there may be differences between the JVI Accepts version and the final, typeset version. The manuscripts remain listed on the JVI Accepts page until the final, typeset versions are published, at which point they are removed from the JVI Accepts page. Any supplemental material intended, and accepted, for publication is not posted until publication of the final, typeset article.

CRedit: Submitting authors can optionally assign CRedit roles within the manuscript submission system at the time of submission. **If CRedit roles have been assigned within the system, those roles are listed for all authors at the end of this message.** The roles will be present only in the XML of the manuscript if it is accepted and published.

Thank you for submitting your work to Journal of Virology.

Sequestration of DDX6 by an RNA Hairpin in the 3'-UTR of the Dengue Genome Mediates Cell Cycle Arrest and Pathogenicity

*Opas Choksupmanee^{1‡}, Worapol Tangkijthavorn^{1,2‡}, Kenneth Hodge^{3‡}, Veerakorn Narkthong²,
Worawich Phornsiricharoenphant⁴, Sarun Tulakarnwong², Chumpol Ngamphiw⁴, Sissades
Tongsima⁴, and Sarin Chimnaronk^{1,2*}*

¹ The Laboratory of RNA Biology, Institute of Molecular Biosciences, Mahidol University, Salaya Campus, Nakhon Pathom, Thailand,

² Siriraj Center of Research Excellence for Systems Pharmacology, Faculty of Medicine, Siriraj Hospital, Mahidol University, Bangkok, Thailand,

³ the Systems Biology Center, Research Affairs, Faculty of Medicine, Chulalongkorn University, 1873 Rama 4 Road, Pathumwan, Bangkok, Thailand,

⁴ National Biobank of Thailand, National Center for Genetic Engineering and Biotechnology, National Science and Technology Development Agency, Thailand Science Park, Pahonyothin Road, Khlong 1, Khlong Luang, Pathum Thani, Thailand.

[‡] These authors contributed equally to this work.

*Corresponding author.

E-mail: sarin.chi@mahidol.ac.th.

Running Title: Characterization of interaction between dengue viral RNA and DDX6 helicase.

Keywords: dengue virus (DENV), viral RNA, untranslated region (UTR), RNA helicase, host-virus interaction, cell cycle, pathogenesis.

Abstract

The extent to which viral genomic RNAs interact with host factors and contribute to host response and disease pathogenesis is not well known. Here, we report that the RNA helicase DDX6 specifically binds to the viral most conserved RNA hairpin in the dengue 3'-UTR, with nanomolar affinities. This interaction requires three conserved residues, Lys³⁰⁷, Lys³⁶⁷, and Arg³⁶⁹, as well as the unstructured extension in the C-terminal domain of DDX6. Interestingly, alanine substitution of these three basic residues resulted in RNA-independent ATPase activity, suggesting a mechanism by which RNA-binding and ATPase activities are coupled in DEAD-box helicases. Furthermore, we used a cross-omics gene enrichment approach to reveal that DDX6 is functionally related to cell cycle regulation and viral pathogenicity, and also demonstrated that DDX6 is sequestered by dengue A3 in infected cells, resulting in cell cycle arrest in G1 phase. Exogenous expression of DDX6 alleviated this effect, viral infection rate and down-regulation of extracellular matrix genes. Disruption of the DDX6-binding site was found in dengue and Zika live-attenuated vaccine strains. Our results suggested that dengue virus has evolved an RNA aptamer against DDX6 to alter host cell states, and conceivably defined DDX6 as a new therapeutic target for prevention of dengue pathogenesis.

Importance

Dengue virus (DENV) is transmitted by mosquitoes to human, infecting 390 million individuals per year globally. About 20% of infected patients shows a spectrum of clinical manifestation, ranging from a mild flu-like syndrome, dengue fever (DF), to life-threatening severe dengue (SD) diseases including dengue haemorrhagic fever (DHF) and dengue shock syndrome (DSS). There is currently no specific treatment for dengue diseases and the molecular mechanisms underlying dengue pathogenesis remain poorly understood. In this study, we combined biochemical, bioinformatics, and high-throughput sequencing approaches to pinpoint a highly conserved interface of the RNA genome of DENV with a human factor named DDX6 in infected cells. The significance of our research is in identifying the mechanism for viral pathogenesis by sequestration of human factor, which allows us to generate a model for live-attenuated dengue vaccine and the design of new therapeutic reagent for dengue diseases.

差出人: **Antiviral Research** EviseSupport@elsevier.com

件名: Successfully received: submission Interference of dengue replication by blocking the access of 3' SL RNA to the viral RNA-dependent RNA polymerase for Antiviral Research

日付: 2020年3月9日 19:18

宛先: sarin.chi@mahidol.ac.th

AR

This message was sent automatically.

Ref: AVR_2020_121

Title: Interference of dengue replication by blocking the access of 3' SL RNA to the viral RNA-dependent RNA polymerase

Journal: Antiviral Research

Dear Dr. Chimnaronk,

Thank you for submitting your manuscript for consideration for publication in Antiviral Research. Your submission was received in good order.

To track the status of your manuscript, please log into EVISE® at:

http://www.evise.com/evise/faces/pages/navigation/NavController.jspx?JRNL_ACR=AVR and locate your submission under the header 'My Submissions with Journal' on your 'My Author Tasks' view.

Thank you for submitting your work to this journal.

Kind regards,

Antiviral Research

Have questions or need assistance?

For further assistance, please visit our [Customer Support](#) site. Here you can search for solutions on a range of topics, find answers to frequently asked questions, and learn more about EVISE® via interactive tutorials. You can also talk 24/5 to our customer support team by phone and 24/7 by live chat and email.

Copyright © 2018 Elsevier B.V. | [Privacy Policy](#)

Elsevier B.V., Radarweg 29, 1043 NX Amsterdam, The Netherlands, Reg. No. 33156677.

Interference of dengue replication by blocking the access of 3' SL RNA to the viral RNA-dependent RNA polymerase

Chairat Tunghirun¹, Veerakorn Narkthong², Wanpen Chaicumpa³, and Sarin Chimnaronk^{1,2}*

¹The Laboratory of RNA Biology, Institute of Molecular Biosciences, Mahidol University, Salaya Campus, Nakhon Pathom 73170,

²Siriraj Center of Research Excellence for Systems Pharmacology, Faculty of Medicine, Siriraj Hospital, Mahidol University, Bangkok 10700,

³Center of Research Excellence on Therapeutic Proteins and Antibody Engineering, Department of Parasitology, Faculty of Medicine, Siriraj Hospital, Mahidol University, Bangkok 10700, Thailand.

Running title: The scFv antibodies that target the RNA-binding interface of dengue RdRp

Keywords: Dengue virus (DENV), viral non-structural protein (NS) 5, RNA-dependent RNA polymerase (RdRp), single-chain variable fragment (scFv), inhibition of viral replication.

Word count: 4,079 (excluding Figure Legends and References)

*To whom correspondence should be addressed. E-mail: sarin.chi@mahidol.ac.th; Tel: +66 2 441 9003 ext. 1383; Fax: +66 2 441 1013.

Abstract

The four circulating serotypes of dengue virus (DENV) occasionally cause potentially fatal symptoms of severe dengue, which there is currently no specific treatment available. Extensive efforts have been made to inhibit viral replication processes by impeding the activity of an exclusive RNA-dependent RNA polymerase (RdRp) in the viral non-structural protein 5 (NS5). In our earlier work, we identified the characteristic, specific interaction between the C-terminal thumb subdomain of RdRp and an apical loop in the 3' stem-loop (SL) element in the DENV RNA genome, which is fundamental for viral replication. Here, we demonstrated a new approach for interfering viral replication via blocking of 3' SL RNA binding to RdRp by the single-chain variable fragments (scFvs). We isolated and cloned 3 different human scFvs that bound to RdRp from DENV serotype 2 and interfered with 3' SL-binding, utilizing a combination of phage-display panning and Alpha methods. When tagged with a cell penetrating peptide, a selected scFv clone, 2E3, entered cells and colocalized with NS5 in cytoplasm of infected HuH-7 cells. 2E3 significantly inhibited DENV RNA replication with sub-nanomolar EC50 values and significantly reduced production of infectious particles. The molecular docking models suggested that 2E3 recognized both palm and thumb subdomains of RdRp, and interacted with Lys⁸⁴¹, a key residue involved in RNA binding. Our results provide a new potential therapeutic molecule specific for flaviviral infection.

Flavors of Flaviviral RNA Structure: towards an Integrated View of RNA Function from Translation through Encapsidation

Kenneth Hodge, Maliwan Kamkaew, Trairak Pisitkun,* and Sarin Chimnaronk*

For many viruses, RNA is the holder of genetic information and serves as the template for both replication and translation. While host and viral proteins play important roles in viral decision-making, the extent to which viral RNA (vRNA) actively participates in translation and replication might be surprising. Here, the focus is on flaviviruses, which include common human scourges such as dengue, West Nile, and Zika viruses, from an RNA-centric viewpoint. In reviewing more recent findings, an attempt is made to fill knowledge gaps and revisit some canonical views of vRNA structures involved in replication. In particular, alternative views are offered on the nature of the flaviviral promoter and genome cyclization, and the feasibility of refining in vitro-derived models with modern RNA probing and sequencing methods is pointed out. By tracing vRNA structures from translation through encapsidation, a dynamic molecule closely involved in the self-regulation of viral replication is revealed.

1. Introduction


Flaviviruses include many of the most prevalent viral scourges known to humanity, such as dengue virus (DENV), West Nile virus (WNV), Zika virus (ZIKV), yellow fever virus (YFV), Japanese encephalitis virus (JEV), St. Louis encephalitis (SLEV), and Murray Valley encephalitis (MVE): a total of 53 species are listed by the International Committee on Taxonomy of Viruses as of 2017.^[1] These viruses contain an approximately 11 000 nt positive-strand RNA genome (Baltimore Group IV) comprising a 5'-untranslated region (UTR) of approximately 100

nucleotides (nt), a single open reading frame, and a 3'-UTR of roughly 500 nt. The genome is initially translated into a single polypeptide with ≈3400 amino acids, which is subsequently proteolytically processed into ten viral proteins.^[2] DENV alone accounts for nearly 400 million infections^[3] and 500 000 hospitalizations per year worldwide.^[4] It is expected that factors such as global warming and urbanization will promote flaviviral infections in a manner outpacing population growth, largely due to enhanced opportunities for the proliferation of the most common flavivirus vectors, mosquitos, and ticks.^[5,6] Much work is still needed to gain a comprehensive view of the flavivirus life cycle in order to develop effective treatments against these infections. In this review, we focus primarily on the flavivirus genus, although we do not hesitate to fill knowledge gaps with work involving the broader *Flaviviridae* family, which includes the hepatitis C virus (HCV) and the bovine diarrhoea virus (BVDV), as well as work from other genera such as *Picornaviridae*.

The current model of the flaviviral RNA life cycle is illustrated in **Figure 1**. The encapsidated RNA genome exists solely as a positive single strand.^[7] Upon internalization, fusion of the virus membrane with the host endosomal membrane allows the release of genomic RNA into the cytoplasm. This RNA serves as the template for translation by the host ribosome at the rough endoplasmic reticulum (ER) to produce the viral nonstructural protein 5 (NS5) possessing RNA-dependent RNA polymerase (RdRp) activity. The combination of viral nonstructural (NS) proteins that interact to amplify viral RNA (vRNA) is known as the “replicase” complex, which is localized in membranous vesicles derived from the ER.^[8] The negative strand is then synthesized by NS5 and is found only in association with the positive strand. This double-stranded form of vRNA (dsRNA) serves as a template for the production of an excess of positive-strand RNA, which may be utilized for further translation, generation of another round of negative strands, or packaged into the maturing virion. vRNA is thus found in dsRNA and (+) single-stranded RNA (ssRNA) forms, as well as a more heterogeneous form associated with (+) ssRNA strands emerging from dsRNA.

Dr. K. Hodge, Dr. T. Pisitkun
 The Systems Biology Center, Research Affairs, Faculty of Medicine
 Chulalongkorn University
 1873 Rama 4 Road, Pathumwan
 Bangkok 10330, Thailand
 E-mail: pisitkut@nhlbi.nih.gov

M. Kamkaew, Dr. S. Chimnaronk
 Laboratory of RNA Biology, Institute of Molecular Biosciences
 Mahidol University
 Salaya Campus
 Nakhon Pathom 73170, Thailand
 E-mail: sarin.chi@mahidol.ac.th

 The ORCID identification number(s) for the author(s) of this article can be found under <https://doi.org/10.1002/bies.201900003>.

DOI: 10.1002/bies.201900003

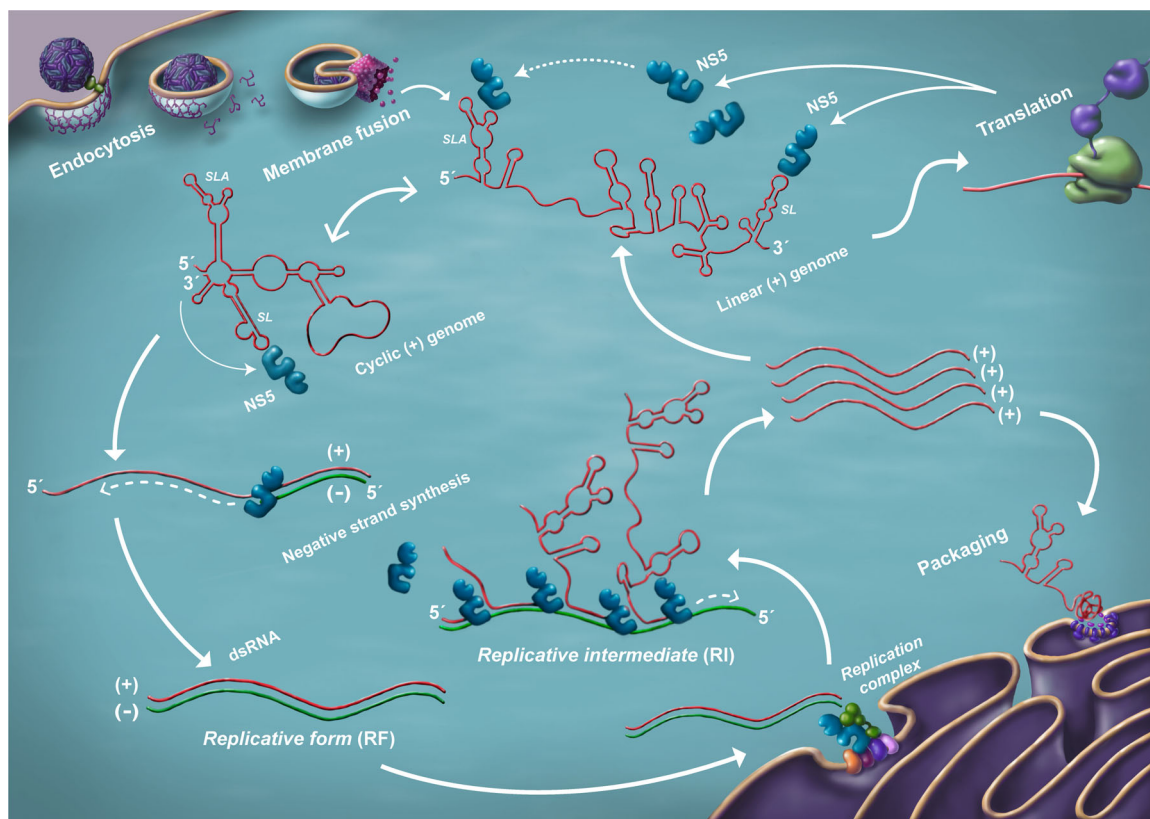


Figure 1. A model of the flaviviral RNA life cycle. Following RNA release into the cytoplasm, as well as translation and viral polyprotein processing, the vRNA cycle begins. The process is thought to occur primarily within or near the ER. Upon accumulation of sufficient replicase complex components, the (+) strand genome switches to a predominantly cyclized form, emphasizing (–) strand generation. The RF and RI are shown. Note that the (–) strand is only seen in a duplex with the (+) strand.

2. Translation of Flaviviral RNA Is Inefficient

Immediately following release from the viral nucleocapsid, translation is the only order of business for flaviviral RNA, as the absence of packaged viral polymerase means that immediate replication is not an option. vRNA can be translated in a canonical cap-dependent manner, in which the 43S ribosomal component scans for a start codon.^[9] Though the initiation context is weak due to the lack of a Kozak consensus sequence upstream of the start codon, a downstream mini-hairpin RNA structure termed “cHP” assists in start codon recognition.^[9] While not universal, the cHP can be observed in both mosquito-borne and tick-borne flaviviruses. Presumably, the structure serves primarily to stall the ribosome over the start codon, as the cHP’s sequence is variable but its stability and location with respect to the start codon clearly correlate with initiation efficiency. It should also be noted that, while lacking a poly(A) tail, the flaviviral 3′-UTR has been shown to interact with poly(A)-binding protein (PABP), another hallmark of cap-dependent translation.^[10]

Translation of dengue vRNA has also been observed in the presence of inhibitors of canonical translation.^[11] However, internal ribosome entry site (IRES)-mediated ribosome binding can be ruled out. This is because no such structures are evident in flaviviral RNA. Also, the addition of a stable 5′-terminal structure inhibited noncanonical translation, suggesting that ribosome binding does not bypass recognition of the vRNA terminus.^[11] Nevertheless, we

note a similarity between the hepatitis virus IRES and the flavivirus 3′-UTR: they are of similar length (350 nt and 450 nt, respectively) and contain specific structures that block degradation by the host exonuclease XRN1.^[12,13] In addition, numerous studies have shown that a variety of alterations to flaviviral 3′-UTRs affect translational output^[14,15] and that these UTRs bind to host factors involved in translation (e.g., PABP^[10] and elongation factor 1- α ^[16]). Conversely, the HCV 3′-UTR and flaviviral 5′-UTR are short relative to their opposing UTRs, and both contain poly(U) sequences of unknown function. One may wonder whether a distant evolutionary event flipped the UTRs that flanked the coding region of the hepatitis virus and the flavivirus ancestor. The flaviviral 3′-UTR, however, does not appear to directly interact with ribosome, given an absence of RNA reads in the 3′-UTR in a ribosomal profiling study.^[17] This work also showed that the viral translation process is quite inefficient in comparison to that of host messenger RNA (mRNA): the authors speculate that such “lazy” translation may reduce the chances of alterations in ER homeostasis that would trigger host defense mechanisms.^[17]

3. Numerous Genomic RNA Structures Are Involved in Replication

Following translation, the first act of the viral NS5 polymerase is to distinguish the viral (+) stranded RNA genome from host

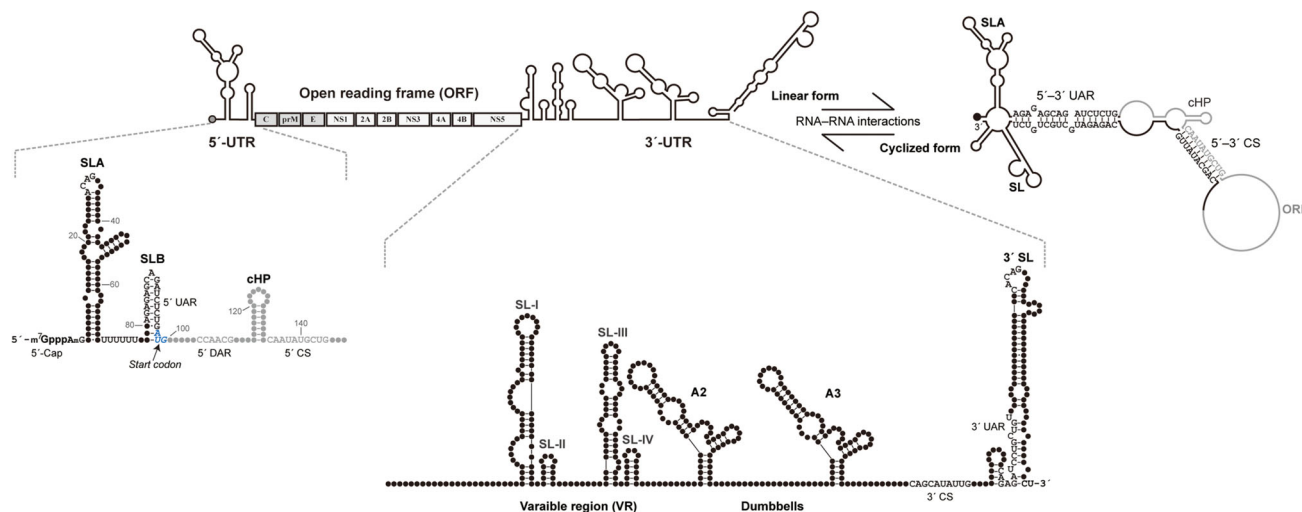


Figure 2. vRNA structures. The complete flaviviral genome contains a single open reading frame (gray) representing ten viral proteins. The flanking 5'- and 3'-UTRs contain RNA elements of relevance to this review, which are annotated. An equilibrium between "linear" and "cyclized" forms is depicted. Upon cyclization, the 5'-SLB structure is eliminated and the terminal 3' structure is no longer associated with SL's stem.

cellular RNAs and generate (–) strand vRNA, which is further used as the template for the production of (+) vRNA. It is thought that the process of vRNA replication occurs in remodeled, ER-derived vesicles.^[17] Here, we highlight (+) strand RNA structures that are relevant to this process.

3.1. Is Cyclization of vRNA Firmly Established?

One observation important in generating the current picture of early steps in flaviviral replication is that of "cyclization" of (+) vRNA through the base pairing of 5'- and 3'-termini (**Figure 2**). Electron microscopy revealed such behavior in alphavirus in the 1970s.^[18] In a mid-1980s flurry of virus sequence analysis studies, Hahn et al.^[19] showed that a number of flaviviruses contained conserved 5'- and 3'-complementary sequences (CS) that could potentially facilitate cyclization. Padmanabhan's group then showed that mutations in these CS regions impaired (–) strand synthesis, while restoring complementarity with a second set of mutations rescued replication.^[20] Gamarik and colleagues later used atomic force microscopy to visualize cyclization of an approximation of DENV RNA.^[21] This work, however, was not without its critics; Lott and Doran^[22] decried an experimental setup that seemed to be designed to produce the expected cyclization result and pointed out the difficulty of distinguishing cyclization (in cis interactions) from concatemerization (in trans). Be that as it may, a long, diverse compendium of experiments apparently support flaviviral genome cyclization.^[23–34] We note that "cyclization" of the replicating form of vRNA does not necessarily mean that the translated form of vRNA is "linear." Indeed, it is established that translating host poly(A)-tailed mRNAs take a circular form, with PABP and eIF4s bridging the two termini.^[35] It is even possible that vRNA can assume more than one cyclized form. For simplicity, we will continue to use the term "cyclization" as opposed to "5'–3' complementarity," but the above caveats should not be ignored.

3.2. Structural RNA Is Enriched in the Viral UTRs

Several groups have contributed to the identification of conserved RNA sequences and structures that play roles in flaviviral replication and translation in addition to the aforementioned 5'–3' CS.^[19,36] Of particular relevance is the conserved 3'-terminal stem-loop structure, designated SL (**Figure 2**), and two long, conserved, repeat sequences termed CS2 and RCS2 that reside in dumbbell structures (A2 and A3 in **Figure 2**) in many flaviviruses.^[37] Later work predicted a 5'-terminal "SLA" (stem-loop A) structure, followed by the SLB structure that contains the start codon.^[21] It was observed that a sequence within SLB, termed the 5'-UAR (upstream AUG region), was complementary to one in the 5' region of SL's stem (**Figure 2**). Currently, at least two other sets of sequences are suspected of engaging in 5'–3' interactions: the "5'–3'-DAR" (downstream AUG region)^[29] and multiple short sequences within the capsid coding region that are complementary with sequences within the mid-3'-UTR.^[38]

3.3. Where Is the Viral Promoter?

Since the generation of the negative strand begins at the (+) 3'-terminus of the template, it would be natural to expect an interaction between viral RdRp and RNA elements in the (+) 3'-UTR. In 2006, Filomatori et al.^[21] combined a number of RNA fragments from DENV UTRs with the purified recombinant RdRp subunit of NS5 in the context of an electrophoretic mobility shift assay (EMSA). Surprisingly, RdRp was found to interact with a 160 nt (+) 5'-terminal input, but not with a 3' input. In vitro polymerase assays yielded parallel results; a combination of RdRp and the (+) 3'-UTR failed to generate (–) complementary products, but a (+) 5' template did. If both the 5' and 3' inputs were present with RdRp, both (–) CS were generated as previously noted in a similar experiment.^[20] These observations gave rise to the notion that the 5'-terminus acts as

the promoter for (–) vRNA synthesis and cyclization places 5'-bound NS5 in proximity to the (+) 3'-terminus. Additional EMSA and RNA footprinting analyses apparently narrowed the site of interaction down to the 5' SLA structure.^[39]

In our recent work using the *in vivo*, albeit heterologous, yeast three-hybrid (Y3H) assay to scan for DENV NS5 and vRNA interactions over the entire viral genome, the results were in opposition to the SLA-promoter viewpoint, revealing that NS5 interacted two orders of magnitude more strongly with the 3' SL than with 5' SLA in the Y3H context.^[40] It is interesting that both DENV SLA and SL have the same sizes of apical loops, both of which contain ACAG sequences in their 5' portions. In fact, the consensus CACAG sequence in the SL top loop (hereafter designated SL-TL) has been recognized as particularly conserved among flaviviruses for more than 30 years:^[41] a study from 2005 shows that a variety of point mutations in SL-TL completely disable replication, but not translation.^[42] In contrast to previous studies conducted by Gamarnik and colleagues, our EMSA confirmed the affinity of RdRp with 3' SL and a sensitive *in vitro* alpha binding assay provided an apparent K_d of ≈ 3 nM for the interaction between RdRp and SL-TL.^[40] It should be noted that two recent studies in which affinities of DENV RdRp with a 5'-UTR fragment containing SLA were measured in solution yielded K_d values ranging from 53 nM to 142 nM.^[43,44]

In a model endorsing a 5' promoter, cyclization is required to bring the 3'-terminus in contact with the viral polymerase. However, a balance between cyclized and linear forms of flaviviral genomes has been hypothesized to play roles not relating to a promoter function: to regulate replication versus translation, to insure generation of full-length RNA strands, to control the ratio of positive to negative strands, and to control the timing of encapsidation.^[19,26,32,37] One study demonstrated that encapsidated DENV RNA exists in cyclized form, while virion-extracted and refolded vRNA is linear.^[45] HCV is also assumed to cyclize,^[46,47] and the promoter for negative-strand synthesis is thought to reside at the 3'-UTR.^[48] The idea of a 3' promoter abolishes the necessity for genomic cyclization in order for NS5 to access the 3'-terminus.

An observation supported by both bioinformatics^[23] and selective 2' hydroxyl acylation analyzed by primer extension (SHAPE)^[49] suggests that the act of cyclization in flaviviruses alters the 3'-terminal SL structure. Since a critical sequence for cyclization, the 3'-UAR, overlaps with the basal 5' region of the SL stem, a base-pairing interaction with the 5'-UAR in SLB results in SL stem shortening, leaving the viral 3'-terminal region free from the stem. Clues to a role played by structural rearrangement of the 3'-end of vRNA are found in earlier *in vitro* RdRp assays, where minor alterations to the 3'-terminus produced large changes in assay output.^[38,48] Also, Gamarnik's group performed a DENV RdRp assay with RNA templates that simply joined SLA to two variants of SL: in one, the 3'-terminus was predicted to be engaged in a stem, but in the other, the terminus was expected to be unpaired.^[39] Though 5'–3' interactions would not be expected with these constructs, only the construct with the unpaired terminus generated the full-length product. Therefore, cyclization of the UTRs per se does not enable replication; rather, a free 3'-terminus is critical. A summary of RdRp activity assays against various RNA inputs is

provided in Table 1; note the obvious dependence of polymerase activity on the structure of the 3'-terminus.

3.4. Why Are There Two NS5-Binding Sites?

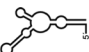
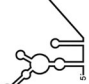



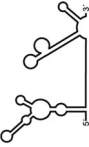
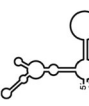

While the ACAG motif in SL-TL (top loop) exhibits strong conservation in all mosquito-borne flaviviruses, the ACAG sequence within SLA is only conserved in DENV and ZIKV. In cases where the TL of 5' SLA (SLA-TL) has been mutated, however, it has been shown to be required for optimal replication.^[21,50] SLA-TL was also shown to be involved in 5' cap methylation of (+) vRNA in WNV.^[51] Intriguingly, footprinting analysis revealed that the UAR cyclization sequence residing in the upstream SLB structure (Figure 2) became highly susceptible to RNase A digestion, thus existing in a single-stranded form in the presence of RdRp.^[39] In contrast, SLA-TL was protected from RNase PhyM in the presence of RdRp. These results suggested that RdRp binding to the SLA-TL stimulated a conformational change of the downstream sequence.

The strong conservation of a 3' terminal uracil (U) and penultimate cytosine (C) on both the positive and the negative flaviviral strands has been noticed in several works.^[52,53] Interestingly, the conserved 3' UUCU terminus is located 46 nt from the 5'-end of SL-TL, while the middle of the UUUUUU tract that straddles SLA and SLB is located 46 nt downstream from the same position in SLA-TL, offering additional similarities between SLA and SL. It seems reasonable that NS5 could stimulate cyclization by disrupting SLB upon binding to SLA-TL, exposing the 5'-UAR. At the other end of the genome, cyclization triggers exposure of the 3'-terminus, providing access to RdRp and initiates (–) vRNA synthesis.^[40] We propose that the dual NS5-binding sites, SLA and SL, may act as sensors of NS5 concentration and that cyclization occurs only when sufficient quantities of NS5 have been translated. While an RdRp–SLA interaction may be important for replication, we favor the admittedly noncanonical view that the default “promoter” should be the 3' SL structure.

3.5. Duplicated RNA Elements Play Roles in Host Switching

Repeat vRNA structures sharing strong sequence identity or multiple motifs seem to be a flavivirus theme. In addition to the aforementioned similarities between SLA and SL, the 3'-UTR of mosquito-borne flaviviruses contains near-identical A2 and A3 dumbbells (Figure 2), as well as structurally similar SLI and SLII elements. These pairings are not commonly seen in flaviviruses with no known vector, making it clear that such duplication almost certainly relates to host-switching.^[54,55] With regard to the dumbbell pair, deletion of the DENV A2 sequence significantly reduced replication in mosquito cells, while the opposite effect was observed upon A3 deletion.^[54] When the experiment was performed in human cells, the trends held but were far less dramatic. This work also showed an accumulation of mutations within the A3 region upon multiple passages in mosquito C6/36 cells. These results were considered to suggest that one structure would be free to mutate to adapt to the host

Table 1. Summary of RdRp affinity and polymerase activity assays with various vRNA fragments.

RNAs	SLA	SLA tail	SL	cySL	SLA-SL	SLA-cySL	cyUTRs	5' + 3'-UTRs
2D structures								
Polymerase activity	Yes ^[44]	Yes ^[39]	No ^[20,21]	n.d.	No ^[39]	Yes ^[39]	Yes ^[20,21]	Yes (both 5' and 3' transcripts were observed) ^[20,21]
RdRp-binding activity	Yes ^[43] No ^[39]	Yes ^[39]	Yes ^[40] No ^[21]	Yes ^[20,40]	n.d.	n.d.	Yes ^[40]	n.d.
Free 3'-tail following the long stem	Yes	Yes	No	Yes	No	Yes	Yes	Yes

n.d., not determined.
“cy” refers to structures as they would exist in cyclized form.

environment, while the other essential structure would remain constant. Relevance to cyclization was further implied as a mutation that eliminated a pseudoknot-forming sequence within the A3 dumbbell, which interacts with the 3' CS involved in 5'–3' pairing, significantly increased viral replication in mosquito cells. Here, we would suggest that research might be furthered by a decreased focus on cyclization and increased focus on the possible protein factors that interact with the dumbbell structures. Sequestration of any host factor that has a strong influence on the immune response could be seen as the primary event and an alteration in cyclization being considered a secondary effect. It is possible that one duplicated structure binds mosquito factors, while the other binds the orthologous human factors. In such a case, repeated passaging in a single cell type would be expected to generate an abundance of mutations in one duplicated structure versus the other. Above, we suggest that the SLA/SL pair could act as sensors as NS5 concentration. It remains possible that other structural pairs could act in a similar fashion.

3.6. Extensive RNA Structure Is Evident within Coding Regions

The combination of modern deep sequencing and RNA probing tools (e.g., SHAPE and dimethyl sulfate [DMS] probing) has greatly increased the opportunities to study the vRNA structure. Not only can the entire genome be investigated, but work can be conducted in an in vivo context. Following examination of the HIV-1,^[56] and HCV genomes using such an approach,^[57,58] a comprehensive survey of the DENV-2 genome was completed in 2018. As with the HIV and HCV works, a high degree of secondary and tertiary structures was uncovered even within coding regions.^[45] Twenty-four RNA “elements” with high levels of predicted base pairing were revealed, 22 of them being found within coding regions. Several, though not all, cases in which synonymous mutations were introduced into DENV-2 showed significant alterations in viral titers and/or vRNA levels in infected cells. One alteration, within the envelope coding region, had particularly potent effects. At the bioinformatic level, DENV-2 sequence comparisons apparently revealed significant decreases in mutation rates in regions with predicted base pairing.

4. There Are Distinct Configurations of Genome-Length vRNA

In 1967, Stollar et al.^[59] first investigated DENV RNA using the methods developed by Baltimore and other virology pioneers. General replication patterns noted in poliovirus^[60,61] apparently held up in flavivirus: 1) generation of a dsRNA viral form shortly after infection that was termed the “replicative form” (RF), 2) high levels of (+) strand vRNA vs (–) strand vRNA, and 3) appearance of a heterogeneous, partially double-stranded form that became known as the “replicative intermediate” (RI) (Figure 1). Later experiments involving JEV,^[62] SLEV,^[63] Kunjin,^[64] and WNV^[7] did not violate these patterns. Over the course of this work, it was found that radiolabeled nucleotide was rapidly incorporated into isolated dsRNA during replication,

suggesting that the newest strands actually displaced somewhat older strands, in contrast to a model where dsRNA was only locally unwound. BVDV (*Flaviviridae*) was also shown to follow the above sequence of events, and RNase A resistance experiments suggested more than one nascent strand per RI.^[65] Another feature of flaviviral RNA was that, unlike alphaviruses, no distinct subgenomic RNAs capable of serving as viral mRNA could be detected in cells infected with flaviviruses—an observation that was important in necessitating the family division of *Flaviviridae* from *Togaviridae*.^[66]

To date, no experiments have detected flaviviral (–) ssRNA. That is, the (–) vRNA exists only as a duplex with (+) vRNA. Using RNase digestion of WNV RNA, followed by 2D polyacrylamide gel electrophoresis analysis (“T1 fingerprinting”), Wengler et al.^[7] were only able to discern negative-stranded vRNA within centrifuged dsRNA fractions, not in ssRNA fractions. However, this absence of viral (–) ssRNA is certainly not a general feature of Group IV viruses. It is, for example, established that poliovirus negative-strand RNA can be found in a single-stranded form, positive strands being found in vesicular structures not occupied by the negative strand.^[67] Some evidence even suggests that HCV may have a (–) ssRNA species.^[68] Conversely, it is thought that negative-strand RNA viruses do not generate immunofluorescence-detectable levels of dsRNA at all.^[69]

Regarding subgenomic flaviviral RNAs (sfRNAs), though no evidence of coding-capable sfRNAs was found, it will be of later interest to note that the early literature was not without reports of low-molecular-weight vRNA species with sedimentation coefficients that placed them under 100 kDa.^[7,62] In the case of WNV, for example, two distinct species of (+) ssRNA were identified at 42 kDa and 65 kDa (or approximately 130 nt and 200 nt, respectively, assuming equal ratios of nucleotides), and hybridization experiments indicated positive polarity. A short vRNA that hybridized with probes representing the MVE 3′-UTR was also found in the brains of infected mice.^[70] A recent wave of sfRNA research has focused on RNA products created by the degradation of the viral genome via the 5′–3′ exonuclease XRN1 until a vRNA structure halts further degradation.^[13] Such single-stranded products are likely the same as those seen 40 years ago.^[71] At this point, we count five forms of genome-scale flaviviral RNA: cyclized and linear (+) vRNA, dsRNA (the RF), heterogeneous (RI), and sfRNA.

5. Mechanisms Underlying the Generation of (+) Strand vRNA Remain to be Delineated

Very little research has been devoted to the means by which the viral polymerase recognizes and initiates (+) strand synthesis. Given that replication occurs within virus-induced membranous vesicles derived from ER, dsRNA is hidden from host mechanisms that normally detect such species, meaning that NS5 may not have to discriminate between a large variety of RNAs in order to initiate vRNA synthesis. The only discrimination required would be between the two dsRNA termini, as every relevant study shows a large (10–100×) excess of positive strand to negative in *Flaviviridae*,^[65,72–76] suggesting preferential recognition of one dsRNA termini versus the other. In

addition to NS5 and the NS3 helicase, host factors apparently contribute to the process of (+) strand synthesis, as in vitro conversion of RF into RI was optimal in the presence of uninfected cell lysate in addition to recombinant NS5 and NS3.^[77] In our view, simple diffusion of NS5 to dsRNA termini is not appealing, particularly given the possibility that *Flaviviridae* polymerase is membrane-anchored during the initiation of positive-strand synthesis,^[75] as shown previously with poliovirus.^[78] Also, at least one study failed to reveal any NS5–dsRNA affinity.^[79] Therefore, we speculate that termini–termini interactions between the (+) strand portion of the dsRNA could be maintained, generating an RNA duplex with frayed ends. Obviously, more work is required to fully understand the molecular mechanisms that viruses utilize to exclusively produce (+) vRNA.

6. Active Switching from Translation to Replication Makes Sense

Having generated quantities of flaviviral protein and RNA, the virus is faced with the luxury of favoring translation over replication, or vice versa. It seems rational to expect that initial replication would not occur at the same time and location as translation, as the vRNA would be translated in the 5′ to 3′ direction, while negative-strand growth would proceed in the opposite direction. Nevertheless, it could be questioned whether, probabilistically, such a ribosome–polymerase collision would be a practical concern. A number of lines of evidence suggested that viruses indeed have switching mechanisms that would minimize this conflict. Gamarnik’s^[80] work with poliovirus replicons showed a near-absence of vRNA synthesis in vitro shortly after the addition of the HeLa lysate; however, RNA synthesis could be induced via the simple addition of cycloheximide, an inhibitor of translation. 3CD, the poliovirus polymerase, which was previously shown to interact with a 5′ cloverleaf structure, was required for this switch to replication.^[81] Such a result makes sense as replication only proceeds when its components reach a critical concentration. Removal of the cloverleaf RNA structure dramatically reduced translation and, perhaps more interestingly, replication, even in the presence of adequate levels of 3CD. Moving to the flavivirus, Lo et al.,^[28] using WNV, and the laboratories of Gamarnik^[21] and Padmanabhan,^[82] using DENV, later showed via a replicon luciferase signal that an initial increase in translated products was followed by a decline. A new wave of translation was observed again ≈24 h after the introduction of the replicon. The downward-sloping portion of this curve, as opposed to a continual increase in the translated products over time, would suggest a period where initial translation products are lost while replication is emphasized, followed by a new wave of translation when (+) vRNA levels reach suitable levels, i.e., an active switch from translation to replication. One HCV study also suggested that a translation/replication switch accompanied an increase in the core protein inhibiting translation.^[83] In addition, the combined presence of DDX6, an RNA helicase known to interact with the DENV 3′-UTR,^[84] and mir-122 at the 5′-terminus of the HCV (+) strand, favors replication vs translation.^[85]

Some evidence points to the cyclized form of vRNA favoring replication over translation. A variety of mutations within the

DENV 3'-UTR were shown to moderately decrease translation, as indicated via replicon luciferase signal, while alterations of the 5' CS that weakened its interaction with the 3' CS actually increased translation moderately.^[14] To complicate the picture, a double mutation that simply exchanged both CS sequences, retaining complementarity, reduced the translation signal by nearly 90%, suggesting a role for the CS sequences that extends beyond mere complementarity. Consistently, mutations or the addition of oligos that would weaken cyclization have the effect of lowering levels of replication.^[15,23–29,32–34,86,87]

7. Do Short Derivatives of vRNA Have Functions?

Several forms of short, noncoding flaviviral RNA have been identified: defective interfering particles (DIPs), microRNA (miRNA)-like sequences, and sfRNA. We must thus expand our collection of flaviviral RNA forms accordingly. Such RNA species likely correspond to the short RNAs found in early pulse/chase studies.^[7] DIPs are so named because they are incapable (defective) of generating progeny in the absence of viable virus and their presence has the effect of hindering viral propagation. Though the notion of DIPs has existed for more than 50 years, their *in vivo* relevance is questionable, as they are typically procured upon multiple passages of infected cells. In flavivirus, one study of dengue DIPs utilized sequencing to elucidate their nature;^[88] not surprisingly, the particles, ranging from 290 to 1030 nt, always contained the complete 5'-UTR and most or all of the 3'-UTR. We note that the 5'-3' joining points of the sequences are significantly enriched for ACA and ACAG sequences, hinting at a role of NS5 in the initial formation of these DIPs.^[40]

The most credible report of an miRNA-like product generated from the flaviviral genome would concern WNV.^[89] In this case, the terminal stem-loop structure (SL) is apparently processed into a 21 nt product that binds to GATA4 mRNA in a mosquito cell line and, in a noncanonical fashion, upregulates GATA4 expression, which in turn enhances viral replication. Unlike the topic of flaviviral miRNAs, that of sfRNAs has received a great deal of high-impact attention over the last five years. sfRNAs are created by the degradation of the viral genome via the 5'-3' exonuclease XRN1. This process is apparently halted in the 5' region of the 3'-UTR via a unique vRNA structure that blocks further degradation.^[13] While both the aforementioned RNAs do contain the terminal SL structure with which NS5 binds, no direct connections between these RNAs and NS5 interactions have been drawn to date. Several works have actually linked the presence of sfRNA to pathogenicity.^[13,90] At this point, the mechanism underlying this pathogenicity remains unknown.

8. What Is Known about vRNA Packaging?

While the assembly of the virion may be described according to localization within the cell, factors whose depletion or enrichment may alter the process, and the means by which vRNA is selectively packaged within capsids, we shall concern ourselves with the latter. Given the broad range of RNAs within the host, as well as documented cases of packaging signals within vRNA (e.g., coronavirus^[91]), it would be rational to engage in a search for repeated or conserved elements within flaviviral RNA that might

specifically interact with the capsid protein. Such elements, however, have not been discovered. Amino acid sequence conservation across flaviviral capsids has been described as “low,”^[92] though general affinity for RNA is not in dispute.

The requirement for specific interactions between capsid and vRNA assumes an environment replete with host factors that would compete for vRNA or capsid. A more exclusive environment, however, might abrogate this need. Indeed, as mentioned above, flaviviruses are thought to carve out their own vesicle-enclosed replication environments. In this case, we might thus look for evidence of coupling between replication and encapsidation. Such linkage has been suggested, and experiments show that only replicating vRNA (versus vRNA whose polymerase has been disabled) is packaged.^[93] Given the difficulty in identifying a packaging signal within flaviviral RNA, we would favor a model in which replicated (+) vRNA is directly presented to the awaiting capsid and structural proteins.

9. vRNA Interactions with Host Proteins May Confound Models Derived from In Vitro Studies

We have now examined flaviviral RNA from translation to packaging. It must be noted that most studies on vRNA structures utilize *in vitro* protocols. However, RNA structures derived from *in vivo* probing do not necessarily resemble those from *in vitro* and *in silico* studies.^[94] The helicase activity of ribosomes causes transient alterations in the structure,^[95] and a multitude of RNA-binding proteins (RBPs) may stabilize structures that would not be preferred in a setting with minimalized components.^[96] Conversely, some thermostable structures have been found to exist largely in denatured states within cells.^[97] To complicate matters further, *in vivo* structures of cellular RNAs have been shown to vary over time, following virus infection.^[95] The potential for in-depth analysis of *in vivo* vRNA structure is seen in the work of Li et al.,^[98] examining Zika vRNA with two different probing methods. The results showed a “moderate” correlation between *in vivo* and *in vitro* structures, in which predicted long-range 5'-3' interactions in vRNA were “generally consistent” with the probing results. However, an important exception was also noted: the absence of interactions between the 5' and 3' CS elements.

While the *in vivo* study of vRNA structures is in its infancy, a number of studies have attempted to globally characterize proteins that bind vRNA. The image of naked vRNA diffusing through a cell whose volume is 30% occupied by macromolecules must therefore be dispelled here.^[99,100] As suggested by the aforementioned case of XRN1, the ability of the virus to utilize, evade, and sequester host factors via vRNA structures and sequences may be critical for viral propagation. While a relative paucity of vRNA-interacting factors might be expected in the protected environment of the viral double-membrane structures where dsRNA appears to reside, a number of experiments have demonstrated roles for host protein-vRNA interactions in translation and replication.^[10,101] Flaviviruses may also sequester factors that ordinarily heighten translation of RNAs involved in an antiviral response; as one example, 3'-UTR interactions with G3BP1, G3BP2, and CAPRIN1 may serve to dampen the interferon response.^[102] vRNA-binding proteins that either increase or

decrease vRNA levels in cells have been identified via protein–RNA crosslinking, followed by vRNA-specific pulldown, identification of relevant proteins via mass spectrometry, and knockdown of proteins of interest.^[103] In one case, knockdown of host-factor YBX1 resulted in an increase in vRNA inside cells despite a decrease in released viral particles, suggesting deficiencies in viral packaging. We would also point out the presence of numerous RNA helicases capable of remodeling vRNA in the handful of studies in which mass spectrometry has been utilized to examine flaviviral RNA-interacting proteins.^[103–105]

10. Conclusions and Outlook

We hope this review enhances a general image of a subtle, sensitive, and highly regulated flaviviral RNA. As seen in recent RNA probing studies, structural elements extend into coding regions representing 95% of the viral genome, possibly illustrating the degree to which vRNA structure and function remains to be explored. Facilitated by next-generation sequencing (NGS), mass spectrometry, and a toolkit of probing methods, research on flaviviral RNA structure and function is entering a new era. In addition to generating entirely novel pictures of vRNA structure, such technology provides opportunities to re-examine early studies with great precision, confirming, contradicting, and adding nuance to canonical viewpoints. It is now possible to examine the complete genome for short- and long-range interactions under any variety of conditions and time points without bias. Such examinations need not be limited to purely single-stranded forms of the genome; new insights may arise by isolating the heterogeneous (RI) form of flaviviral RNA. One may find that in vitro and in silico methods that attempted to resolve RNA structure may have in vivo alternatives that account for a vRNA that could be largely occupied by host factors. We look forward to the delineation of critical interactions involving these structures, given their obvious relevance to antiviral drug development.

Acknowledgements

The authors thank Dr. David Michael Payne for his useful comments on the manuscript. This work was supported by Grants-in-Aids for Research from Mahidol University, Thailand, and by grants (RSA6080066 and IRG5780009) from the Thailand Research Fund (TRF) to S.C. K.H. is supported by Rachadaphiseksompot Fund for Postdoctoral Fellowship, Chulalongkorn University, Thailand.

Conflict of Interest

The authors declare no conflict of interest.

Keywords

Dengue virus (DENV), flaviviruses, host–virus interactions, viral RNA genome, untranslated region (UTR), nonstructural protein 5 (NS5), RNA-dependent RNA polymerase (RdRp)

Received: January 7, 2019
Revised: May 2, 2019
Published online: June 18, 2019

- [1] M. J. Adams, E. J. Lefkowitz, A. M. Q. King, B. Harrach, R. L. Harrison, N. J. Knowles, A. M. Kropinski, M. Krupovic, J. H. Kuhn, A. R. Mushegian, M. Nibert, S. Sabanadzovic, H. Sanfaçon, S. G. Siddell, P. Simmonds, A. Varsani, F. M. Zerbini, A. E. Gorbalenya, A. J. Davison, *Arch. Virol.* **2017**, *162*, 2505.
- [2] T. Nowak, P. M. Färber, G. Wengler, G. Wengler, *Virology* **1989**, *169*, 365.
- [3] S. Bhatt, P. W. Gething, O. J. Brady, J. P. Messina, A. W. Farlow, C. L. Moyes, J. M. Drake, J. S. Brownstein, A. G. Hoen, O. Sankoh, M. F. Myers, D. B. George, T. Jaenisch, G. R. W. Wint, C. P. Simmons, T. W. Scott, J. J. Farrar, S. I. Hay, *Nature* **2013**, *496*, 504.
- [4] J. A. Streit, M. Yang, J. E. Cavanaugh, P. M. Polgreen, *Emerg. Infect. Dis.* **2011**, *17*, 914.
- [5] B. D. Slenning, *Vet. Pathol.* **2010**, *47*, 28.
- [6] D. J. Gubler, *Nat. Med.* **2004**, *10*, 129.
- [7] G. Wengler, G. Wengler, H. J. Gross, *Virology* **1978**, *89*, 423.
- [8] S. Welsch, S. Miller, I. Romero-Brey, A. Merz, C. K. E. Bleck, P. Walther, S. D. Fuller, C. Antony, J. Krijnse-Locker, R. Bartenschlager, *Cell Host Microbe* **2009**, *5*, 365.
- [9] K. Clyde, E. Harris, *J. Virol.* **2006**, *80*, 2170.
- [10] C. Polacek, P. Friebe, E. Harris, *J. Gen. Virol.* **2009**, *90*, 687.
- [11] D. Edgil, C. Polacek, E. Harris, *J. Virol.* **2006**, *80*, 2976.
- [12] S. L. Moon, J. G. Blackinton, J. R. Anderson, M. K. Dozier, B. J. T. Dodd, J. D. Keene, C. J. Wilusz, S. S. Bradrick, J. Wilusz, *PLoS Pathog.* **2015**, *11*, e1004708.
- [13] G. P. Pijlman, A. Funk, N. Kondratieva, J. Leung, S. Torres, L. van der Aa, W. J. Liu, A. C. Palmenberg, P. Y. Shi, R. A. Hall, A. A. Khromykh, *Cell Host Microbe* **2008**, *4*, 579.
- [14] W. W. Chiu, R. M. Kinney, T. W. Dreher, *J. Virol.* **2005**, *79*, 8303.
- [15] K. L. Holden, D. A. Stein, T. C. Pierson, A. A. Ahmed, K. Clyde, P. L. Iversen, E. Harris, *Virology* **2006**, *344*, 439.
- [16] J. L. Blackwell, M. A. Brinton, *J. Virol.* **1997**, *71*, 6433.
- [17] D. W. Reid, R. K. Campos, J. R. Child, T. Zheng, K. W. K. Chan, S. S. Bradrick, S. G. Vasudevan, M. A. Garcia-Blanco, C. V. Nicchitta, *J. Virol.* **2018**, *92*, e01766.
- [18] M. Hsu, H. J. Kung, N. Davidson, *Cold Spring Harb Symp. Quant. Biol.* **1974**, *38*, 943.
- [19] C. S. Hahn, Y. S. Hahn, C. M. Rice, E. Lee, L. Dalgarno, E. G. Strauss, J. H. Strauss, *J. Mol. Biol.* **1987**, *198*, 33.
- [20] S. You, R. Padmanabhan, *J. Biol. Chem.* **1999**, *274*, 33714.
- [21] C. V. Filomatori, M. F. Lodeiro, D. E. Alvarez, M. M. Samsa, L. Pietrasanta, A. V. Gamarnik, *Genes Dev.* **2006**, *20*, 2238.
- [22] W. B. Lott, M. R. Doran, *Trends Biochem. Sci.* **2013**, *38*, 350.
- [23] D. E. Alvarez, C. V. Filomatori, A. V. Gamarnik, *Virology* **2008**, *375*, 223.
- [24] D. E. Alvarez, M. F. Lodeiro, S. J. Luduena, L. I. Pietrasanta, A. V. Gamarnik, *J. Virol.* **2005**, *79*, 6631.
- [25] J. Corver, E. Lenches, K. Smith, R. A. Robison, T. Sando, E. G. Strauss, J. H. Strauss, *J. Virol.* **2003**, *77*, 2265.
- [26] A. A. Khromykh, H. Meka, K. J. Guyatt, E. G. Westaway, *J. Virol.* **2001**, *75*, 6719.
- [27] R. M. Kofler, V. M. Hoenninger, C. Thurner, C. W. Mandl, *J. Virol.* **2006**, *80*, 4099.
- [28] M. K. Lo, M. Tilgner, K. A. Bernard, P. Y. Shi, *J. Virol.* **2003**, *77*, 10004.
- [29] P. Friebe, E. Harris, *J. Virol.* **2010**, *84*, 6103.
- [30] P. Friebe, J. Peña, M. O. F. Pohl, E. Harris, *Virology* **2012**, *422*, 346.
- [31] P. Friebe, P. Y. Shi, E. Harris, *J. Virol.* **2011**, *85*, 1900.
- [32] S. M. Villordo, D. E. Alvarez, A. V. Gamarnik, *RNA* **2010**, *16*, 2325.
- [33] B. Zhang, H. Dong, D. A. Stein, P. L. Iversen, P. Y. Shi, *Virology* **2008**, *373*, 1.
- [34] Z.-Y. Liu, X.-F. Li, T. Jiang, Y.-Q. Deng, Q. Ye, H. Zhao, J.-Y. Yu, C.-F. Qin, *eLife* **2016**, *5*, e17636.
- [35] S. E. Wells, P. E. Hillner, R. D. Vale, A. B. Sachs, *Mol. Cell* **1998**, *2*, 135.

- [36] T. Grange, M. Bouloy, M. Girard, *FEBS Lett.* **1985**, *188*, 159.
- [37] V. Proutski, E. A. Gould, E. C. Holmes, *Nucleic Acids Res.* **1997**, *25*, 1194.
- [38] L. de Borja, S. M. Villordo, N. G. Iglesias, C. V. Filomatori, L. G. Gebhard, A. V. Gamarnik, *J. Virol.* **2015**, *89*, 3430.
- [39] C. V. Filomatori, N. G. Iglesias, S. M. Villordo, D. E. Alvarez, A. V. Gamarnik, *J. Biol. Chem.* **2011**, *286*, 6929.
- [40] K. Hodge, C. Tunghirun, M. Kamkaew, T. Limjindaporn, P. Yenichsomanus, S. Chimnaronk, *J. Biol. Chem.* **2016**, *291*, 17437.
- [41] G. Wengler, E. Castle, *J. Gen. Virol.* **1986**, *67*, 1183.
- [42] M. Tilgner, T. S. Deas, P. Y. Shi, *Virology* **2005**, *331*, 375.
- [43] P. J. Bujalowski, W. Bujalowski, K. H. Choi, *J. Virol.* **2017**, *91*, e00047.
- [44] M. Kamkaew, S. Chimnaronk, *Protein Expression Purif.* **2015**, *112*, 43.
- [45] E. A. Dethoff, M. A. Boerneke, N. S. Gokhale, B. M. Muhire, D. P. Martin, M. T. Sacco, M. J. McFadden, J. B. Weinstein, W. B. Messer, S. M. Horner, K. M. Weeks, *Proc. Natl. Acad. Sci. U. S. A.* **2018**, *115*, 11513.
- [46] C. Thurner, C. Witwer, I. L. Hofacker, P. F. Stadler, *J. Gen. Virol.* **2004**, *85*, 1113.
- [47] M. Yi, S. M. Lemon, *J. Virol.* **2003**, *77*, 3557.
- [48] J. W. Oh, G. T. Sheu, M. M. C. Lai, *J. Biol. Chem.* **2000**, *275*, 17710.
- [49] J. Sztuba-Solinska, T. Teramoto, J. W. Rausch, B. A. Shapiro, R. Padmanabhan, S. F. J. Le Grice, *Nucleic Acids Res.* **2013**, *41*, 5075.
- [50] M. F. Lodeiro, C. V. Filomatori, A. V. Gamarnik, *J. Virol.* **2009**, *83*, 993.
- [51] B. Zhang, H. Dong, Y. Zhou, P. Y. Shi, *J. Virol.* **2008**, *82*, 7047.
- [52] A. A. Khromykh, N. Kondratieva, J. Y. Sgro, A. Palmenberg, E. G. Westaway, *J. Virol.* **2003**, *77*, 10623.
- [53] G. Wengler, G. Wengler, *Virology* **1981**, *113*, 544.
- [54] L. de Borja, S. M. Villordo, F. L. Marsico, J. M. Carballada, C. V. Filomatori, L. G. Gebhard, H. M. Pallarés, S. Lequime, L. Lambrechts, I. Sánchez vargas, C. D. Blair, A. V. Gamarnik, *mBio* **2019**, *10*, e02506.
- [55] S. M. Villordo, C. V. Filomatori, I. Sánchez-Vargas, C. D. Blair, A. V. Gamarnik, *PLoS Pathog.* **2015**, *11*, e1004604.
- [56] N. A. Siegfried, S. Busan, G. M. Rice, J. A. E. Nelson, K. M. Weeks, *Nat. Methods* **2014**, *11*, 959.
- [57] D. M. Mauger, M. Golden, D. Yamane, S. Williford, S. M. Lemon, D. P. Martin, K. M. Weeks, *Proc. Natl. Acad. Sci. U. S. A.* **2015**, *112*, 3692.
- [58] N. Pirakitikulr, A. Kohlway, B. D. Lindenbach, A. M. Pyle, *Mol. Cell* **2016**, *62*, 111.
- [59] V. Stollar, R. W. Schlesinger, T. M. Stevens, *Virology* **1967**, *33*, 650.
- [60] D. Baltimore, Y. Becker, J. E. Darnell, *Science* **1964**, *143*, 1034.
- [61] D. Baltimore, *Proc. Natl. Acad. Sci. U. S. A.* **1964**, *51*, 450.
- [62] E. Zebowitz, J. K. Leong, S. C. Doughty, *Infect. Immun.* **1974**, *10*, 204.
- [63] D. W. Trent, C. C. Swensen, A. A. Qureshi, *J. Virol.* **1969**, *3*, 385.
- [64] R. W. Boulton, E. G. Westaway, *Arch. Virol.* **1977**, *55*, 201.
- [65] Y. Gong, R. Trowbridge, T. B. Macnaughton, E. G. Westaway, A. D. Shannon, E. J. Gowans, *J. Gen. Virol.* **1996**, *77*, 2729.
- [66] E. G. Westaway, M. A. Brinton, Y. Gaidamovich, M. C. Horzinek, A. Igarashi, L. Kääriäinen, O. K. Lvov, J. S. Porterfield, P. K. Russell, D. W. Trent, *Intervirology* **1985**, *24*, 183.
- [67] R. Bolten, D. Egger, R. Gosert, G. Schaub, L. Landmann, K. Bienz, *J. Virol.* **1998**, *72*, 8578.
- [68] M. Shindo, A. M. Di Bisceglie, T. Akatsuka, T.-L. Fong, L. Scaglione, M. Donets, J. H. Hoofnagle, S. M. Feinstone, *Proc Natl Acad Sci U S A* **1994**, *91*, 8719.
- [69] F. Weber, V. Wagner, S. B. Rasmussen, R. Hartmann, S. R. Paludan, *J. Virol.* **2006**, *80*, 5059.
- [70] N. Urosevic, M. van Maanen, J. P. Mansfield, J. S. Mackenzie, G. R. Shellam, *J. Gen. Virol.* **1997**, *78*, 23.
- [71] E. G. Chapman, D. A. Costantino, J. L. Rabe, S. L. Moon, J. Wilusz, J. C. Nix, J. S. Kieft, *Science* **2014**, *344*, 307.
- [72] P. D. Uchil, V. Satchidanandam, *Virology* **2003**, *307*, 358.
- [73] C. J. Chen, M. D. Kuo, L. J. Chien, S. L. Hsu, Y. M. Wang, J. H. Lin, *J. Virol.* **1997**, *71*, 3466.
- [74] T. L. Fong, M. Shindo, S. M. Feinstone, J. H. Hoofnagle, A. M. Di Bisceglie, *J. Clin. Invest.* **1991**, *88*, 1058.
- [75] J. E. Tomassini, E. Boots, L. Gan, P. Graham, V. Munshi, B. Wolanski, J. F. Fay, K. Getty, R. LaFemina, *Virology* **2003**, *313*, 274.
- [76] M. S. Diamond, M. Zachariah, E. Harris, *Virology* **2002**, *304*, 211.
- [77] K. Raviprakash, K. R. Porter, C. G. Hayes, M. Sinha, *Am. J. Trop. Med. Hyg.* **1998**, *58*, 90.
- [78] D. Egger, L. Pasamontes, R. Bolten, V. Boyko, K. Bienz, *J. Virol.* **1996**, *70*, 8675.
- [79] M. R. Szymanski, M. J. Jezewska, P. J. Bujalowski, C. Bussetta, M. Ye, K. H. Choi, W. Bujalowski, *J. Biol. Chem.* **2011**, *286*, 33095.
- [80] A. V. Gamarnik, R. Andino, *Genes Dev.* **1998**, *12*, 2293.
- [81] R. Andino, G. E. Rieckhof, D. Baltimore, *Cell* **1990**, *63*, 369.
- [82] M. Manzano, E. D. Reichert, S. Polo, B. Falgout, W. Kasprzak, B. A. Shapiro, R. Padmanabhan, *J. Biol. Chem.* **2011**, *286*, 22521.
- [83] J. Zhang, O. Yamada, H. Yoshida, T. Iwai, H. Araki, *Virology* **2002**, *293*, 141.
- [84] A. M. Ward, K. Bidet, A. Yinglin, S. G. Ler, K. Hogue, W. Blackstock, J. Gunaratne, M. A. Garcia-Blanco, *RNA Biol.* **2011**, *8*, 1173.
- [85] J. M. Biegel, E. Henderson, E. M. Cox, G. Bonenfant, R. Netzband, S. Kahn, R. Eager, C. T. Pager, *Virology* **2017**, *507*, 231.
- [86] T. S. Deas, I. Binduga-Gajewska, M. Tilgner, P. Ren, D. A. Stein, H. M. Moulton, P. L. Iversen, E. B. Kauffman, L. D. Kramer, P. Y. Shi, *J. Virol.* **2005**, *79*, 4599.
- [87] P. J. Bredenbeek, E. A. Kooi, B. Lindenbach, N. Huijman, C. M. Rice, W. J. Spaan, *J. Gen. Virol.* **2003**, *84*, 1261.
- [88] D. Li, W. B. Lott, K. Lowry, A. Jones, H. M. Thu, J. Aaskov, *PLoS One* **2011**, *6*, e19447.
- [89] M. Hussain, S. Torres, E. Schnetzler, A. Funk, A. Grundhoff, G. P. Pijlman, A. A. Khromykh, S. Asgari, *Nucleic Acids Res.* **2012**, *40*, 2210.
- [90] E. G. Chapman, S. L. Moon, J. Wilusz, J. S. Kieft, *eLife* **2014**, *3*, e01892.
- [91] K. Narayanan, C. J. Chen, J. Maeda, S. Makino, *J. Virol.* **2003**, *77*, 2922.
- [92] L. A. Byk, A. V. Gamarnik, *Annu. Rev. Virol.* **2016**, *3*, 263.
- [93] A. A. Khromykh, A. N. Varnavski, P. L. Sedlak, E. G. Westaway, *J. Virol.* **2001**, *75*, 4633.
- [94] C. K. Kwok, Y. Tang, S. M. Assmann, P. C. Bevilacqua, *Trends Biochem. Sci.* **2015**, *40*, 221.
- [95] O. Mizrahi, A. Nachshon, A. Shitrit, I. A. Gelbart, M. Dobesova, S. Brenner, C. Kahana, N. Stern-Ginossar, *Mol. Cell* **2018**, *72*, 862.
- [96] J. Tyrrell, J. L. McGinnis, K. M. Weeks, G. J. Pielak, *Biochemistry* **2013**, *52*, 8777.
- [97] S. Rouskin, M. Zubradt, S. Washietl, M. Kellis, J. S. Weissman, *Nature* **2014**, *505*, 701.
- [98] P. Li, Y. Wei, M. Mei, L. Tang, L. Sun, W. Huang, J. Zhou, C. Zou, S. Zhang, C. F. Qin, T. Jiang, J. Dai, X. Tan, Q. C. Zhang, *Cell Host Microbe* **2018**, *24*, 875 e5.
- [99] S. B. Zimmerman, S. O. Trach, *J. Mol. Biol.* **1991**, *222*, 599.
- [100] R. Milo, *Bioessays* **2013**, *35*, 1050.

- [101] P. D. Nagy, J. Pogany, *Nat. Rev. Microbiol.* **2011**, *10*, 137.
- [102] K. Bidet, D. Dadlani, M. A. Garcia-Blanco, *PLoS Pathog.* **2014**, *10*, e1004242.
- [103] S. L. Phillips, E. J. Soderblom, S. S. Bradrick, M. A. Garcia-Blanco, *mBio* **2016**, *7*, e01865.
- [104] G. Manokaran, E. Finol, C. Wang, J. Gunaratne, J. Bahl, E. Z. Ong, H. C. Tan, O. M. Sessions, A. M. Ward, D. J. Gubler, E. Harris, M. A. Garcia-Blanco, E. E. Ooi, *Science* **2015**, *350*, 217.
- [105] O. V. Viktorovskaya, T. M. Greco, I. M. Cristea, S. R. Thompson, *PLoS Neglected Trop. Dis.* **2016**, *10*, e0004921.



**2019 - The 7th Burapha University International
Conference on Interdisciplinary Research**

“Break the Barriers, Design the Future”



Visualization of viral replication process via fluorescent dengue RNA

Chutima Chokesaksrikul^a, Sarin Chimnaronk^{a,b,*}

^aLaboratory of RNA Biology, Institute of Molecular Biosciences, Mahidol University, 25/25 Phutthamonthon 4 Road, Salaya, Nakhon Pathom 73170, Thailand.

^bSiriraj Center of Research Excellence for Systems Pharmacology, Faculty of Medicine, Siriraj Hospital, Mahidol University, Bangkok 10700, Thailand.

Abstract

Dengue virus (DENV) is a member of the family *Flaviviridae*, possessing a positive single-stranded RNA genome of approximately 10.7 kb in size. The notion of viral RNA replication begins with the synthesis of a negative-strand RNA, which serves as the template for massive production of positive stranded genomic RNA. During replication, viral RNA is believed to exist in single and double stranded, and a mix of both forms. However, a reliable proof for the replication model as well as precise molecular mechanism are still missing. This study aims at visualization of viral replication process in host cell using fluorescent RNA replicon. We designed and constructed a new two-color replicon containing the mCherry gene and the dBroccoli RNA aptamer to directly observe viral protein and RNA molecules, respectively. We show here that viral RNA was observed in an interesting punctate pattern at the nuclear periphery in HuH-7 cell. Combining with co-immunostaining, we found that NS5 was co-localized with dBroccoli signals at the nuclear border, suggesting a state where NS5 bound to the positive stranded genome to synthesize the negative strand. In addition, viral dsRNA signals were clearly seen in the cytoplasm with no overlap with dBroccoli signals. Our results provide a new useful tool for dissection of viral RNA states in host cell to expand our understanding of viral replication mechanism.

© 2019 Published by Burapha University.

Keywords: Dengue virus (DENV); viral replication; replicon RNA; RNA aptamer; immunofluorescence.

*Corresponding author. Tel.: +66-(0)2-441-9003 ext. 1383.
E-mail address: sarin.chi@mahidol.ac.th

1. Introduction

The four serotypes of dengue virus (DENV-1–4) are transmitted to humans by *Aedes* mosquitoes and are the etiological agent of dengue fever (DF) and dengue hemorrhagic fever (DHF) (Gubler, 1998). DENV infection is one of the major public health concerns for which there are still no specific antiviral drug or effective vaccine. DENV belongs to the flavivirus genus within family *Flaviviridae*, possessing a positive single-stranded RNA genome of approximately 10.7 kb in size. The ten viral proteins are encoded by a single open reading frame (ORF) consisting of three structural proteins of capsid (C), pre-membrane (prM), and envelope (E), which form the viral particle, and seven non-structural (NS) proteins of NS1, NS2A, NS2B, NS3, NS4A, NS4B, and NS5. The viral ORF is flanked by highly structured 5′ and 3′-untranslated regions (UTRs) containing multiple conserved *cis*-acting RNA elements which play regulatory roles in translation and replication of the viral genome (Clyde et al., 2008; Gebhard et al., 2011; Kato and Hishiki, 2016). The NS proteins are fundamental for replication of the viral genome but they are not detectable in viral particles (Chambers et al., 1990).

DENV invades host cells by viral E glycoprotein binding to the receptors, followed by a release of the RNA genome into cytoplasm. The viral RNA is translated into a single viral pre-polypotein, which is proteolytically processed into 10 viral proteins at the endoplasmic reticulum (ER) membrane. Thereafter, the viral genome replication occurs within virus-induced, reorganized intracellular membranes containing the virus replication complex (RC) (Gillespie et al., 2010). RC is thought to comprise of viral RNA, viral NS proteins and host proteins. The viral NS3 and NS5 proteins are the major enzymatic components of RC, which promote efficient viral replication in close association with cellular host factors (Welsch et al., 2009). NS3 consists of two functional domains of the serine protease and the RNA helicase in its N- and C-termini, involved in viral protein maturation and RNA replication, respectively (Lou et al., 2008; Wang et al., 2009). NS5 is also constituted by two distinct enzymes, an N-terminal methyltransferase (MTase) and a C-terminal RNA-dependent RNA polymerase (RdRp), required for capping and synthesis of the viral RNA genome, respectively (Davidson, 2009).

In viral RNA (vRNA) replication, the positive-sense RNA is first used as a template by RdRp of NS5 to synthesize a complementary negative-sense RNA. The negative-strand RNA product exists as a dsRNA intermediate, so-called the replicative form (RF), base-pairing with positive-strand RNA template (Westaway et al., 2003). The 3′-end of negative-sense RNA in RF binds to RdRp of NS5 to initiate generation of the positive-sense RNA genome. It is reported that several nascent positive-sense RNA molecules are synthesized at the same time from one negative stranded template before capping by NS5 MTase, the model of which is called the replicative intermediate form (RI) (Saeedi and Geiss, 2013). Efficient replication of vRNA within RC relies on complex RNA–RNA, RNA–protein and protein–protein interactions (Chen et al., 1997; Phong et al., 2011). Using electron microscopy and tomography, virus-induced vesicles were shown to be derived from the invagination of ER membrane (Davidson, 2009) and contain all NS proteins and dsRNA (Davidson, 2009; Chen et al., 1997; Phong et al., 2011). However, this model of viral RNA replication remains largely elusive due to the lack of molecular evidence.

Replicon is an RNA fragment of viral genomes, which contains the intact 5′- and 3′-UTRs, and all essential viral NS protein genes for efficient viral RNA replication and translation. Therefore, replicon is capable of self-replication like virus inside host. Generally, the replicon contains a fluorescence protein in the place of structural proteins to allow direct monitoring viral protein synthesis. Recently, our research group has developed a new DENV replicon that also contains the dBroccoli RNA aptamer for direct visualization of viral RNA molecules in living cells. RNA aptamer is a single-stranded RNA capable of binding to specific ligand such as small molecules, metal ions, or proteins with high affinity. In 2011, an RNA aptamer showing a specific tertiary structure binding a fluorophore of 3,5-difluoro-4-hydroxybenzylidene imidazolinone (DFHBI) and exhibiting green fluorescence was identified via *in vitro* evolution or SELEX (Paige et al., 2011; Warner et al., 2014). This

study aims to use DENV replicon having both protein and RNA reporters to investigate and interactions with vRNA during the replication process in human cells.

2. Methodology

2.1. Preparation of replicon RNAs by *in vitro* transcription

The pUC19 plasmid encoding the DENV-2 replicon that has the mCherry red fluorescent protein gene, NS2/NS3 cleavage site sequences, FMDV2A sequences, and the E protein transmembrane sequences in the place of the viral prM and E proteins. Moreover, the dBroccoli RNA aptamer was inserted into the 3'-UTR after the stop codon of viral ORF. This replicon was previously constructed in our group. The transcription templates were synthesized by PCR using a forward primer, Class_T7_No.GGG_New (5'-GAA ATT ACG ACT CAC TAT TAG TTG TTA GTC TAC GTG GAC CGA C-3') containing the T7 promoter (underlined), and a reverse primer, DV2_Rev_no_RE_sites (5'-GGT GCT GTT GAA TCA ACA GGT TCT-3'). PCR was performed with Phusion® HF DNA polymerase. Desired PCR product bands were purified from 1% agarose gel using FavorPrep™ GEL/PCR Purification Kit.

DsDNA templates were subjected to the *in vitro* run-off transcription using the RiboMAX™ Large Scale RNA Production System, according to the manufacturer's protocol. The reactions were incubated at 37°C for 4-6 hours before quenching by adding 1 µl of DNase I per 1 µg of DNA template and incubating at 37°C for 15 minutes. Finally, DENV replicon RNAs were purified by the RNeasy® Mini Kit (QIAGEN, USA), quantified by spectrophotometer, and stored at -30°C until use.

2.2. Cell culture and RNA transfection

HuH-7 (Hepatocellular carcinoma cells) were cultured in Dulbecco's Modified Eagle Medium (DMEM) with 10% fetal bovine serum (FBS) and 1x penicillin and streptomycin. Cells were grown at 37°C with 5% CO₂ and passaged every 4-5 days. During the passaging step, 50 µl of cell suspension was mixed with 50 µl of 0.4% trypan blue, and transferred to hemocytometer counting chamber (Baxter Scientific) for counting the number of impermeable cells in the four major squares and the total number of cells per ml was calculated.

The replicon RNAs were transfected into HuH-7 cells at 24 hours after plating cells (5,000 cells/well) in FluoroBrite DMEM in 96-well plate using the Lipofectamine® 3000 reagent (Invitrogen™, USA). Replicon RNAs and Lipofectamine® 3000 were diluted in 5 µl of 1xOpti-MEM before mixing both solutions together, and then incubated at room temperature for 15 minutes. The reactions were then added directly to the well. The fluorescence images of transfected cells were visualized under the DeltaVision™ Ultra fluorescence microscope for living cell imaging or under the ZEISS LSM 800 confocal laser scanning microscope for fixed cell imaging.

2.3. Staining and immunofluorescence

For live cell imaging, thirty minutes prior to imaging, cell culture media were replaced by the imaging medium consisting of 10 µM DFHBI, to stain RNA aptamer, and 5 µl of 200 ng/µl Hoechst® 33342 (Thermo Fisher Scientific, USA) to stain the nucleus.

To fix cells, the cell culture media were replaced by 100 µl of 4% paraformaldehyde. Cells were then incubated at room temperature for 30 minutes, and washed three times by 100 µl of PBS. Cell permeabilization was achieved by incubation at room temperature for a minute in 100 µl of 0.1% Triton X-100 in PBS, and at 4°C for overnight in 100 µl of Odyssey® Blocking Buffer (PBS). The immuno-probing was performed using the primary antibody (1:1000 dilution) of the rabbit polyclonal anti-NS5 antibody (Thermo Fisher Scientific,

USA) or the mouse monoclonal anti-dsRNA antibody [English and Scientific Consulting, Hungary (SCICONS)] and the secondary antibody conjugated to Alexa 647 dye (1:2000 dilution).

Table 1. Excitation and emission wavelengths used in this study.

Fluorophores	Excitation (nm)	Emission (nm)
mCherry	587	610
dBroccoli aptamer	472	507
Hoechst 33342	350	461
Alexa Fluor 647	650	665

2.4. Image analysis

The images were subjected to co-localization analysis using the CellProfiler™ 3.0 software. We used Hoechst-stained nucleus as primary objects or references to identify cell positions, and to search for punctate features in the images. Identified features in red and green channels were overlaid on each other to identify co-localization.

3. Results and Discussion

3.1. The first two-color DENV replicon

We have designed and constructed a new two-color DENV replicon containing the mCherry red fluorescence protein and the dBroccoli aptamer that shows green fluorescence upon binding to DFHBI (Fig. 1). We inserted the NS2B/NS3 cleavage site and the FMDV2A ribosome skipping peptide for cleavage of mCherry from C and NS1 proteins. The dsDNA template was amplified and validated (Fig. 2), prior to the *in vitro* run-off transcription. The transcription of long replicon RNA showed an expected band of approximately 9.7 kb with smearing pattern on 1% denaturing agarose gel (Fig. 3). This is a commonly observed nature of long RNA in electrophoresis due to incomplete denaturing of secondary structures in long RNA. The final yield of purified transcribed replicon was approximately 25 µg per 50 µl reaction.

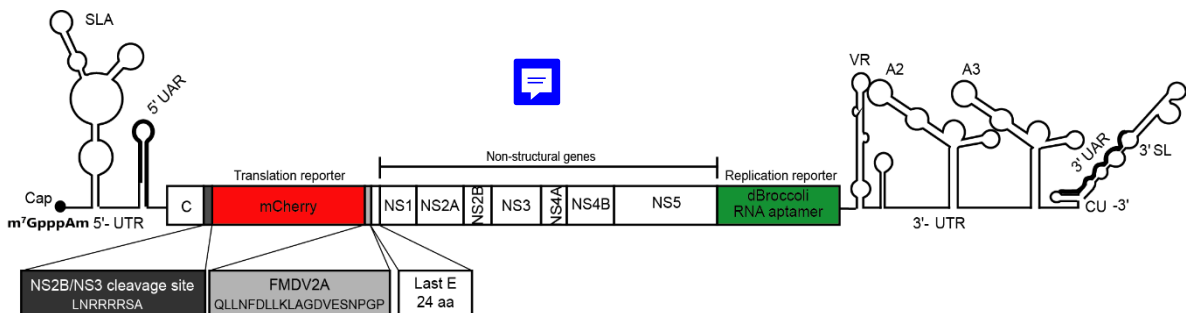


Fig. 1. The DENV replicon construct used in this study. The viral prM and E genes were replaced by the mCherry gene flanked by the NS2/NS3 cleavage site (dark gray) and FMDV2A (light gray) followed by the last 24 amino acids of E protein. The dBroccoli RNA aptamer was inserted into between the stop codon and the 3'-UTR.

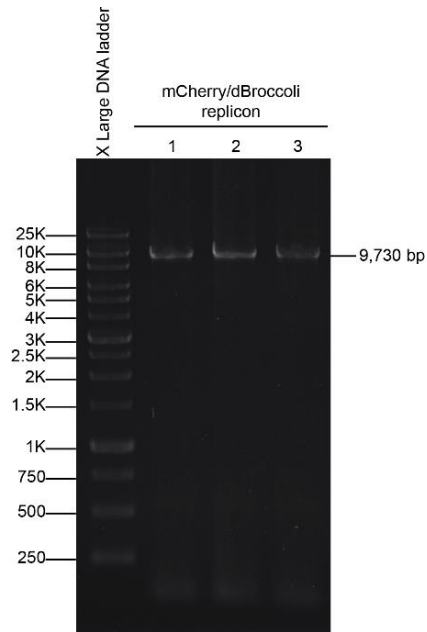


Fig. 2. 1% agarose gel electrophoresis (AGE) of amplified replicon templates (9,730 bp).

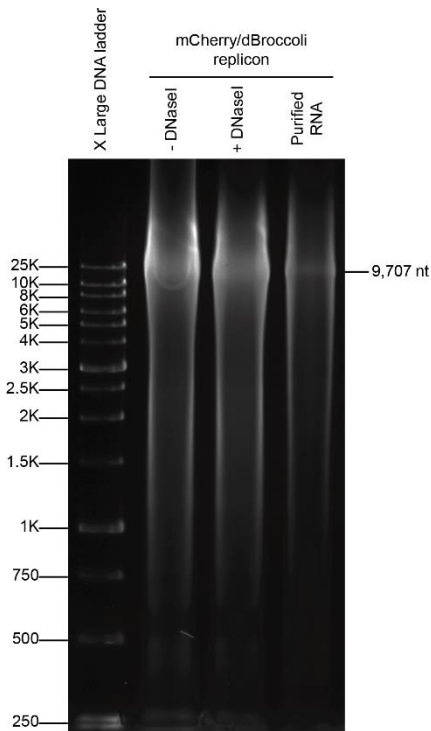


Fig. 3. 1% denaturing AGE of transcription products. The expected size of replicon was 9,707 nt.

3.2. Fluorescent viral RNA in tube and in cell

To confirm that dBroccoli aptamer folded properly in the context of transcribed replicon and was capable of binding DFHBI and fluorescing, we tested by mixing 2.5 μ g of purified replicon RNA with 10 μ M DFHBI in a 10 μ l solution for 15-30 minutes at room temperature. The results clearly showed strong fluorescence under blue light only in the presence of both replicon with dBroccoli and DFHBI (Fig. 4), suggesting that dBroccoli is intact in our replicon. These results prompted us to further investigate the RNA fluorescence in HuH-7 cells.

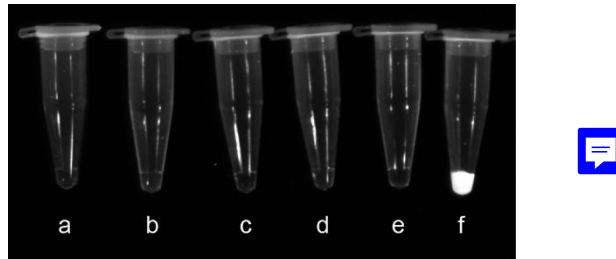


Fig. 4. Fluorescence signals of *in vitro* transcribed replicon RNAs. Tubes from left to right contained (a) PBS, (b) DFHBI, (c) replicon without dBroccoli, (d) replicon without dBroccoli and DFHBI, (e) the mCherry/dBroccoli replicon, and (f) the mCherry/dBroccoli replicon and DFHBI.

Since it was known that transfection of long RNA into mammalian cells is not straightforward, we extensively optimized replicon RNA transfection using Lipofectamine® 3000. We found that 100 ng RNA yielded the best balance between signal intensity and cell viability. 48 hours post transfection (hpt) into hepatic HuH-7 cells which has been well established as a target organ for DENV infection (Dissanayake and Seneviratne, 2018), we observed red mCherry signal spread over cytoplasm as we expected. The results confirmed that our replicon was capable to replicate in HuH-7. In contrast, the green dBroccoli signal showed interesting specific localization as a punctate pattern around the nucleus in living cells (Fig. 5). To our knowledge, this viral RNA localization pattern has not been reported so far. These results validated our new two-color viral replicon for visualizing both viral protein and RNA at the same time.

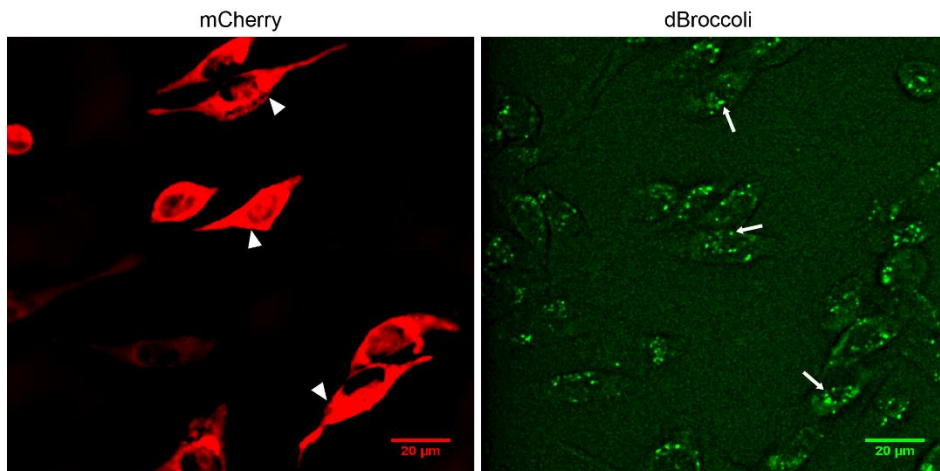


Fig. 5. Live cell images (40x objective) of HuH-7 cells at 48 hours after transfection with DENV replicon.

3.3. Dissection of replication process by co-immunofluorescence

Next, we attempted to use our replicon to visualize the viral replication process in cell. To do this, we have extensively optimized the protocol of immunostaining to maximize the signal-to-noise ratio because we had to use 4 different fluorescence channels. One of the keys was to thoroughly wash fixed cells with 100 mM glycine to remove all residual paraformaldehyde and DFHBI staining had to be performed before permeabilization. We here immunostained two key factors in viral replication, which were NS5 and dsRNA. The confocal images revealed dBroccoli signal was seen in cytoplasm as in live cell imaging (Fig. 6). As expected, DENV-2 NS5 protein mainly showed both nucleus and nuclear peripheral localization (Fig. 6(a)), as previously reported (Hannemann et al., 2013; Kapoor et al., 1995; Kumar et al., 2013; Miller et al., 2006; Pryor et al., 2007; Tay et al., 2013). On the other hand, dsRNA was observed in the cytoplasm (Fig. 6(b)), in agreement with earlier reports (Son et al., 2015; Uchida et al., 2014; Welsch et al., 2009).

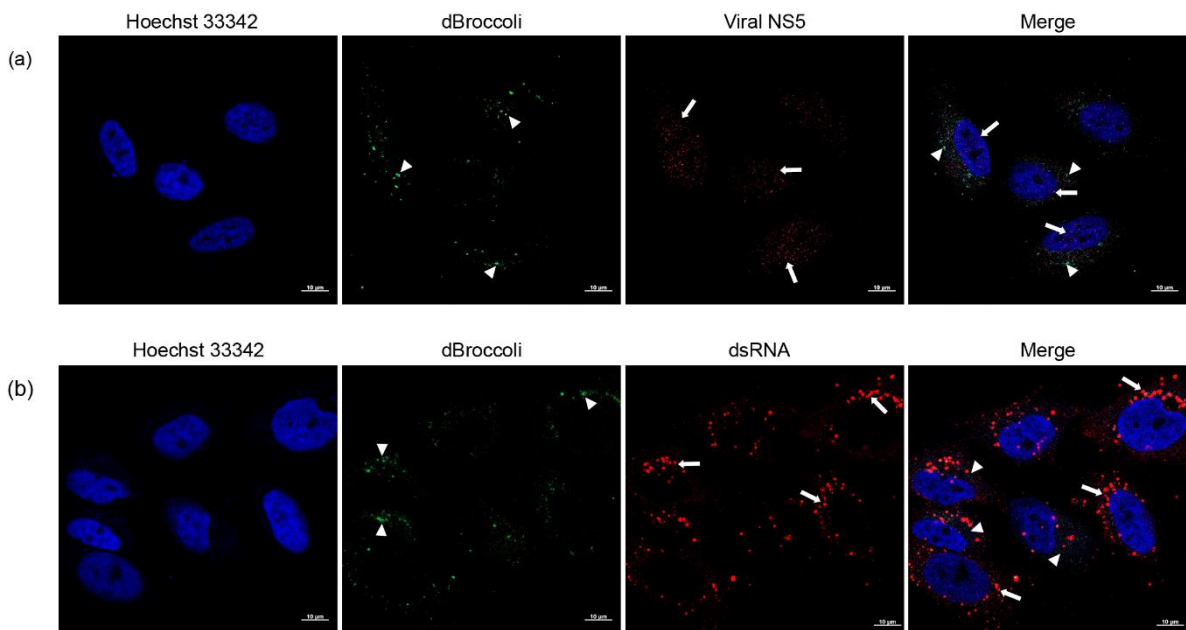


Fig. 6. Fixed cell images (63x objective) of HuH-7 cells at 24 hours after transfection with DENV replicon. Cells were co-immunostained with antibodies against viral NS5 (a) or dsRNA (b).

Images were further subjected to quantitative analysis by the CellProfiler™ 3.0 software. The fluorescence signals were picked up as spots (punctates) and aligned together with Hoechst signals. There was NS5 co-localized with dBroccoli at the nuclear periphery (white arrows in Fig. 7(a)). These locations should indicated where NS5 bound to positive vRNA at an initial step of replication, synthesizing negative stranded vRNA. In contrast, no significant overlap of dsRNA with dBroccoli signals (Fig. 7(b)), as expected because correctly folded dBroccoli aptamer should be found only in positive single stranded RNA but not in dsRNA forms. Taken together, our replicon dissected the states of viral RNA during replication in human cell.

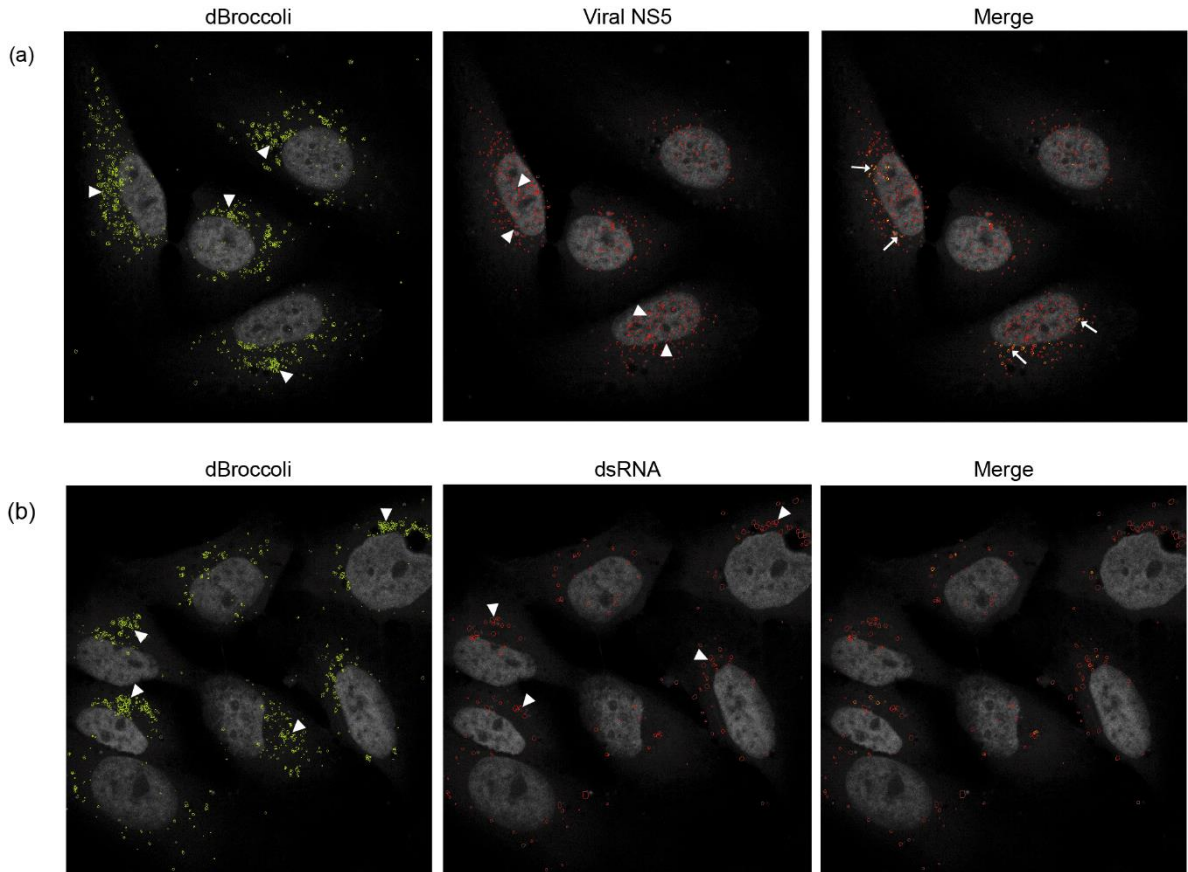


Fig. 7. Quantitative analysis of the images in Fig. 6 using the CellProfiler™ 3.0 software. dBroccoli signals were picked as green spots, and (a) viral NS5 and (b) dsRNA are in red. Co-localized spots are in yellow (also indicated by white arrows).

4. Conclusions

This work demonstrated, for the first time, a new two-color DENV replicon that is capable of visualization of viral RNA and protein syntheses at the same time in both live and fixed cells. We found that DENV positive RNAs showed punctate localization at the nuclear periphery, and some co-localized with NS5, suggesting an initial complex in viral replication. Our study has an important implication for the use of fluorescence replicon in dissecting viral replication steps in cell. Future studies will be performed to further distinguish RF and RI states of vRNAs in cell.

Acknowledgements

This work was supported by Grants-in-Aids for scientific research from Mahidol University, Thailand, and by the Mid-Career Grant (RSA6080066) from the Thailand Research Fund (TRF) to SC.

References

- Chambers, T.J., Hahn, C.S., Galler, R., Rice, C.M., 1990. Flavivirus genome organization, expression, and replication. *Annual Review of Microbiology* 44, p. 649-688.
- Chen, C.J., Kuo, M.D., Chien, L.J., Hsu, S.L., Wang, Y.M., Lin, J.H., 1997. RNA-protein interactions: involvement of NS3, NS5, and 3' noncoding regions of Japanese encephalitis virus genomic RNA. *Journal of Virology* 71, p. 3466-3473.
- Clyde, K., Barrera, J., Harris, E., 2008. The capsid-coding region hairpin element (cHP) is a critical determinant of dengue virus and West Nile virus RNA synthesis. *Virology* 379, p. 314-323.
- Davidson, A.D., 2009. Chapter 2. New insights into flavivirus nonstructural protein 5. *Advances in Virus Research* 74, p. 41-101.
- Dissanayake, H.A., Seneviratne, S.L., 2018. Liver involvement in dengue viral infections. *Reviews in Medical Virology* 28.
- Gebhard, L.G., Filomatori, C.V., Gamarnik, A.V., 2011. Functional RNA elements in the dengue virus genome. *Viruses* 3, p. 1739-1756.
- Gubler, D.J., 1998. Dengue and dengue hemorrhagic fever. *Clinical Microbiology Reviews* 11, p. 480-496.
- Hannemann, H., Sung, P.Y., Chiu, H.C., Yousuf, A., Bird, J., Lim, S.P., Davidson, A.D., 2013. Serotype-specific differences in dengue virus non-structural protein 5 nuclear localization. *Journal of Biological Chemistry* 288, p. 22621-22635.
- Kapoor, M., Zhang, L., Ramachandra, M., Kusakawa, J., Ebner, K. E., Padmanabhan, R., 1995. Association between NS3 and NS5 proteins of dengue virus type 2 in the putative RNA replicase is linked to differential phosphorylation of NS5. *Journal of Biological Chemistry* 270, p. 19100-19106.
- Kato, F., Hishiki, T., 2016. Dengue Virus Reporter Replicon is a Valuable Tool for Antiviral Drug Discovery and Analysis of Virus Replication Mechanisms. *Viruses* 8.
- Kumar, A., Buhler, S., Selisko, B., Davidson, A., Mulder, K., Canard, B., Bartenschlager, R., 2013. Nuclear localization of dengue virus nonstructural protein 5 does not strictly correlate with efficient viral RNA replication and inhibition of type I interferon signaling. *Journal of Virology* 87, p. 4545-4557.
- Luo, D., Xu, T., Watson, R.P., Scherer-Becker, D., Sampath, A., Jahnke, W., Lescar, J., 2008. Insights into RNA unwinding and ATP hydrolysis by the flavivirus NS3 protein. *The EMBO Journal* 27, p. 3209-3219.
- Miller, S., Sparacio, S., Bartenschlager, R., 2006. Subcellular localization and membrane topology of the Dengue virus type 2 Non-structural protein 4B. *Journal Biological Chemistry* 281, p. 8854-8863.
- Paige, J.S., Wu, K.Y., Jaffrey, S.R., 2011. RNA mimics of green fluorescent protein. *Science* 333, p. 642-646.
- Phong, W.Y., Moreland, N.J., Lim, S.P., Wen, D., Paradkar, P.N., Vasudevan, S.G., 2011. Dengue protease activity: the structural integrity and interaction of NS2B with NS3 protease and its potential as a drug target. *Bioscience Reports* 31, p. 399-409.
- Pryor, M.J., Rawlinson, S.M., Butcher, R.E., Barton, C.L., Waterhouse, T.A., Vasudevan, S.G., Davidson, A.D., 2007. Nuclear localization of dengue virus nonstructural protein 5 through its importin alpha/beta-recognized nuclear localization sequences is integral to viral infection. *Traffic* 8, p. 795-807.
- Saeedi, B.J., Geiss, B.J., 2013. Regulation of flavivirus RNA synthesis and capping. *Wiley Interdisciplinary Reviews RNA* 4, p. 723-735.
- Son, K.N., Liang, Z., Lipton, H.L., 2015. Double-stranded RNA is detected by immunofluorescence analysis in RNA and DNA virus infections, including those by negative-sense RNA viruses. *Journal of Virology* 89, p. 9383-9392.
- Tay, M.Y., Fraser, J.E., Chan, W.K., Moreland, N.J., Rathore, A.P., Wang, C., Jans, D.A., 2013. Nuclear localization of dengue virus (DENV) 1-4 non-structural protein 5; protection against all 4 DENV serotypes by the inhibitor Ivermectin. *Antiviral Research* 99.
- Uchida, L., Espada-Murao, L.A., Takamatsu, Y., Okamoto, K., Hayasaka, D., Yu, F., Morita, K., 2014. The dengue virus conceals double-stranded RNA in the intracellular membrane to escape from an interferon response. *Scientific Reports* 4, p. 7395.
- Wang, C.C., Huang, Z.S., Chiang, P.L., Chen, C.T., Wu, H.N., 2009. Analysis of the nucleoside triphosphatase, RNA triphosphatase, and unwinding activities of the helicase domain of dengue virus NS3 protein. *FEBS Letters* 583, p. 691-696.
- Warner, K.D., Chen, M.C., Song, W., Strack, R.L., Thorn, A., Jaffrey, S.R., Ferre-D'Amare, A.R., 2014. Structural basis for activity of highly efficient RNA mimics of green fluorescent protein. *Nature Structural and Molecular Biology* 21, p. 658-663.
- Welsch, S., Miller, S., Romero-Brey, I., Merz, A., Bleck, C.K., Walther, P., Bartenschlager, R., 2009. Composition and three-dimensional architecture of the dengue virus replication and assembly sites. *Cell Host and Microbe* 5, p. 365-375.
- Westaway, E.G., Mackenzie, J.M., Khromykh, A.A., 2003. Kunjin RNA replication and applications of Kunjin replicons. *Advances in Virus Research* 59, p. 99-140.



**2019 - The 7th Burapha University International
Conference on Interdisciplinary Research**

“Break the Barriers, Design the Future”

Correlation of Dengue Severity with Cell Cycle Alteration

Veerakorn Narkthong^{a,b}, Chamras Promtmas^a, Sarin Chimnaronk^{b,c*}

^aDepartment of Biomedical Engineering, Faculty of Engineering, Mahidol University, 999 Phutthamonthon 4 Road, Salaya, Nakorn Pathom, 73170,

^bSiriraj Center of Research Excellence for Systems Pharmacology, Faculty of Medicine, Siriraj Hospital, Mahidol University, Bangkok 10700,

^cInstitute of Molecular Biosciences, Mahidol University, 25/25 Phutthamonthon 4 Road, Salaya, Nakorn Pathom, 73170, Thailand.

Abstract

Dengue is one of the significant mosquito-borne viral infections of public health concern, for which currently no effective drug is available. Dengue virus (DENV) is an enveloped positive-sense single strand RNA virus, belonging to the genus flavivirus within family *Flaviviridae*, and has four antigenically related serotypes designated as DENV-1–4. All the four serotypes can cause clinical manifestation ranging from mild flu-like illness, known as dengue fever (DF) to potentially lethal complications of dengue hemorrhagic fever (DHF) and dengue shock syndrome (DSS), referred to as severe dengue (SVD). To date, precise molecular mechanisms that trigger SVD remain largely elusive and a molecular marker associated with the sign of SVD has not been identified. We hypothesized that virus–host interactions contributes to the onset of SVD and observed cell phenotypes implicating dengue severity in a model human hepatic HuH-7 cell line at the single-cell level via high-content imaging analysis (HCA). In this study, we show that the four DENV serotypes are divided into two distinct genotypic groups of serotypes 1 and 3, and 2 and 4. Each group is also distinguishable by the probability of SVD development in Thai patients, suggesting critical involvement of viral RNA sequences in disease pathogenesis. We further found that the reduction of cell numbers upon infection with four DENV serotypes recapitulated the clinical statistics and evolutionary relationship, and was attributed to the reduction of cell population in the S phase of cell cycle. Our study reveals a new *in vitro* model for estimation of SVD.

© 2019 Published by Burapha University.

Keywords – Dengue virus (DENV), cell cycles, cell phenotypes, severe dengue (SVD), high-content imaging analysis (HCA).

*Corresponding author. Tel.: +66-(0)2-441-9003 ext. 1383.

E-mail address: sarin.chi@mahidol.ac.th

1. Introduction

Dengue infection is the most critical mosquito-borne viral disease in the world – and the most rapidly spreading – with a 30-fold increase in global incidence over the past 50 years. The disease has become a serious health problem worldwide as more than 100 countries are in the risk area (Rodenhuis-Zybert et al., 2010). The disease is caused by dengue virus (DENV) and spread to human through the bite of an infected *Aedes* species (*Ae. aegypti* or *Ae. albopictus*) mosquito. DENV is an enveloped RNA virus belonging to the genus flavivirus within family *Flaviviridae*, and has four antigenically related serotypes designated as DENV-1–4. DENV possesses a single-strand positive-sense RNA genome with a size of approximately 10.7 kb, which encodes ten viral proteins. All the four DENV serotypes can cause clinical manifestation and show similar patterns of systemic dissemination at 3-7 days after infection. The symptoms of dengue diseases are classified into 2 groups by WHO 2009 criteria including dengue fever (DF) which is a common illness of DENV infection and dengue hemorrhagic fever (DHF) or dengue with a warning sign which potentially lead to death (WHO, 2009). Clinical manifestations of DF include fever, rash, hemorrhagic symptoms, headache, ocular pain, arthralgia, myalgia, nausea, and vomiting. DF can develop to DHF emerging the warning signs such as abdominal pain, mucosal bleeding, persistent vomiting, liver enlargement and restlessness, and occasionally progresses to dengue shock syndrome (DSS) for 2-7 days after illness, which displays severe bleeding, severe plasma leakage, and severe organ involvement that lead to death (Rothman, 2011). Most DENV infections pass with minimal or no symptoms. In contrast, severe diseases can lead to a mortality rate of up to 20% of affected individuals but with expert management and primarily careful fluid replacement, this can be reduced to less than 1% (Rothman, 2011 and Screaton et al., 2015). Approximately 3.6 billion people are living in the endemic area, with an estimation of 400 million cases of DENV infection every year, of which 0.5 million cases require hospitalization care (Sim and Hibberd, 2016). In 2018, Thailand Department of Disease Control reported the number of DENV patients being around 70,000 cases and 0.13% were dead. Notably, ~50% of death were caused by DENV-2. The lethal cases were mostly found in patients that were more than 60 years old (Department of disease control, Thailand, 2019). Currently, there are no specific drug for dengue diseases and preventive vaccine have not been so successful (Bente, 2006; Whitehead, 2007; and Swaminathan and Khanna, 2019).

Primates are the only vertebrates known to be infected by DENV in nature. Both humans and non-human primates are susceptible to dengue virus infection, but the viral strains isolated from humans and non-human primates are genetically distinct, indicating that these transmission cycles diverged in the distant past (Wang et al, 2000). Infection with one DENV serotype confers long-term protective immunity against re-infection with the same serotypes but not against other serotypes (Rothman, 2011). Also, DENV infection has been known for a while that secondary infection by distinct DENV serotypes increases the risk of development of severe dengue (SVD). However, it was also shown that SVD can be observed in primary infection, especially in infants and children below 15 years old (Jain and Chaturvedi, 2010). The severity of secondary infection of DENV is explained by the antibody-dependent enhancement mechanism (ADE) theory which is based on increasing cellular uptake of infectious virus-antibody complexes in secondary infection in both adults and children (Haslwanter, 2017). However, the role of ADE in human infectious still remains controversial (Screaton et al., 2015), and ADE cannot serve as a classifier for the severity of dengue diseases. Moreover, the precise molecular mechanism of SVD remains poorly understood and a feasible *in vitro* or *in vivo* model enabling selection or prediction of virus strains associated with SVD is not existing (Yauch and Shresta, 2008). Attempts to identify the relationship of violence in the pathogenesis with the host and viral genomes failed to render clear explanation (Flipse et al., 2013). Hence, further studies are definitely required to identify a specific biomarker for SVD and to comprehensively understand the diseases mechanisms.

Since SVD could not be fully explained by viral serotypes and genotypes as mentioned above, we here explored cell *phenotypes* upon infection and asked if some phenotypes could explain the SVD trend in patients. The idea is based on our hypothesis that virus–host interactions contribute to the onset of SVD, which should be able to be observed by changes in cell phenotypes.

2. Materials and Methods

2.1. Cell culture and virus infection

Kidney epithelial from African green monkey cell line (Vero) and human liver cell line (HuH-7) were cultured in Dulbecco's modified minimal essential medium (DMEM: Gibco™) supplemented with 10% inactivated fetal bovine serum (Merck), and 1% penicillin-streptomycin (Gibco™). Cells were incubated in a humidified incubator at 37°C with 5% CO₂.

DENV stocks were obtained by inoculating monolayers of C6/36 cells with the virus at a multiplicity of infection (MOI) of 0.1. Cells were cultured for 5-12 days (serotypes dependent) in L-15 medium supplemented with 1% heat-inactivated FBS, 10% TPB, 1.2% penicillin and streptomycin. Virus titers were quantified by the Focus Forming Unit (FFU) assay with Vero cells. HuH-7 cells were cultured in 96-well plates (PerkinElmer) overnight, and infected with DENV-1 (Hawaii), DENV-2 (16681), DENV-3 (H87), and DENV-4 (H241) at an MOI of 0.1-20 at 37°C for 2 hours. Viruses were removed by two washes with supplemented-DMEM, and infected cells were maintained at 37°C with 5% CO₂.

2.2. Immunofluorescence staining

2.2.1. Cell cycle – Cells were labeled with 10 µM of EdU (Invitrogen) for 30-60 minutes. Initially, cells were fixed with 4% paraformaldehyde in PBS at room temperature for 15 minutes, and washed 3 times with PBS prior to permeabilization with 100 µl of cold-pure methanol for 15 minutes at room temperature. Then, cells were washed 3 times with PBS prior to an addition of 30 µl of EdU solution consisting of 1 M of Tris pH 8.5, 4 mM of CuSO₄, 10 µM fluorescent azide dye, and 50 mM ascorbic acid for 30 minutes at room temperature.

2.2.2. Virus and Nucleus – Cells were blocked with the Odyssey (PBS) blocking buffer (Li-COR) at room temperature for at least 1 hour. DENVs were labelled using 30 µl of primary antibody (mouse-monoclonal anti-dsRNA antibody: SCICONS) dilution (1:1000 in blocking buffer) for overnight in the moisture control box at 4°C in dark. After a three-time wash with 0.1% Tween in PBS (PBS-T), the secondary antibody (Alexa Fluor® 647 donkey anti-mouse: ThermoFisher) at 1:1000 dilution was reacted with cells in the blocking buffer for 2 hours at room temperature. Then, cells were washed with PBS-T (3 times) and PBS (2 times) before labelling the nucleus using 1:1000 diluted 4',6-diamidino-2-phenylindole (DAPI) in PBS for 1 hour at room temperature. Cells were washed (3×) with PBS and stored at 4°C in PBS.

2.3. High content imaging and data analysis

Cells were imaged under the high-content imaging system (PerkinElmer). Excitation and emission filters were selected appropriately without overlapping each other's wavelengths including emission 430-500 nm and excitation 355-385 nm for DAPI signal, 655-760 and 615-645 nm for Alexa647 signal, and 500-550 and 460-490 nm for EdU signal. 20× objective lens (Air, NA 0.4) was used for high image quality for quantitative analysis using the CellProfiler software. The MATLAB software was used for data management and modelling.

3. Results and Discussion

Bioinformatic analyses of existing clinical data and dengue sequences

To assess the circumstance of infection and severe cases for each DENV serotype in Thailand, we collected all available clinical data from literatures with a strict criteria to include only studies that had clear specification of DF, DHF, and DSS, according to WHO criteria, as well as DENV serotypes. We, however, precluded data regarding primary or secondary infections, genders, and ages. Four studies passed our criteria (Vaughn, 1999; Kalayanaroj and Nimmannitya, 2000; Nisalak, 2003; and Anantapreecha, 2005). The collected data were rearranged according to viral serotypes (1–4) and severity (common dengue or DF and severe dengue or DHF and DSS). We then calculated and normalized the possibility of SVD for each serotype in each study. The results showed that the median possibility of SVD is highest in individuals infected with DENV-2, followed by DENV-4, DENV-1, and DENV-3 (**Fig. 1**). The results also indicated two DENV groups with higher and lower SVD probability.

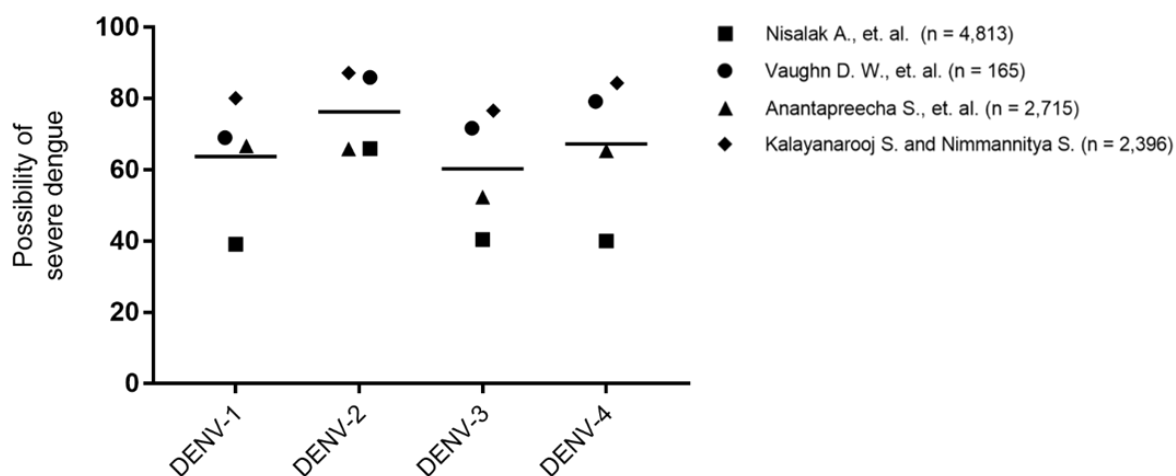


Figure 1. Plots of possibility of SVD for each DENV serotypes in Thai patients, based on four previously-reported clinical data (Vaughn, 1999; Kalayanaroj and Nimmannitya, 2000; Nisalak, 2003; and Anantapreecha, 2005). Median possibilities are indicated by black lines.

Next, we asked if this varied SVD probability might stem from viral genotypes. We performed sequence alignments of entire DENV genomes from 4 serotypes, and built a phylogenetic tree (**Fig. 2**). The results clearly showed the same grouping as in the probability of SVD development in Thai patients that DENV-1 and DENV-3 are in a close genotypic relationship, whereas DENV-2 is more related to DENV-4. Our analysis suggested critical involvement of viral RNA sequences in disease pathogenesis. It is noted that a previous study that used only the sequence of the DENV E genes to construct the phylogenetic tree classified DENV-2 and DENV-4 into different groups (HKatzeknick, 2015). This implied that interactions between host receptors and DENV E are not a major cause for SVD.

In vitro DENV infection

We next sought to explore cell phenotypes that could serve as indicator for SVD. To do this, we decided to utilize a human hepatic cell line, HuH-7, as an *in vitro* infection model. It has been known that DENV is capable of infecting C6/36 (Sakoonwatanyoo et al., 2006), BHK (Phanthanawiboon et al., 2014), Vero (Kinney et al.,

2005; Farias et al. 2013; and Phanthanawiboon et al., 2014), Monocyte, Dendritic (Noisakran et al., 2010) and HuH-7 (Stein et al., 2011; and Pando-Robles et al., 2014) cells. To normalize the infection efficiency varied by DENV serotypes, we first measured infection ability of 4 representative DENV strains in various MOI and HPI (hours post infection) in HuH-7. Each DENV strain was initially propagated in C6/36 cells and quantitated by FFU in Vero cells. The infectivity of the virus was calculated by mean intensity of dsRNA signal per cytoplasm area. The results clearly showed that each DENV strain did not equally infect HuH-7 at the same MOI (**Fig. 3**). For example, at MOI of 5 at 48 HPI, the infection efficiencies were approximately 70%, 95%, 50%, and 50% for DENV-1–4, respectively. DENVs could have differences in affinity with cell surface receptors and replication rate in HuH-7. In addition, the pattern of infection rates was not well consistent with the order of serotypes in SVD (**Fig. 1**). In order to investigate cell phenotypes in the same number of infected cells, we decided to use MOI of 10, 2.5, 20, and 10 for DENV-1–4, respectively, which showed more than 80% infection at 48 HPI.

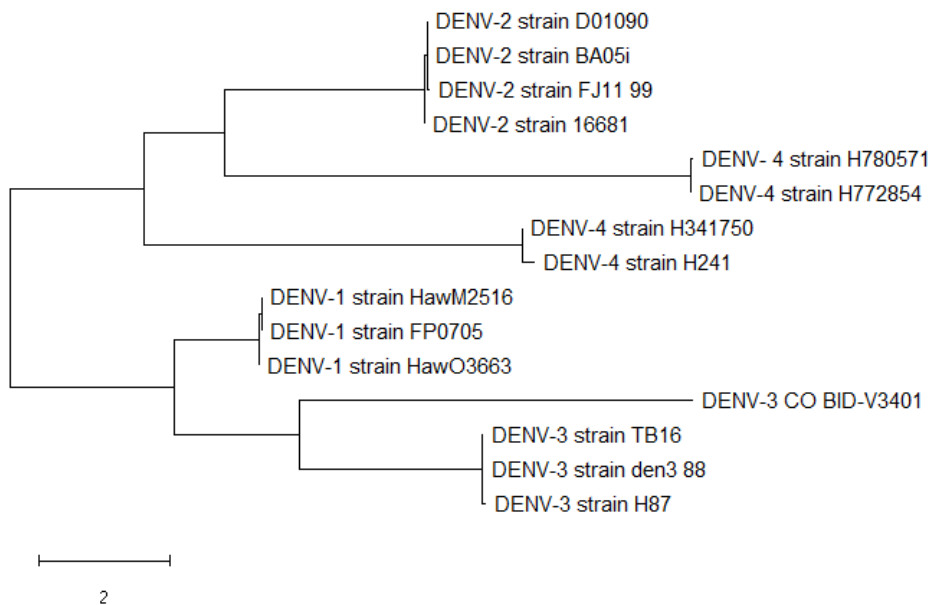


Figure 2. A phylogenetic tree (n = 15) shows the evolutionary relationships inferred by Neighbor-Joining method. Entire DENV genome sequences were aligned with MEGA. The evolutionary distances were computed using the Maximum Composite Likelihood method.

Phenotypes of DENV-infected cells

We first explored the simplest phenotype of cell viability. Surviving cells after infection with 4 serotypes of DENV were quantitated by mean intensity of DAPI per nucleus area. As shown in **Fig. 4**, the number of HuH-7 cells significantly reduced upon infection in order of DENV-2, DENV-4, DENV-1, and DENV-3. Interestingly, the order recapitulated SVD possibility in patients (**Fig. 1**), suggesting that our *in vitro* infection model is useful for investigation of cell phenotypes for DENV infection. The reduction in cell number could be accounted for by cell death and/or cell proliferation. Given that cell proliferation has so far not been intensively investigated in DENV-infected cells, we decided to dissect cell proliferation through cell cycles analysis.

Here, we took an advantage of the high-content imaging analysis (HCA) system to quantitate three different fluorescence signals for cell nuclei, viral RNA, and DNA replication in individual cells. This system allowed us to fractionate only infected cells into 4 different cell cycles of G1, Early S, late S and G2/M phases at the single

cell level. The results showed that the distribution of infected cells in the early S phase (ES) significantly reduced by approximately 3% in DENV-1, 15% in DENV-2, and 7% in DENV-4, compared to that of non-infected cells (**Fig. 5**). In contrast, DENV-3 caused slightly increase (~3%) in the S phase population. The reduction of cells in S phase contributed to increasing cells in G1 and G2/M phases. In particular, DENV-1, DENV-2, and DENV-4 caused approximately 4%, 11%, and 8%, respectively, increasing G1 population. The results revealed that DENV infection induced cell cycle dysregulation with different magnitudes among serotypes for the first time. Again, the order of reduction in the S phase was consistent with SVD possibility and cell numbers (**Figs. 1 and 4**). These results strongly indicated a correlation between SVD in patients and cell cycle alteration in our *in vitro* model. It is not known, however, how DENV modulates cell cycle in infected cell. Our results suggested that the viral genome itself plays a crucial role in SVD, and thus, it is possible that there is such a signal in the viral genome to induce cell cycle changes and SVD. Our work also has implication for detecting cell cycle change by a new biosensor for estimation of SVD.

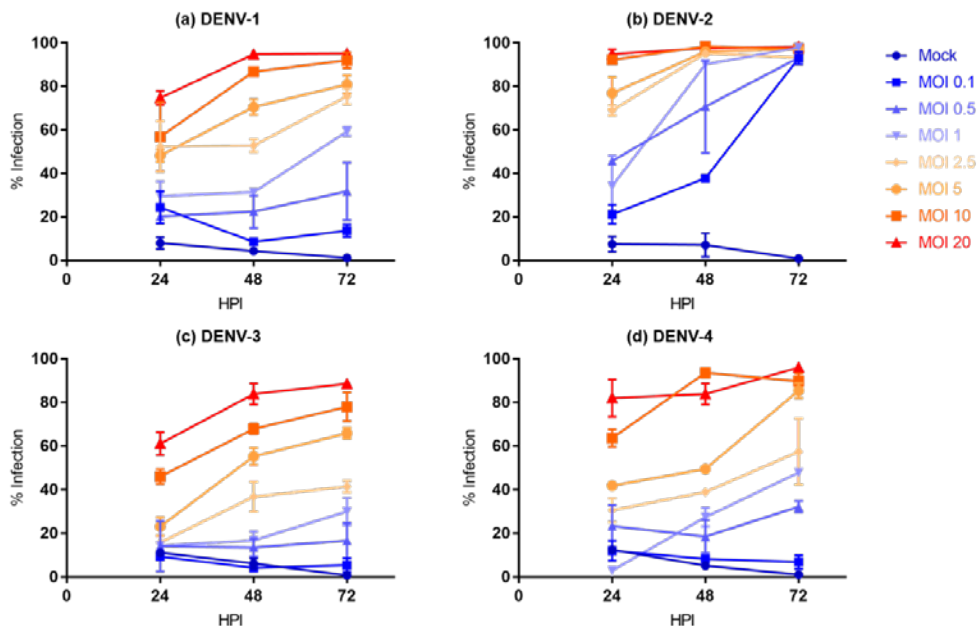


Figure 3. Infectivity of DENV-1 (a), DENV-2 (b), DENV-3 (c), and DENV-4 (d) in HuH-7 in various MOI (0.1-20) and HPI (24-72) conditions.

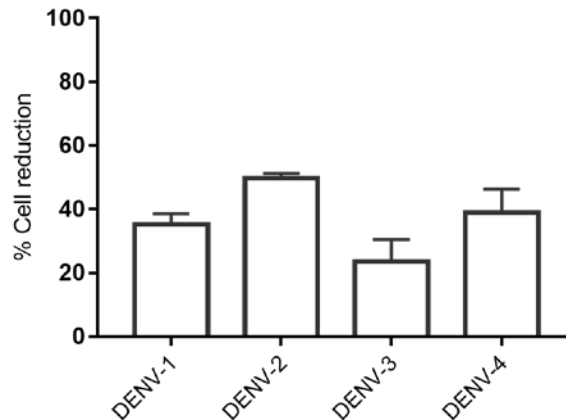


Figure 4. Reduction in cell numbers upon infection with different DENV serotypes.
It is noted that the percent infection was adjusted to be the same.

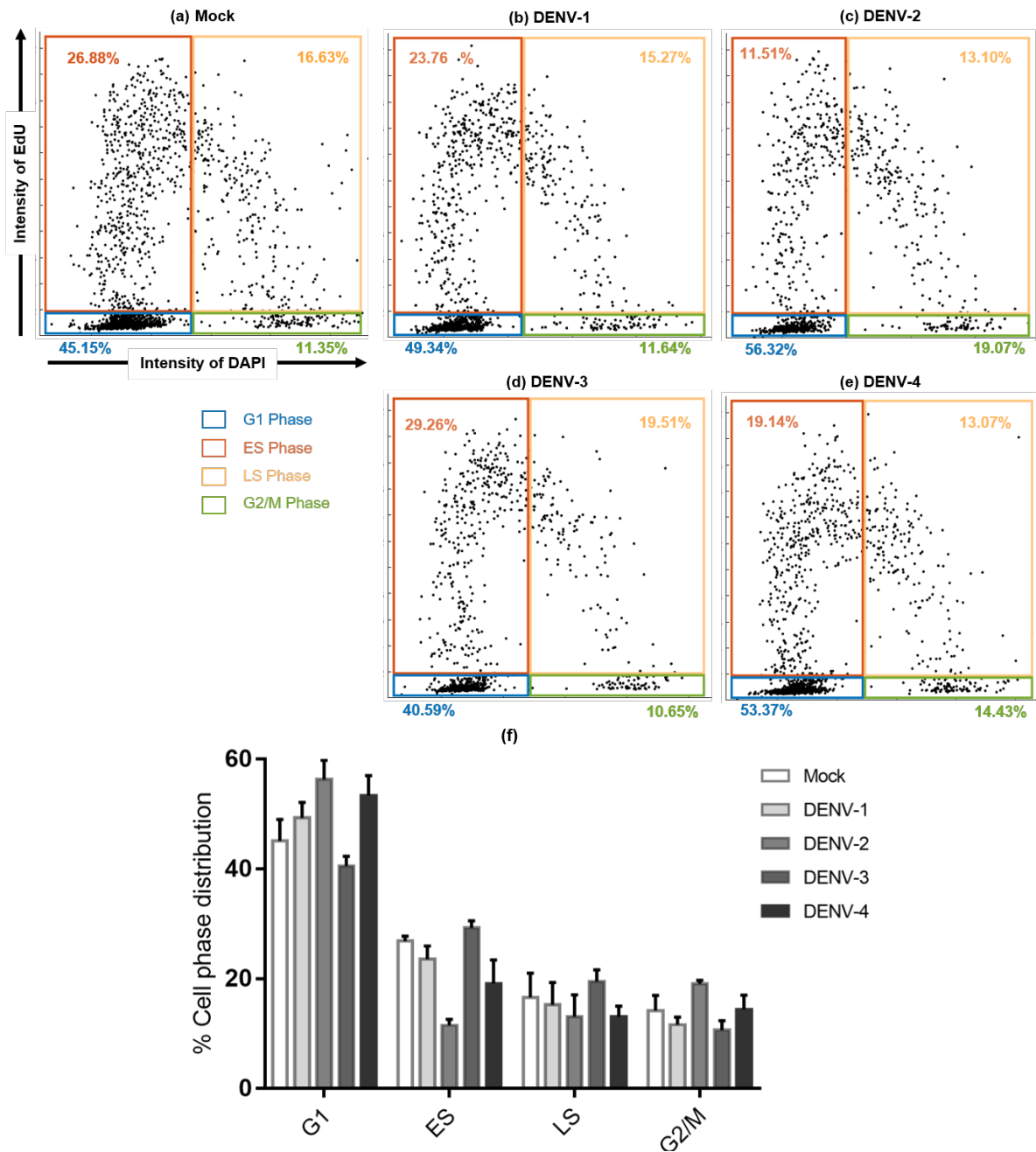


Figure 5. Cell cycle plots of non-infected cells (a) and DENV-infected cells (b-e) by the mean intensity of DAPI and EdU staining. Cell cycles are divided into four quadrants of G1 (blue), ES (red), LS (yellow), and G2/M (green) phases. The population of cells in each phase are shown in (f).

4. Conclusion

In this work, we combined bioinformatic analysis with an in vitro infection model to demonstrate that the four DENV serotypes are divided into two distinct groups of serotypes 1 and 3, and 2 and 4. The two groups are distinguishable by their genotypes, possibility of SVD in patients, infected cell viability, and cell cycle alteration in infected cell. Moreover, the rank order of DENV serotypes for severity is consistent with that of the magnitude of cell cycle alteration as serotypes $2 > 4 > 1 > 3$. Our data suggests that the cell cycle likely plays important roles in SVD development in human. Our study reveals a new in vitro model for estimation of SVD, and the use of cell cycle as an indicator for SVD.

Acknowledgements

We thank Prof. Pathai Yenchitsomanus (Division of Medical Molecular Biology at the Department of Research and Development, Faculty of Medicine, Siriraj Hospital) for providing DENV strains used in this study. This work was supported by Grants-in-Aids for scientific research from Mahidol University, Thailand, and by the Mid-Career Grant (RSA6080066) from the Thailand Research Fund (TRF) to SC. This work was also supported by the Center of Excellence on Medical Biotechnology (CEMB), S&T Postgraduate Education and Research Development Office (PERDO), Office of Higher Education Commission (OHEC), Thailand (Research Grant SD-59-002-04).

References

1. Rodenhuis-Zybert IA, Wilschut J, Smit JM. Dengue virus life cycle: viral and host factors modulating infectivity. *Cell Mol Life Sci*. 2010;67(16):2773-86.
2. World Health Organization. (2009). Dengue guidelines for diagnosis, treatment, prevention and control: new edition. World Health Organization. <http://www.who.int/iris/handle/10665/44188>.
3. Rothman AL. Immunity to dengue virus: a tale of original antigenic sin and tropical cytokine storms. *Nat Rev Immunol*. 2011;11(8):532-43.
4. Screaton G, Mongkolsapaya J, Yacoub S, Roberts C. New insights into the immunopathology and control of dengue virus infection. *Nat Rev Immunol*. 2015;15(12):745-59.
5. Sim S, Hibberd ML. Genomic approaches for understanding dengue: insights from the virus, vector, and host. *Genome Biol*. 2016;17:38.
6. Department of Disease Control, Thailand (2019). Dengue fever forecast report Thailand 2019. <https://ddc.moph.go.th/th/site/newsview/view/696>.
7. Swaminathan S, Khanna N. Dengue vaccine development: Global and Indian scenarios. *Int J Infect Dis*. 2019.
8. Whitehead SS, Blaney JE, Durbin AP, Murphy BR. Prospects for a dengue virus vaccine. *Nat Rev Microbiol*. 2007;5(7):518-28.
9. Wang et. al. Evolutionary Relationships of Endemic/Epidemic and Sylvatic Dengue viruses. *Journal of Virology*. 2000;74:3227-34.
10. Jain A, Chaturvedi UC. Dengue in infants: an overview. *FEMS Immunol Med Microbiol*. 2010;59(2):119-30.
11. Haslwanter D, Blaas D, Heinz FX, Stiasny K. A novel mechanism of antibody-mediated enhancement of flavivirus infection. *PLoS Pathog*. 2017;13(9):e1006643.
12. Yauch LE, Shresta S. Mouse models of dengue virus infection and disease. *Antiviral Res*. 2008;80(2):87-93.
13. Flipse J, Wilschut J, Smit JM. Molecular mechanisms involved in antibody-dependent enhancement of dengue virus infection in humans. *Traffic*. 2013;14(1):25-35.
14. Nisalak A. et al. Serotype-specific dengue virus circulation and dengue disease in Bangkok, Thailand from 1973 to 1999. *Am J Trop Med Hyg*. 2003;191-202.
15. Vaughn D. A. et al. Dengue viremia titer, antibody response pattern, and virus serotype correlate with disease severity. *Infectious diseases society of America*. 1999;181:2-9.
16. Anantapreecha S, Chanama S, A An, Naemkhunthot S, Sa-Ngasang A, Sawanpanyalert P, et al. Serological and virological features of dengue fever and dengue haemorrhagic fever in Thailand from 1999 to 2002. *Epidemiol Infect*. 2005;133(3):503-7.
17. Kalayanaroj S. and Nimmannitya S. Clinical and laboratory presentations of dengue patients with different serotypes. *Dengue Bulletin*. 2000;24:53-9.
18. HKatzeknick L. C. et al. Dengue virus cluster antigenically but not as discrete serotypes. *SCIENCE*. 2015;349:1338-42.
19. Sakoonwatanyoo P, Boonsanay V, Smith DR. Growth and production of the dengue virus in C6/36 cells and identification of a laminin-binding protein as a candidate serotype 3 and 4 receptor protein. *Intervirology*. 2006;49(3):161-72.
20. Phanthanawiboon S, A An, Panngarm N, Limkittikul K, Ikuta K, Anantapreecha S, et al. Isolation and propagation of Dengue virus in Vero and BHK-21 cells expressing human DC-SIGN stably. *J Virol Methods*. 2014;209:55-61.

21. Farias KJ, Machado PR, da Fonseca BA. Chloroquine inhibits dengue virus type 2 replication in Vero cells but not in C6/36 cells. *ScientificWorldJournal*. 2013;2013:282734.
22. Kinney RM, Huang CY, Rose BC, Kroeker AD, Dreher TW, Iversen PL, et al. Inhibition of dengue virus serotypes 1 to 4 in vero cell cultures with morpholino oligomers. *J Virol*. 2005;79(8):5116-28.
23. Noisakran S, Onlamoon N, Songprakhon P, Hsiao HM, Chokeyphaibulkit K, Perng GC. Cells in dengue virus infection in vivo. *Adv Virol*. 2010;2010:164878.
24. Pando-Robles V, Osés-Prieto JA, Rodríguez-Gandarilla M, Meneses-Romero E, Burlingame AL, Batista CV. Quantitative proteomic analysis of Huh-7 cells infected with Dengue virus by label-free LC-MS. *J Proteomics*. 2014;111:16-29.
25. Stein DA, Perry ST, Buck MD, Oehmen CS, Fischer MA, Poore E, et al. Inhibition of dengue virus infections in cell cultures and in AG129 mice by a small interfering RNA targeting a highly conserved sequence. *J Virol*. 2011;85(19):10154-66.
26. Bente D. A. R-HR. Models of dengue virus infection. *Drug Discov Today Dis Model*. 2006;3(1):93-103.

PO016

Identification of human poly(A)-binding proteins as dengue NS5 interactors in infected cell

Jakkrit Jantiya^a, Surat Punyahathaikul^b, Kenneth Hodge^c, Trairak Pisitkun^c,
and Sarin Chimnaronk^{a*}

^aLaboratory of RNA Biology, Institute of Molecular Biosciences, Mahidol University,

^bCenter for Vaccine Development, Institute of Molecular Biosciences, Mahidol University, 25/25 Phutthamonthon 4 Road, Salaya, Nakhon Pathom 73170, Thailand,

^cThe Systems Biology Center, Research Affairs, Faculty of Medicine, Chulalongkorn University, 1873 Rama 4 Road, Pathumwan, Bangkok 10330, Thailand.

***E-mail:** sarin.chi@mahidol.ac.th

Dengue virus (DENV) infection is one of the major public health concerns worldwide for which no effective drug is currently available. This study aims to provide a comprehensive view of host-virus interactions for development of new drug targets. Here we used an engineered, tagged dengue virus (etDENV) that contains an octahistidine tag and a FLAG tag inserted into the NS5 gene to facilitate isolation of proteins associated with NS5 in infected cells. The human hepatoma cell line, HuH-7, were infected with either etDENV or the wild type DENV-2 as a control, and tagged NS5 was isolated with anti-FLAG M2 affinity gels. We obtained about 0.5 µg NS5 from 10⁶ cells as estimated by the Western blot analysis. The tandem mass spectrometry identified 540 human proteins that co-immunoprecipitated with NS5. The number of NS5-interactors was significantly reduced to 96 upon the treatment of RNase prior to immunoprecipitation, suggesting a contamination with a subset of viral RNA-interacting proteins. There were 83 proteins shared by two datasets, including at least 4 functional groups of the poly(A)-binding, ATP-binding, mRNA splicing, and the translational initiation, in six distinct protein complexes. A few NS5 interactors identified in this work were previously reported including BCLAF1, RBM3 and THRAP3. Functional analysis of an uncharacterized protein complex in DENV infection is underway.

Keywords: Dengue virus (DENV), non-structural protein 5 (NS5), immunoprecipitation (IP), tandem mass spectrometry (MS/MS), interaction network

Proc09

Identification of human poly(A)-binding proteins as dengue NS5 interactors in infected cell

Jakkrit Jantiya^a, Surat Punyahathaikul^b, Kenneth Hodge^c, Trairak Pisitkun^d,
and Sarin Chimnaronk^{a*}

^aLaboratory of RNA Biology, Institute of Molecular Biosciences, Mahidol University,

^bCenter for Vaccine Development, Institute of Molecular Biosciences, Mahidol University,
25/25 Phutthamonthon 4 Road, Salaya, Nakhon Pathom 73170, Thailand,

^cThe Systems Biology Center, Research Affairs, Faculty of Medicine, Chulalongkorn
University, 1873 Rama 4 Road, Pathumwan, Bangkok 10330, Thailand.

*E-mail: sarin.chi@mahidol.ac.th

Abstract

Dengue virus (DENV) infection is one of the major public health concerns worldwide for which no effective drug is currently available. This study aims to provide a comprehensive view of host-virus interactions for development of new drug targets. Here we used an engineered, tagged dengue virus (etDENV) that contains an octahistidine tag and a FLAG tag inserted into the NS5 gene to facilitate isolation of proteins associated with NS5 in infected cells. The human hepatoma cell line, HuH-7, were infected with either etDENV or the wild type DENV-2 as a control, and tagged NS5 was isolated with anti-FLAG M2 affinity gels. We obtained about 0.5 µg NS5 from 10⁶ cells as estimated by the Western blot analysis. The tandem mass spectrometry identified 540 human proteins that co-immunoprecipitated with NS5. The number of NS5-interactors was significantly reduced to 96 upon the treatment of RNase prior to immunoprecipitation, suggesting a contamination with a subset of viral RNA-interacting proteins. There were 83 proteins shared by two datasets, including at least 4 functional groups of the poly(A)-binding, ATP-binding, mRNA splicing, and the translational initiation, in six distinct protein complexes. A few NS5 interactors identified in this work were previously reported including BCLAF1, RBM3 and THRAP3. Functional analysis of an uncharacterized protein complex in DENV infection is underway.

Keywords: Dengue virus (DENV), non-structural protein 5 (NS5), immunoprecipitation (IP), tandem mass spectrometry (MS/MS), interaction network

Introduction

Dengue fever is a mosquito-borne tropical disease, caused by dengue virus (DENV), which infects ~400 million people in more than 110 countries with approximately 10,000-20,000 deaths per year [1]. DENV is transmitted by female mosquitos of *Aedes* species that take a blood meal from a person infected with the virus. Nowadays, there is still no specific treatment and effective vaccine for the dengue diseases [2].

DENV is an enveloped virus belonging to the genus flavivirus within the family *Flaviviridae*. DENV possesses a positive single-stranded RNA genome that is translated by host ribosome into a single polypeptide at the endoplasmic reticulum (ER), which is further cleaved into 10 individual proteins by host and viral proteases [3]. The DENV proteins are composed of three structural proteins of C (capsid), prM (pre-

membrane/membrane) and E (envelope), which are assembled into the virus particle, and seven non-structural proteins (NS) of NS1, NS2A, NS2B, NS3, NS4A, NS4B, and NS5. Viral NS proteins are assembled together to form a membrane-bound replication complex (RC) that catalyzes RNA replication [4,5]. Of those, NS5 is the largest viral protein within RC and shows the most conserved amino acid sequences among DENV proteins (5). NS5 has a size of ~103 kDa and consists of two distinct enzymatic activities that play vital roles in replication. Its one-third N-terminal domain is 2'-O methyltransferase (MTase) involved in capping of the viral genome. The C-terminal region comprises of an RNA-dependent RNA polymerase (RdRp) required for viral RNA synthesis [6]. In addition, a group of host proteins were earlier reported for their interactions with RC to assist viral replication process [8]. For example, NS5 interacts with STAT2 to suppress host innate immune response [7]. Hence, a study of the global interaction network of NS5 with host factors should provide deep understanding of host-dependent viral replication, and clues to drug targets.

To explore NS5-interacting network in an environment of DENV infection, we utilized our engineered, tagged dengue virus (etDENV) that contains an octahistidine (8×His) tag and a FLAG tag (DYKDDDDK) in the MTase domain of NS5 for the infection and immunoprecipitation of NS5 interactors from human hepatic cells, the natural target of DENV [9]. Our study unveiled NS5-host factors interactions with a high accuracy in the context of real infection.

Experimental

Propagation of viruses

The Vero (African green monkey kidney epithelial) cells were infected with DENV at an MOI of 0.1 in 1x VP-SFM (virus production serum free medium). After infection, the cytopathic effect (CPE) was monitored until 50% cells die without lysis. Then, cells were collected by the freeze-thaw method. The virus titers were quantitated with the plaque forming assay (PFU) and the virus stocks were stored at -80°C

Protein extraction and FLAG immunoprecipitation (IP)

Human HuH-7 cells (a well differentiated hepatocyte-derived carcinoma cell line) were infected with DENV serotype 2 (DENV-2) strain 16681 or etDENV at an MOI of 5. Forty-eight hours after infection (hpi), cells were lysed by the lysis buffer (25 mM Tris pH 7-8, 150 mM NaCl, 0.1% SDS, 0.5% sodium deoxycholate and 1% Triton X-100) supplemented with protease inhibitor, DNase I and phosphatase inhibitor. NS5 was isolated by incubating with EZview Red Anti-FLAG M2 affinity gels (SIGMA) overnight at 4°C on a tube rotator. Then, beads were washed with TBS buffer (50 mM Tris-Cl pH 7.6 and 150 mM NaCl) 8-10 times. The Western blot was performed to quantitate protein yields and purity of NS5 from FLAG-IP.

Western blot analysis

Samples were loaded onto 10% SDS-PAGE. Electrophoresis was performed for 2 hours. The membrane was then blocked by immersing in 50 ml blocking solution (5% skim milk in PBS-T) for 1 hour. The membrane was washed 3 times with PBS-T for 5 minutes prior to incubation with the primary antibody (1:5000 rabbit anti-NS5 polyclonal antibody in PBS-T) for 1 hour at room temperature. After 3 washes with PBS-T for 5 minutes, the membrane was incubated with the secondary antibody (1:10000 goat anti-rabbit FITC-labelled antibody) for 1 hour at room temperature. Chemiluminescence reaction was performed using the PierceTM ECL Western Blotting Substrate at room temperature for 5 minutes. Bands were visualized by X-ray films in the dark room. The band intensity was quantitated by the ImageJ program.

Mass spectrometry (MS) and data analysis

Pulldown protein fractions were digested on beads with trypsin for LC-MS/MS analysis [10]. Sample were eluted from beads in the elution buffer 1 (5 ng/ μ l trypsin, 2 M urea, 50 mM Tris-HCl pH 7.5 and 1 mM DTT) and incubated for 30 min at room temperature. Then, the peptide in the solution was alkylated with the elution buffer 2 (2 M urea, 50 mM Tris-HCl pH 7.5, and 5 mM IAA) for 30 min at room temperature, and continued the incubation at 35°C overnight to complete tryptic digestion. Following digestion, sample were cleaned and concentrated by using C18 jupiter ZipTips. Then, the tandem mass spectrometer (Q-Exactive Plus, Thermo) was used to identify NS5 and its interacting proteins. The raw data were analyzed using MaxQuant, a quantitative proteomics software package designed for analyzing large-scale mass-spectrometric data sets. The NS5 protein–protein interacting network was generated using the STRING 10.5 database [11], and reconstructed via the Cytoscape program [12] to indicate the number of peptide fragments weighted against molecular mass for all nodes.

Results

Propagation of etDENV

Both etDENV and DENV-2 were propagated in Vero cells in a large-scale adequate for later IP and MS experiments. The obtained virus titers were 1.3×10^7 and 4.7×10^6 PFU/ml for etDENV and DENV-2, respectively as quantitated by plaque forming assay (PFA) (**Fig. 1**). The results confirmed our previous investigation that the tag in NS5 does not disturb the folding and function of NS5 in viral replication in host [9].

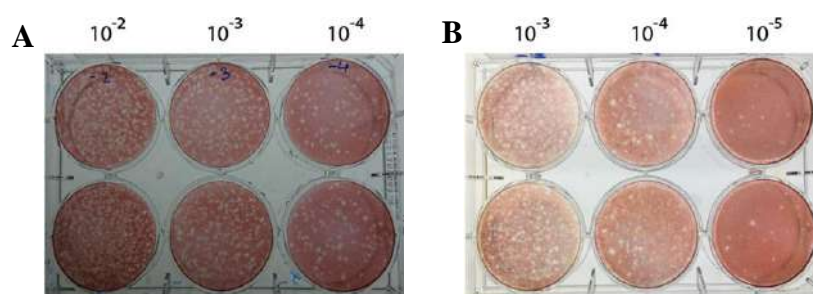


Figure 1. Plaque forming assay of (A) the wild type DENV-2 strain 16681, and (B) etDENV. The assay was performed with technical duplicates.

Isolation of tagged NS5 from infected cells

NS5 in etDENV has both 8×His and FLAG tags. Our preliminary test showed that FLAG IP rendered less background contamination than nickel affinity pulldown. In this study, we performed FLAG-IP of NS5 with biological duplicates in HuH-7 cells. The Western blot analysis validated IP efficiency (**Fig. 2**). As expected, no NS5 band was observed in IP fraction from DENV-2. By comparing band intensity with the purified recombinant DENV RdRp, the yields of tagged NS5 were estimated to be 0.73 and 0.49 μ g per 10^6 cells from 2 IP rounds. We observed a trace of NS5 in flow-through and wash fractions of etDENV. This could be because of inadequate FLAG beads or overloaded protein amount. Nonetheless, NS5 isolated in this study has very high quality and quantity sufficient for the MS/MS analysis.

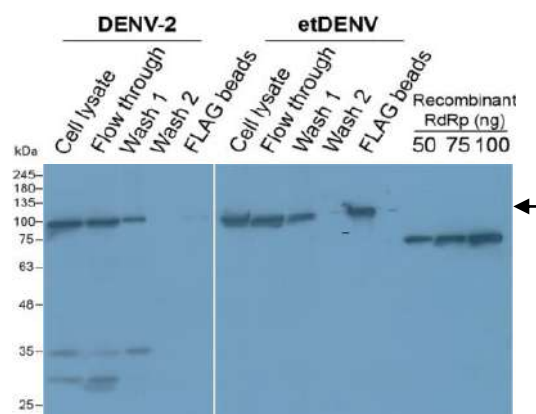


Figure 2. Western blot of FLAG-IP of NS5 from DENV- and etDENV-infected HuH-7. A black arrow indicates tagged NS5 bands of 105.7 kDa.

Interactome of DENV NS5 in human liver cell

Five hundred and forty human proteins were identified by mass spectrometry with NS5 IP, and classified into five functional Gene Ontology (GO) groups (Fig. 3B). Since the NS5 interactor list was largely occupied by RNA-binding proteins, it was possible that a number of identified interactors did not directly interact with NS5 but rather bound to viral RNA where NS5 also bound during viral replication. To minimize this bias, we improve the list by an addition of RNase during IP to remove viral RNA-interacting proteins. The results revealed 96 proteins that were classified into four GO groups (Fig. 3B). Of those, 83 proteins were identical between two IP experiments with and without RNase (Fig. 3A) and were enriched in poly(A)-binding and RNA-binding proteins. To visualize the interaction network, we assigned weights to each protein by dividing the MS peptide counts by molecular mass and abundance in the liver to eliminate MS biases. The resulting NS5 ‘interactome’ map is shown in Fig. 4, revealing six different cellular complexes. Two known complexes are translational machinery and spliceosome, whereas four complexes have not been characterized so far. While further functional study of these complexes in viral replication should be required, our results obviously showed specific, complex, though shaped, interaction network of host–virus during viral replication process. It is also noted that some identified NS5-interacting proteins in this work were previously reported including YBX1 and HSP90 [13,14], and THRAP3 and BCLAF1 [15], validating our NS5-IP/MS system.

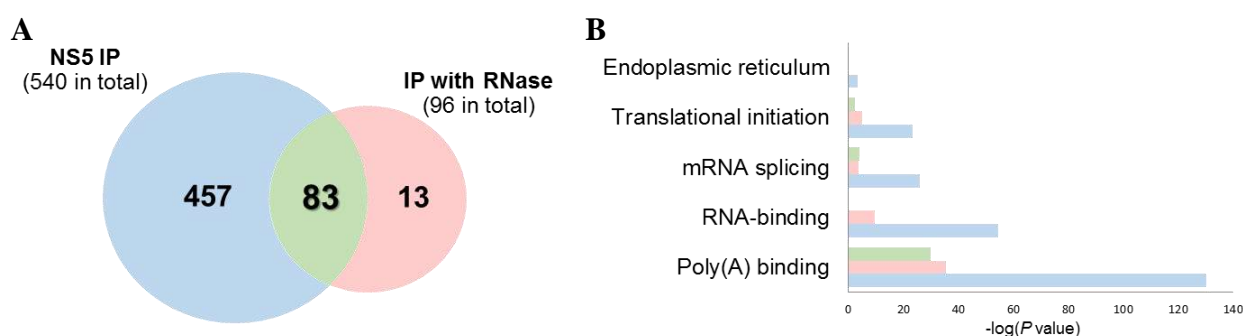


Figure 3. (A) Venn diagram of NS5-interacting proteins. Eighty-three proteins were found in the intersection (green) of two experiments (light blue and pink). (B) GO groups of NS5 interactors according to DAVID.

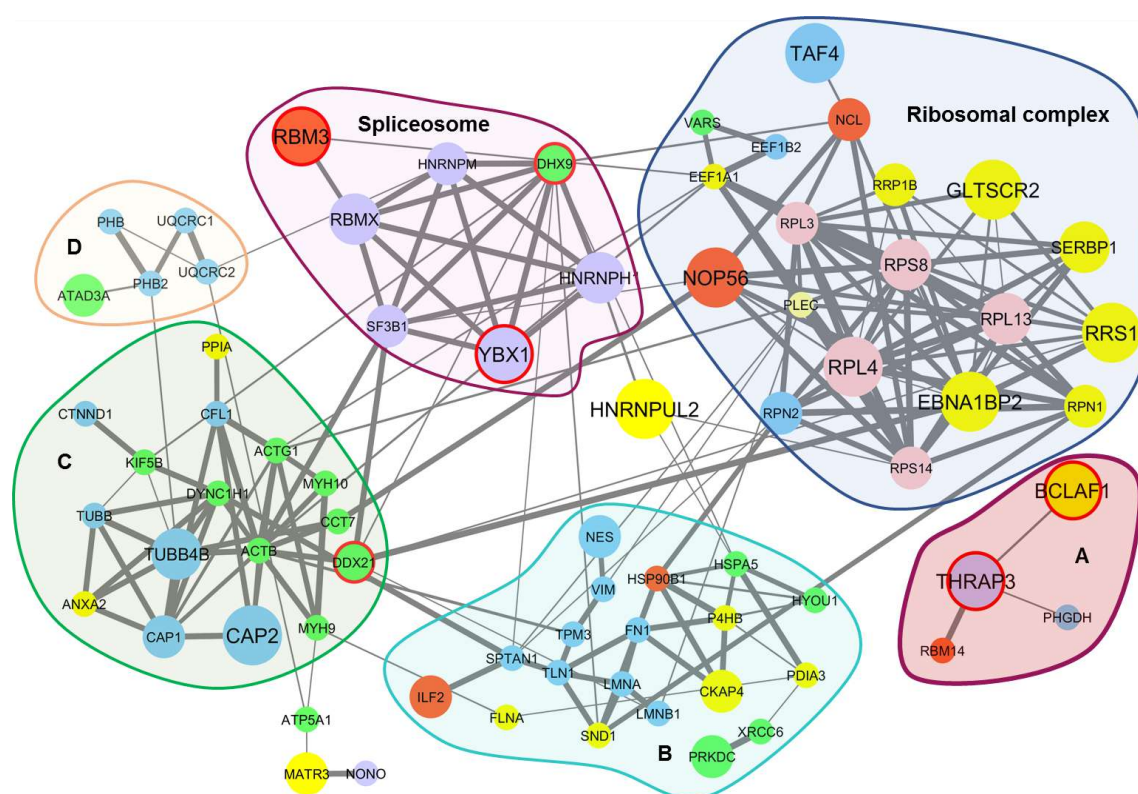


Figure 4. NS5 interactome in HuH-7. Node colors indicate four enriched groups: yellow, poly(A) binding proteins; orange, ATP-binding proteins; purple, mRNA splicing; pink, ribosomal proteins; and blue, unannotated function. Node sizes implicate identification confidence. Proteins also identified in previous studies are marked by red circles.

Discussion and Conclusion

In this study, we demonstrated an improved procedure of isolation of tagged NS5 and its interacting proteins from infected HuH-7 cells. Our pipeline provided superior performance to any previous publications in all aspects such as lower background, high recovery rate of NS5 peptides, high accuracy with peptide cut-off and weighted protein nodes, and most importantly, the experiment was achieved in virus-infected cells. We note that DENV NS3 was found to be a major interactor of NS5 in our study (data not shown) as corroborated by a previous study showing that the thumb domain of NS5 interacted with the C-terminal region in the RNA helicase domain of NS3 [16]. Upon RNase treatment, our NS5 interactome map was occupied by poly(A)-binding proteins. We do not have a clear explanation for interactions between NS5 and poly(A)-binding proteins, and their functions in viral replication require further study. NS5 interactors also include mRNA splicing factors such as YBX1, HNRNPH1, HNRNPM, RBMX, SF3B1, DHX9, NONO and THRAP3, which are generally localized in the nucleus [17]. A previous study reported that NS5 interacted with spliceosome to interfere with cellular splicing [13]. We have a great interest in an uncharacterized complex A comprised of THRAP3 and BCLAF1 (Fig. 4), which was also reported to interact with NS5 [15], and showed relatively big node sizes in our map. Understanding functions and structures of viral RC absolutely requires further study such as gene knock-in/out, *in vitro* reconstitution and cryo-electron microscopy.

Acknowledgment

This work was supported by Grants-in-Aids for Research from Mahidol University, Thailand, and by Grants (RSA6080066) from the Thailand Research Fund (TRF) to SC. KH was supported by Rachadaphiseksompot Fund for Postdoctoral Fellowship, Chulalongkorn University, Thailand.

References

- [1] Bhatt S, Gething PW, Brady OJ, Messina JP, Farlow AW, Moyes CL, et al. The global distribution and burden of dengue. *Nature*. 2013;496(7446):504-7.
- [2] Carabali M, Hernandez LM, Arauz MJ, Villar LA, Ridde V. Why are people with dengue dying? A scoping review of determinants for dengue mortality. *BMC Infect Dis*. 2015;15:301-.
- [3] Gould EA, Solomon T. Pathogenic flaviviruses. *Lancet (London, England)*. 2008;371(9611):500-9.
- [4] Lescar J, Soh S, Lee LT, Vasudevan SG, Kang C, Lim SP. The Dengue Virus Replication Complex: From RNA Replication to Protein-Protein Interactions to Evasion of Innate Immunity. In: Hilgenfeld R, Vasudevan SG, editors. *Dengue and Zika: Control and Antiviral Treatment Strategies*. Singapore: Springer Singapore; 2018. p. 115-29.
- [5] Lim SP, Wang Q-Y, Noble CG, Chen Y-L, Dong H, Zou B, et al. Ten years of dengue drug discovery: Progress and prospects. *Antiviral Res*. 2013;100(2):500-19.
- [6] Lim SP, Noble CG, Shi PY. The dengue virus NS5 protein as a target for drug discovery. *Antiviral Res*. 2015;119:57-67.
- [7] Ashour J, Laurent-Rolle M, Shi PY, Garcia-Sastre A. NS5 of dengue virus mediates STAT2 binding and degradation. *J Virol*. 2009;83(11):5408-18.
- [8] Dey L, Mukhopadhyay A. DenvInt: A database of protein-protein interactions between dengue virus and its hosts. *PLoS Negl Trop Dis*. 2017;11(10):e0005879-e.
- [9] Poyomtip T, Hodge K, Matangkasombut P, Sakuntabhai A, Pisitkun T, Jirawatnotai S, et al. Development of viable TAP-tagged dengue virus for investigation of host-virus interactions in viral replication. *J Gen Virol* 2016;97(3):646-58.
- [10] Hubner NC, Bird AW, Cox J, Splettstoesser B, Bandilla P, Poser I, et al. Quantitative proteomics combined with BAC TransgeneOmics reveals in vivo protein interactions. *J Cell Biol*. 2010;189(4):739-54.
- [11] Szklarczyk D, Morris JH, Cook H, Kuhn M, Wyder S, Simonovic M, et al. The STRING database in 2017: quality-controlled protein-protein association networks, made broadly accessible. *Nucleic Acids Res*. 2017;45(D1):D362-D8.
- [12] Shannon P, Markiel A, Ozier O, Baliga NS, Wang JT, Ramage D, et al. Cytoscape: a software environment for integrated models of biomolecular interaction networks. *Genome Res*. 2003;13(11):2498-504.
- [13] De Maio FA, Risso G, Iglesias NG, Shah P, Pozzi B, Gebhard LG, et al. The Dengue Virus NS5 Protein Intrudes in the Cellular Spliceosome and Modulates Splicing. *PLoS Pathog*. 2016;12(8):e1005841.
- [14] Fischl W, Bartenschlager R. Exploitation of cellular pathways by Dengue virus. *Curr Opin Microbiol*. 2011;14(4):470-5.
- [15] Shah PS, Link N, Jang GM, Sharp PP, Zhu T, Swaney DL, et al. Comparative flavivirus-host protein interaction mapping reveals mechanisms of Dengue and Zika virus pathogenesis. *Cell*. 2018;175(7):1931-45.e18.
- [16] Tay MY, Saw WG, Zhao Y, Chan KW, Singh D, Chong Y, et al. The C-terminal 50 amino acid residues of dengue NS3 protein are important for NS3-NS5 interaction and viral replication. *J Biol Chem*. 2015;290(4):2379-94.
- [17] Chen YI, Moore RE, Ge HY, Young MK, Lee TD, Stevens SW. Proteomic analysis of in vivo-assembled pre-mRNA splicing complexes expands the catalog of participating factors. *Nucleic Acids Res*. 2007;35(12):3928-44.

PO017***In silico* screening of inhibitor specific to dengue non-structural protein 5**

Lakkana Thaveepornkul^a, Chartchai Krittanai^a, Pilaipan Puthavathana^b
and Sarin Chimnaronk^{a*}

^a*Institute of Molecular Biosciences, Mahidol University, 25/25 Phutthamonthon 4 Road, Salaya, Nakhon Pathom 73170, Thailand.*

^b*Faculty of Medical Technology, Mahidol University, 999 Phutthamonthon 4 Road, Salaya, Nakhon Pathom 73170, Thailand.*

***E-mail :** *sarin.chi@mahidol.ac.th*

Dengue virus (DENV) (infects about 390 million people annually around the world and there is still no effective drug available). This study aims at performing virtual screening of drug-like small molecules that bind to two specific regions in the DENV non-structural protein 5 (NS5), which have so far not been utilized as antiviral drug targets. The first site is in the C-terminal thumb subdomain of RNA-dependent RNA polymerase (RdRp), which interacts with the viral RNA to initiate replication. The second site is located at the interface between methyltransferase (MTase) (and RdRp domains in NS5, where domain-domain interactions are important for viral viability). The grids covering both sites were generated and optimized, and a total of 689,461 compounds from the ZINC database were individually docked *in silico* onto the structures of the DENV-2 RdRp domain (PDB :5K5M) (and the full-length DENV-3 NS5 (PDB :4V0R) (using the AutoDock procedure). Top 43 hit molecules ranked by their binding affinity (ΔG (scores-) 10.0 to -11.0 kcal/mol) (were further analyzed for their interactions with NS5 using PyMOL). Finally, seven inhibitor candidates : ZINC09202280, ZINC09781412, ZINC21660843, ZINC33012732, ZINC11916580, ZINC14994931, and ZINC09250034 were selected for *in vitro* assays. We found that all compounds had no cytotoxicity in HuH-7 cell at the concentration of 1 μ M, but the anti-DENV effect was hardly detectable by the focus-forming unit (FFU) (assay at this concentration). Further work should be required to improve inhibitor selection and validation processes.

Keywords: Dengue virus (DENV), non-structural protein 5 (NS5), RNA-dependent RNA polymerase (RdRp), *in silico* screening.

Proc10

In silico screening of inhibitor specific to dengue non-structural protein 5

Lakkana Thaveepornkul^a, Chartchai Krittanai^a, Pilaipan Puthavathana^b
and Sarin Chimnaronk^{a*}

^a*Institute of Molecular Biosciences, Mahidol University, 25/25 Phutthamonthon 4 Road, Salaya, Nakhon Pathom 73170, Thailand.*

^b*Faculty of Medical Technology, Mahidol University, 999 Phutthamonthon 4 Road, Salaya, Nakhon Pathom 73170, Thailand.*

**E-mail: sarin.chi@mahidol.ac.th*

Abstract

Dengue virus (DENV) infects about 390 million people annually around the world and there is still no effective drug available. This study aims at performing virtual screening of drug-like small molecules that bind to two specific regions in the DENV non-structural protein 5 (NS5), which have so far not been utilized as antiviral drug targets. The first site is in the C-terminal thumb subdomain of RNA-dependent RNA polymerase (RdRp), which interacts with the viral RNA to initiate replication. The second site is located at the interface between methyltransferase (MTase) and RdRp domains in NS5, where domain-domain interactions are important for viral viability. The grids covering both sites were generated and optimized, and a total of 689,461 compounds from the ZINC database were individually docked in silico onto the structures of the DENV-2 RdRp domain (PDB: 5K5M) and the full-length DENV-3 NS5 (PDB: 4V0R) using the AutoDock procedure. Top 43 hit molecules ranked by their binding affinity (ΔG) scores (-10.0 to -11.0 kcal/mol) were further analyzed for their interactions with NS5 using PyMOL. Finally, seven inhibitor candidates: ZINC09202280, ZINC09781412, ZINC21660843, ZINC33012732, ZINC11916580, ZINC14994931, and ZINC09250034 were selected for in vitro assays. We found that all compounds had no cytotoxicity in HuH-7 cell at the concentration of 1 μ M, but the anti-DENV effect was hardly detectable by the focus-forming unit (FFU) assay at this concentration. Further work should be required to improve inhibitor selection and validation processes.

Keywords: Dengue virus (DENV), non-structural protein 5 (NS5), RNA-dependent RNA polymerase (RdRp), in silico screening.

Introduction

DENV infects up to 390 million people each year and ~500,000 individuals experience potentially life-threatening complications, including hemorrhage and shock [1]. Currently, there is still no approved drug available for treatment of the diseases, and drug candidates that were subjected to clinical trials showed so far no significant reduction of viral load and fever [2]. In addition, an only approved DENV vaccine failed to fully protect infection by either of 4 DENV serotypes [3]. Therefore, there is an urgent need for new antiviral agents to prevent or cure DENV infection.

DENV possesses a single positive stranded RNA genome of about 10.7 kilobases in size, which encodes 10 viral proteins [4]. Of those, the non-structural protein 5 (NS5) is the most attractive anti-viral drug target because it shows the highest amino-acid conservation of 67–82% among four DENV serotypes, and plays crucial role in viral

replication in host [5]. NS5 contains two fundamental enzymatic activities of methyltransferase (MTase) and RNA-dependent RNA polymerase (RdRp), localized in its N- and C-terminal domains, respectively. Although numerous studies have been attempt to identify inhibitors against NS5's activities; however, the design of specific inhibitors with no off-target and side-effect could be difficult because the amino acid sequences and structural configurations of NS5 are highly homologous to other eukaryotic MTase and RNA polymerases.

To address this issue, this study aims at *in silico* screening of inhibitors that targets to two characteristic sites in DENV NS5, which have not been targeted so far.

Experimental

In silico screening

The full-length DENV NS5 (PDB: 4V0R) and RdRp (PDB: 5K5M) structures were obtained from the Protein Data Bank for preparing the docking model and generating the grids that covered target sites using AutoDockTools and Chimera programs. A total of 642,759 ligands (ZincLrg) and 46,702 ligands (ZincSm) of small compounds that extracted from the ZINC database were then individually docked onto DENV proteins using the supercomputer at Texas University by accessed the DrugDiscovery@TACC (<https://drugdiscovery.tacc.utexas.edu/#/>). Ligands with acceptable ΔG scores were manually analyzed for their 3D interactions with DENV proteins using the PyMOL program.

Cells, virus, and compounds

C6/36 (*Aedes albopictus*, mosquito cell line) cells were grown at 28°C in L-15 media supplemented with 10% fetal bovine serum (FBS) and 10% tryptose phosphate broth (TPB). Vero (African green monkey kidney cell line) and HuH-7 (hepatocarcinoma cell line) cells were grown at 37°C at 5% CO₂ in Minimum Essential Media (MEM) and Dulbecco's Modified Eagle Media (DMEM) supplemented with 10% FBS, respectively. DENV-2 strain 16681 were propagated in C6/36 cells, titered by FFU assay and stored at -80°C until use. The candidate compounds were purchased from MolPort and dissolved in dimethyl sulfoxide (DMSO) to a final concentration of 10 mM and stored at -30°C.

Cytotoxicity (MTS) and antiviral assays

HuH-7 cells were seeded at 5×10^3 cells per well in 96-well plates and incubated with 5-fold serial dilutions of each compound from 100 μ M to 1.28 nM in a total of 100 μ l at 37 °C at 5% CO₂ for 48 h. Then, 20 μ l of CellTiter 96® AQueous One Solution (Promega) was added into each well and incubated for 2 h. Absorbance was measured at 490 nm using a 96-well plate reader. For antiviral assay, HuH-7 cells were seeded in 96-well plates (3×10^4 cells per well) and incubated at 37 °C at 5% CO₂ for 48 h. Cells were infected with DENV-2 at MOI 0.1 for 2 h. Then virus was removed, and 200 μ l of compounds at a final concentration of 1 μ M in DMEM was added into infected cells. After 48 h, cell culture supernatants were collected and subjected to the FFU assay to measure viral titers.

Focus forming unit (FFU) assay

The protocol mainly followed John et al. [6]. Vero cells were seeded in 96-well plate (3×10^4 cells per well) and cultured at 37°C, 5% CO₂ for 24 h. Cells were infected with 50 μ l of 10-fold serial dilutions of DENV in MEM supplemented with 3% FBS, and incubated for 2 h at room temperature on the rocker. The CMC semisolid overlay media (2X-MEM media supplemented with 6% FBS and 3% carboxymethyl cellulose) was added and incubated for 3 days at 37°C with 5% CO₂. The overlay media was then removed, and cells were washed with PBS prior to fixation with 3.7% formaldehyde in

PBS 100 μ l for 10 min. Cells were opened with an addition of 100 μ l of 1% Triton-X100 for 10 min. After 3-time PBS washes, the primary antibody (mouse anti-flavivirus group antigen monoclonal antibody, Millipore) was added and incubated for 2 h at room temperature, following by the reaction with the secondary antibody (goat anti-mouse IgG – HRP conjugated, Abcam) at 37°C for 2 h. The positive viral foci were visualized by staining with diaminobezidine (DAB) and foci forming units per sample unit volume (FFU/ml) were calculated.

Results and Discussions

Virtual screening of NS5 inhibitor

To identify inhibitors strictly specific to DENV NS5 to minimize possible off-target effects, we targeted two unique sites, designated here T (Figure 1A) and I sites (Figure 1B), located in the C-terminal thumb subdomain of RdRp and at the interface between MTase and RdRp, respectively. The T site was reported to interact with the 3' end of viral RNA genome to initiate replication [7], and the I site is essential for flavivirus replication [8]. Both sites are highly specific to DENV because the T site shows different amino acid sequence and structure from human RNA polymerase, and the I site is formed only in flaviviral NS5 in which the MTase and RdRp domains are directly linked together. Initially, the T site was challenged. Since the T site binds RNA, it is composed of positively-charged amino acid residues including R770, R773, K841 and R856. We optimized the grid to cover the whole positively-charged patch with the box dimensions of $25 \times 25 \times 25$ Å. Docking with ZincLrg and ZincSm resulted in the ΔG ranging from -8.0 to -10.9 kcal/mol. Top 18 molecules showing the ΔG lower than -10.0 kcal/mol were selected and categorized into 5 groups based on their binding modes to RdRp, and one representative compound from each group was selected to pursue according to the ΔG , solubility, and commercial availability. These are ZINC09202280, ZINC09781412, ZINC21660843 and ZINC33012732 (Table 1).

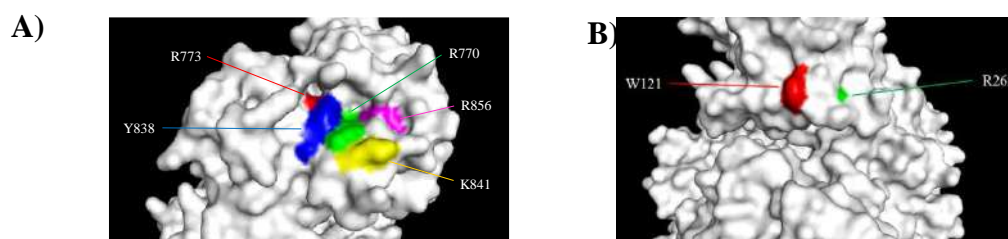
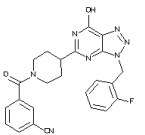
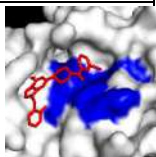
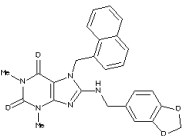
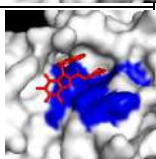
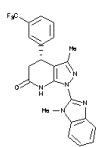
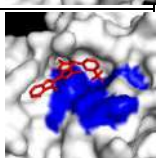
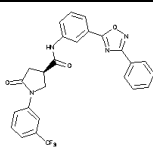
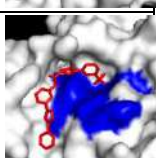
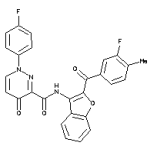
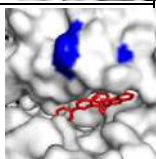
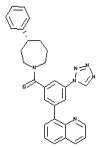
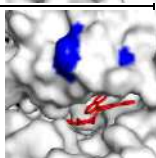
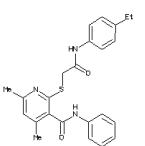
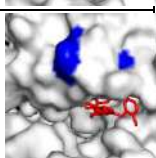


Figure 1. (A) T site on DENV-2 RdRp (PDB: 5K5M) (B) I site on DENV-3 full-length NS5 (PDB: 4V0R)

On the other hand, the I site includes hydrophobic residues of F567, W121, P585, and R265, whose mutations severely impaired viral RNA replication [8]. The grid of $20 \times 20 \times 20$ Å, encompassing W121 and R265 was generated for the docking. The docking yielded the ΔG ranging from -8.7 to -11.8 kcal/mol, and top 25 molecules with the ΔG lower than -11.0 kcal/mol were categorized into 7 groups. Three compounds of ZINC11916580, ZINC14994931 and ZINC09250034 (Table 1) were selected for the cell-based assay. When compare the ΔG between two target sites, the I site rendered lower binding energy because of deeper binding groove compared to the shallow pocket on the surface of T site. The selected compounds showed drug-like compound properties following the Lipinski's rules that recommended for drug development [9]. Moreover, none of those compounds have been reported for their antiviral activity. So the biological evaluation of compounds should to confirm further in cell-based assays.

Table 1 .Small compounds identified and selected for further validation in this study .

ZINC ID	Structure	Molecular formula (Molecular weight [g/mol])	Lipophilicity (log <i>P</i>)	Binding score (kcal/mol)	Binding model
ZINC 09202280		C ₂₄ H ₂₀ FN ₇ O ₂ (457.469)	2.16	-10.2	
ZINC 09781412		C ₂₆ H ₂₃ N ₅ O ₄ (469.501)	4.28	-10.6	
ZINC 21660843		C ₂₂ H ₁₈ F ₃ N ₅ O (425.414)	3.98	-10.4	
ZINC 33012732		C ₂₆ H ₁₉ F ₃ N ₄ O ₃ (492.457)	4.84	-10.3	
ZINC 11916580		C ₂₇ H ₁₇ F ₂ N ₃ O ₄ (485.446)	5.00	-11.8	
ZINC 14994931		C ₂₉ H ₂₆ N ₆ O (474.568)	4.40	-11.7	
ZINC 09250034		C ₂₄ H ₂₅ N ₃ O ₂ S (419.55)	5.01	-11.6	

Examination of cytotoxicity and antiviral effect

Next, all compounds were subjected to the MTS assay to assess their cytotoxicity in human hepatic HuH-7 cell .Lipophilicity (log*P*) indicate the solubility of compounds, the more lipophilic compounds will have less soluble in aqueous media. According to Lipinski's rules, log*P* value of compounds should be lower than 5. The selected compounds had log*P* value between 2.16 to 5.01, only ZINC11916580 which has log*P* value 5.00 was not dissolved in DMSO and not further pursued .The absorbances were average and calculated as percentage of cell viability compared with untreated cells using GraphPad Prism software. All tested compounds showed dose-dependent response as increasing concentration affected cell viability. At the highest tested concentration of 100 μ M, ZINC14994931 and ZINC09250034 were insoluble forming

crystals in DMEM. All compounds had no obvious effect on cell viability at the concentration of 0.8 μ M (Figure 2A). Hence, we decided to examine their antiviral activities at the concentration of 1 μ M.

We used human hepatic HuH-7 cell in this study because it is a DENV-targeting cell with high infectivity [10]. We found that at this concentration, all compounds failed to show significant reduction in DENV production in HuH-7 cells (Figure 2B). Nonetheless, the ability of compound to inhibit DENV activity can rely on DENV serotypes, cell types, and cell permeability.

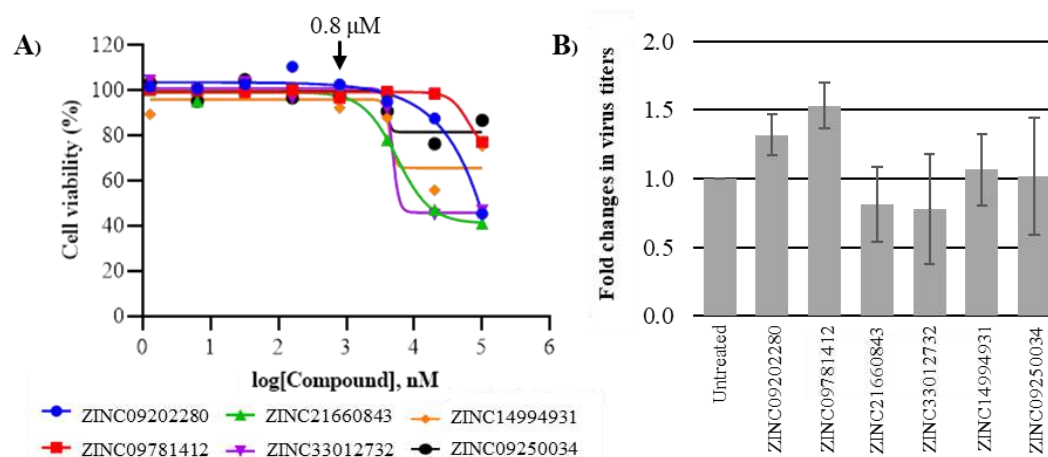


Figure 2. (A) MTS cell viability assay at 48 h after exposure. (B) Fold changes in virus titers in culture supernatant at 48 h post-infection (hpi).

Conclusion

In this study, we identified compounds from the ZINC database library, which could bind to two unique sites of DENV NS5 via the *in silico* screening. Selected 6 compounds had no cytotoxicity at 1 μ M; however, they showed not significant reduction in viral titers at this concentration. We will address this issue in the future by increasing the compound concentration and examining with the other DENV serotypes.

Acknowledgment

We thank Texas Advanced Computing Center, University of Texas Medical Branch for providing an access to the supercomputer. This work was supported by Grants-in-Aids for scientific research from Mahidol University, Thailand, and by the Mid-Career Grant (RSA6080066) from the Thailand Research Fund (TRF) to SC.

References

- [1] Li Y, Wu S. Dengue: what it is and why there is more. *Sci Bull Sci Found Philipp*. 2015;60(7):661-4.
- [2] Low JGH, Ooi EE, Vasudevan SG. Current status of dengue therapeutics research and development. *J Infect Dis*. 2017;215(Suppl 2):S96-S102.
- [3] Moi ML, Takasaki T, Kurane I. Human antibody response to dengue virus: implications for dengue vaccine design. *Trop Med Health*. 2016;44(1):1.
- [4] Lai J-H, Lin Y-L, Hsieh S-L. Pharmacological intervention for dengue virus infection. *Biochem Pharmacol*. 2017;129:14-25.
- [5] Lim SP, Noble CG, Shi P-Y. The dengue virus NS5 protein as a target for drug discovery. *Antiviral Res*. 2015;119:57-67.

- [6] John AM, Jittmittraphap A, Chattanadee S, Alwin Prem Anand A, Shenbagarathai R, Leaungwutiwong P. In vitro analysis of synthetic peptides in blocking the entry of dengue virus. *Virus Research*. 2019;260:142-50.
- [7] Hodge K, Tunghirun C, Kamkaew M, Limjindaporn T, Yenchitsomanus P-t, Chinnaronk S. Identification of a conserved RNA-dependent RNA Polymerase (RdRp)-RNA interface required for flaviviral replication. *J Biol Chem*. 2016;291(33):17437-49
- [8] Li X-D, Shan C, Deng C-L, Ye H-Q, Shi P-Y, Yuan Z-M, et al. The interface between methyltransferase and polymerase of NS5 is essential for flavivirus replication. *PLoS Negl Trop Dis*. 2014;8(5):e2891.
- [9] Mignani S, Rodrigues J, Tomas H, Jalal R, Singh PP, Majoral J-P, et al. Present drug-likeness filters in medicinal chemistry during the hit and lead optimization process: how far can they be simplified? *Drug Discovery Today*. 2018;23(3):605-15.
- [10] Lin Y-L, Liu C-C, Lei H-Y, Yeh T-M, Lin Y-S, Chen RM-Y, et al. Infection of five human liver cell lines by dengue-2 virus. 2000;60(4):425-31.
- [11] Vicente CR, Herlinger K-H, Fröschl G, Malta Romano C, de Souza Areias Cabidelle A, Cerutti Junior C. Serotype influences on dengue severity: a cross-sectional study on 485 confirmed dengue cases in Vitória, Brazil. *BMC Infect Dis*. 2016;16:320.

Proceedings PP009-3

Investigation of host–dengue virus interaction via proteomics

Jakkrit Jantiva¹, Kenneth Hodge², Trairak Pisitkun², and Sarin Chimnarong^{1,*}

¹ Laboratory of RNA Biology, Institute of Molecular Biosciences, Mahidol University, Salaya Campus, Nakhon Pathom 73170, Thailand,

² The Systems Biology Center, Research Affairs, Faculty of Medicine, Chulalongkorn University, 1873 Rama 4 Road, Pathumwan, Bangkok 10330, Thailand.

*Email: sarin.chi@mahidol.ac.th

ABSTRACT

Dengue virus (DENV) infection is one of the major public health concerns worldwide for which currently no effective drug is available. DENV utilizes the viral non-structural protein 5 (NS5) to replicate its RNA genome in infected cells and suppress the host immune interferon response. Given that NS5 is the largest (~103 kDa) and the most conserved viral protein (with ~65% sequence identity among the four serotypes), NS5 represents a promising antiviral target for drug development. To obtain deep insight into viral NS5–host interaction, we used our recently developed engineered-tagged DENV or etDENV, which harbors a tandem His-FLAG tag in NS5, to isolate the whole NS5-interacting human factors from hepatoma HuH-7 cells at 48 hours after infection. The nickel-affinity pull down and immunoprecipitation (IP) with anti-FLAG beads were examined, providing final NS5 protein yields of approximately 3.1 and 0.8 µg from 1.5×10^7 cells, respectively. Although nickel affinity gave higher protein amount, FLAG-IP yielded better protein purity on SDS-PAGE. Therefore, FLAG-IP fractions were used for preparing sample for a tandem mass spectrometer. In this study, we confirmed viral NS3 as a major NS5-interacting protein. The results also revealed an interaction map containing 204 human proteins, including several machineries such as protein translation, chaperone, RNA processing, and nucleoprotein. Further study to characterize roles played by those proteins with NS5 in viral replication should accelerate antiviral drug research.

Keywords: Dengue virus (DENV), non-structural protein 5 (NS5), immunoprecipitation (IP), mass spectrometry (MS)

INTRODUCTION

Dengue fever is a mosquito-borne tropical disease, caused by dengue virus (DENV), which infects ~400 million people in more than 110 countries with approximately 10,000-20,000 deaths per year (1). DENV is transmitted by female mosquitos of *Aedes* species that take a blood meal from a person infected with the virus. Nowadays, there is still no specific treatment and effective vaccine for the dengue diseases (2).

DENV is an enveloped virus belonging to the genus flavivirus within the family *Flaviviridae*. DENV possesses a positive single-stranded RNA genome that serves as the template for both viral protein and RNA syntheses in host cells. The viral RNA genome is

translated by host ribosome into a single polypeptide at the endoplasmic reticulum (ER), which is further cleaved into 10 individual proteins by host and viral proteases (3). The DENV proteins are composed of three structural proteins of C (capsid), prM (pre-membrane/membrane) and E (envelope), which are assembled into the virus particle, and seven non-structural proteins (NS) of NS1, NS2A, NS2B, NS3, NS4A, NS4B, and NS5. Of those, NS5 shows the most conserved amino acid sequences amongst DENV proteins (4). NS5 has a size of ~103 kDa and bears two distinct enzymatic activities that play vital roles in virus replication. Its one-third N-terminal domain is 2'-O methyltransferase (MTase) involved in capping of viral genome. The C-terminal region comprises of an RNA-dependent RNA polymerase (RdRp) required for viral RNA synthesis (4). NS5 also plays a role in suppression of the host immune interferon response via its interaction with the STAT2 protein (5). Therefore, NS5 becomes the most attractive target for antiviral drug development. Since it has been known that the virus also requires host proteins to ensure its replication in host cells (6), a study of the global interaction network of NS5 with host factors should be required to provide deep understanding of host-dependent viral replication, and clues to targeting drug design.

We recently developed an engineered-tagged dengue virus (etDENV) that contains an octahistidine tag and a FLAG tag (DYKDDDDK) in the MTase domain of the NS5 gene to facilitate protein purification via both His and FLAG tag pull downs. It also has been shown that tag insertion did not disturb the folding and function of NS5 in infected cells (7). In this study, we utilize etDENV to isolate the protein interaction network of NS5 in infected hepatic cells, a natural target of DENV, with a high accuracy via combining immunoprecipitation of tagged-NS5 and mass spectrometry analysis.

MATERIALS AND METHODS

Protein extraction

The HuH-7 (human hepatocyte cells) cells were cultured in DMEM supplemented with 10% fetal bovine serum (FBS) at 5% CO₂ at 37°C. 1.5×10^7 cells were infected with dengue virus serotype 2 strain 16681 or etDENV at MOI = 5 in 2% FBS DMEM media when the cell confluences reached 80-90%. 48 hours after infection, cells were collected from the dish using a plastic cell scraper, and gently transferred into a microcentrifuge tube. Cells were washed with PBS, and lysed by the lysis buffer containing 50 mM HEPES pH 7.2, 150 mM KCl, 25 mM imidazole, 1× Protease inhibitor, 1% Triton X-100, 1× Phosphatase Inhibitor and 7 U ml⁻¹ DNase I for 30 min on ice. Cell lysate was cleared by centrifugation at 15,000 r.p.m. for 15 min at 4°C, and the supernatant was collected.

Nickel-NTA affinity and FLAG immunoprecipitation (IP)

A 25 µl of Ni-NTA agarose beads (QIAGEN) or 20 µl of EZview Red Anti-FLAG M2 affinity gels (SIGMA) was transferred to a new tube and centrifuged at 3,000 or 8,000 r.p.m, respectively, at 4°C for 1 min. Beads were collected and thoroughly washed by 200 µl of ddH₂O for 3 times. Then, beads were equilibrated twice with the lysis buffer. Clear cell lysate was mixed with beads at 4°C for 2 hours to allow tagged NS5 binding to resins.

Unbound protein fraction (flow through) was collected, and beads were washed with the wash buffer (50 mM HEPES pH 7.2, 150 mM NaCl, 25 mM imidazole for Ni-NTA, and PBS for M2 beads) for 8 times. In Ni-affinity, bound proteins were eluted from beads via 20 μ l of the elution buffer containing 50 mM HEPES pH 7.2, 150 mM NaCl, 250 mM imidazole. In FLAG-IP, bound proteins were left on beads.

Western blot analysis

A 10 μ l of protein samples was loaded onto SDS-PAGE. A PVDF membrane and 6 pieces of filter papers were cut to the same size as the gel. The membrane was rinsed with 100% methanol for 1 min, followed by ddH₂O for 2 min. The SDS gel, the membrane, and all filter papers were soaked in the transfer buffer (190 mM glycine, 10% MeOH, and 100 mM Tris base) for 5 min. The blotting apparatus was assembled by placing 3 filter papers at the center of the blotting plate, followed by the PVDF membrane, SDS-PAGE gel, and 3 filter papers. Electroblothing was performed for 1 hour. The membrane was then blocked by immersing in 50 ml blocking solution (5% skim milk in PBS-T) for 1 hour. The membrane was washed 3 times with PBS-T for 5 min. The membrane was incubated with primary antibody (1:5000 rabbit anti-NS5 polyclonal antibody (Invitrogen) in PBS-T) for 1 hour at room temperature. After 3 washes with PBS-T for 5 min, the membrane was incubated with secondary antibody (1:10000 goat anti-rabbit FITC-labelled antibody (Dako)) for 1 hour at room temperature, washed 3 times with PBS-T. Chemiluminescence reaction was performed by the PierceTM ECL Western Blotting Substrate at room temperature for 5 min. Bands were visualized by X-ray films in the dark room.

Mass spectrometry (MS) and data analysis

Concentrated samples from FLAG-IP were digested on bead in the buffer 1 (5 ng/ μ l trypsin, 2 M Urea, 50 mM Tris-HCl pH 7.5, and 1 mM DTT) for 30 min at room temperature. Peptides were collected into a new microcentrifuge tube, and were alkylated twice with 50 μ l of the buffer 2 (2 M Urea, 50 mM Tris-HCl pH 7.5, and 5 mM IAA). The reaction was further incubated at room temperature overnight to complete tryptic digestion (do not heat at 37°C because urea can carbamylate peptides). The reaction was quenched at 4°C. Peptide pool was desalted with an octadecyl C18 resin before injection into a tandem mass spectrometer (Q-Exactive Plus, Thermo). Mass spectrums were analyzed using MaxQuant that is a quantitative proteomics software package designed for analyzing large-scale mass-spectrometric data sets. The NS5 protein-protein interacting network was generated using the STRING 10.5 database (8), and reconstructed via the Cytoscape program (9) to indicate the number of peptide fragments weighted against molecular mass for all nodes.

RESULTS

Expression of tagged NS5

Protein extraction was performed at 48 hours after infection to ensure sufficient protein yield for the mass spectrometry analysis. We utilized the Western blot to estimate the total amount of NS5 in the cell lysate based on the purified recombinant DENV RdRp protein (73.5 kDa) (10) (**Fig. 1**). As expected, the NS5 bands from etDENV were slightly above that of DENV-2 due to the octahistidine and FLAG tag (1.01 kDa) in its MTase domain (**Fig. 1A**). According to the recombinant RdRp protein standard, there was approximately 7.3 μg (70.9 pmol) or 4.2×10^{13} molecules of NS5 from 1.5×10^7 cells.

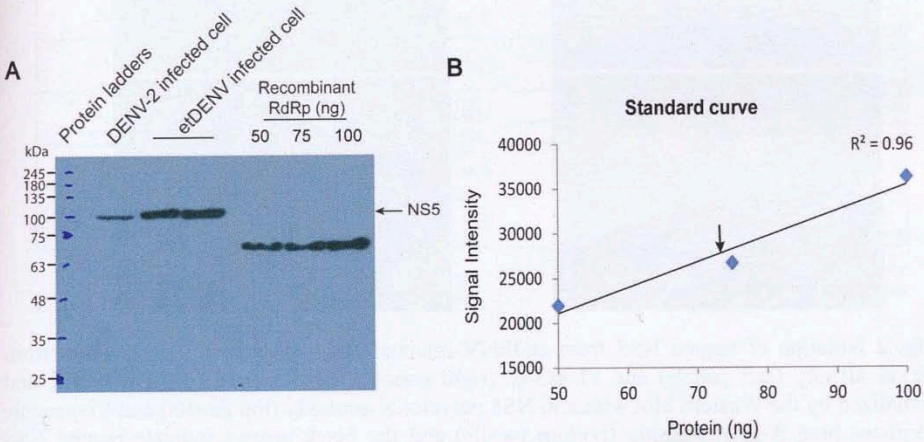


Fig. 1 Estimation of NS5 amount in infected cells. (A) Cell lysate from DENV-2 and etDENV infected cells were analyzed by the Western blot with an anti-NS5 polyclonal antibody. (B) Intensities of the recombinant RdRp on the Western blot were plotted as a standards curve to quantitate NS5 amount (black arrow) in infected HuH-7.

Isolation of tagged NS5 from infected cells

To isolate tagged NS5 and its interacting proteins, we compared nickel affinity with FLAG-IP by protein yields and purity estimated by the Western blot and SDS-PAGE, respectively (**Fig. 2**). The nickel affinity yielded about 3.1 μg of NS5 whereas FLAG-IP gave 0.8 μg from 1.5×10^7 cells. Both approaches showed a very high efficiency because there was only little amount of NS5 found in flow through and wash fractions (**Fig. 2**). While nickel affinity showed higher protein yield, FLAG-IP had better protein purity. We decided to use FLAG-IP to prepare the sample for mass spectrometry. Nonetheless, NS5 fractions obtained in this study have a very high quantity and quantity sufficient for the proteomic analysis. We note that isolation of NS5 from infected cells via etDENV and FLAG-IP in this study showed superb quality and quantity, which was not possible in earlier studies that used anti NS5 antibodies for IP.

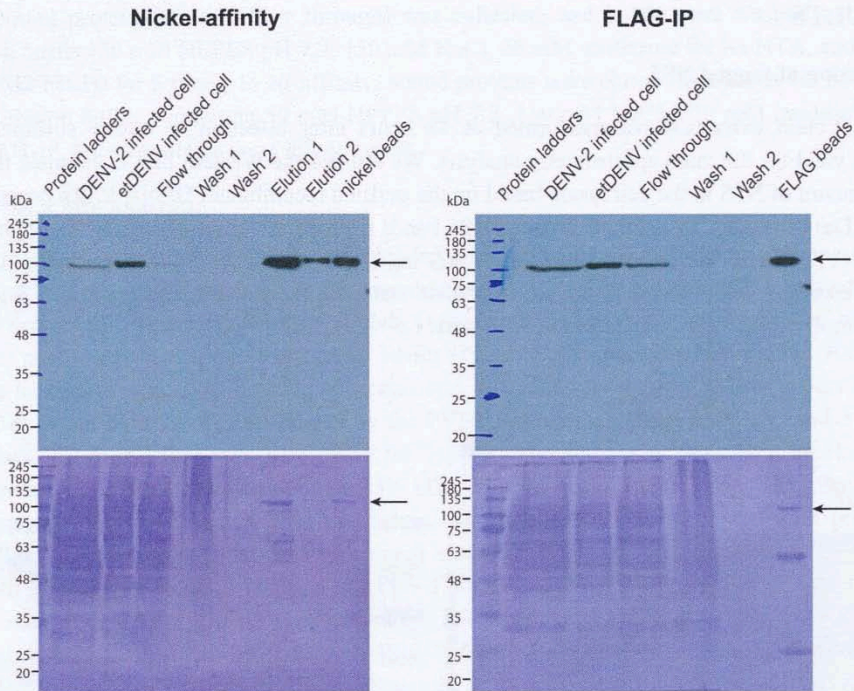


Fig. 2 Isolation of tagged NS5 from etDENV-infected HuH-7. Each protein fraction from nickel affinity (left panels) and FLAG-IP (right panels) was resolved by SDS-PAGE and visualized by the Western blot with anti NS5 polyclonal antibody (top panels) and Coomassie (brilliant blue R-250) staining (bottom panels) and the black arrows indicate tagged NS5 bands (105.7 kDa).

Interactome of DENV NS5 in human liver cells

The mass spectrometry identified NS5 peptides with 76% coverage of the whole amino acid sequence, indicating a very high-quality and purity of protein preparation. The second abundant peptides of DENV proteins were identified as NS3, confirming that NS3 (the viral protease and RNA helicase) is the major NS5-interacting protein in infected cells (**Table 1**). Next, we searched for human proteins that were co-purified with NS5. We identified 204 proteins with high-confidence, having peptide counts beyond 2. The STRING map and Gene Ontology (GO) were used to cluster the interaction networks. In addition, to increase accuracy, we assigned weights to each protein by dividing the peptide counts by molecular mass and abundance in the liver to eliminate biases towards proteins size and amount in cells. The resulting NS5 interaction network is shown in **Fig. 3**. The 'interactome' map revealed at least three different cellular machineries including the ribosome and translational factors, the RNA processing complex, nucleoprotein complex. While further functional study of these complexes in viral replication should be required, our results obviously showed specific, complex, though shaped, interaction network of host-virus during viral replication process. It is also noted that some identified NS5-interacting proteins in this work were previously reported including FASN, HSP90, and YBX1 (11-13), again validating our NS5-IP/MS system.

Table 1 DENV proteins identified by NS5 IP with mass spectrometry

Proteins	Size (amino acid)	MS count	Count relative to protein residues
Capsid	114	3	2.6
M	166	1	0.6
E	389	6	1.5
NS1	456	4	0.9
NS2A	212	0	0
NS2B	133	0	0
NS3	618	25	4.0
NS4A	147	1	0.7
NS4B	251	0	0
NS5	900	81	9.0

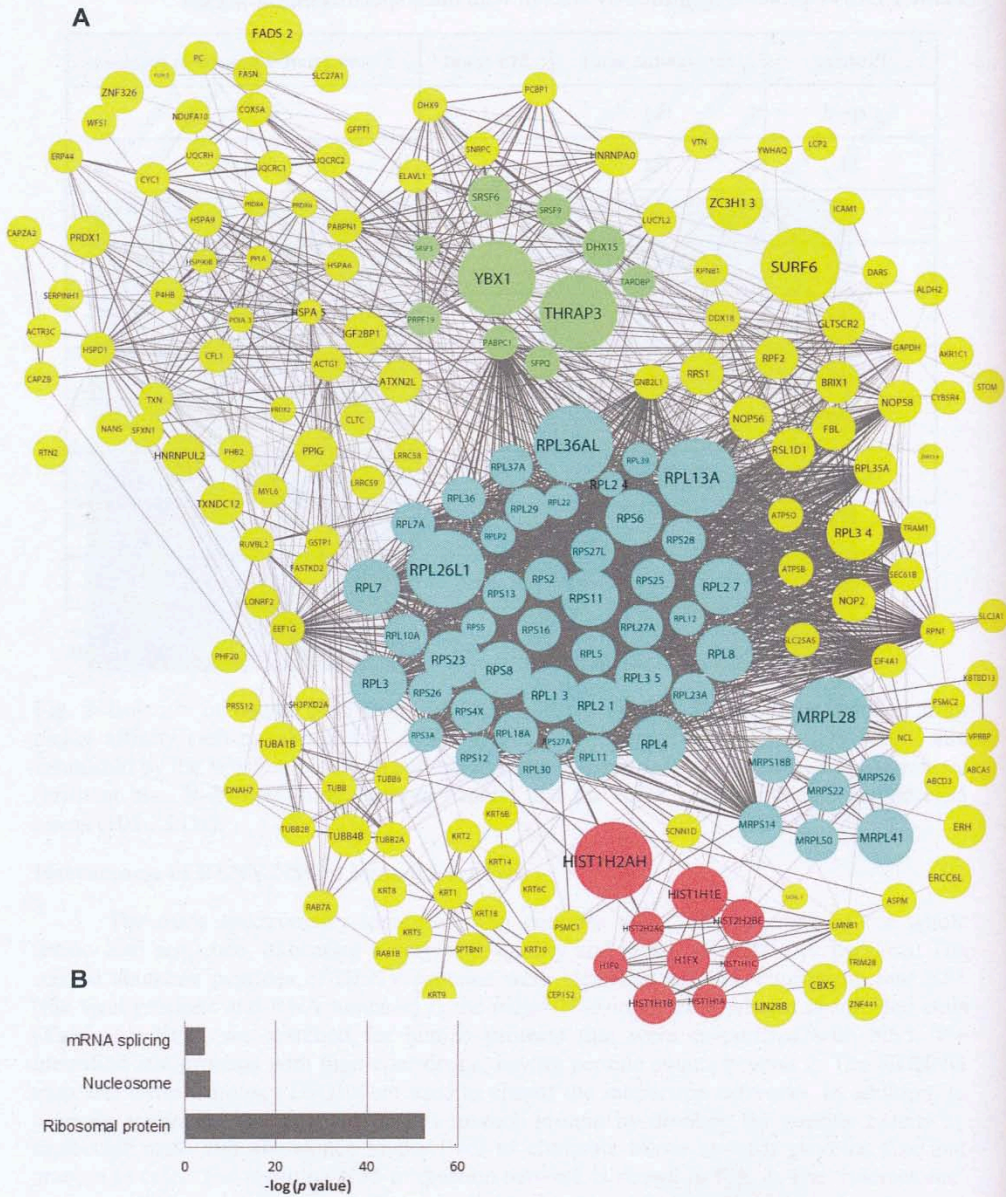


Fig. 3 NS5 interactome in HuH-7. The protein-protein interaction network of NS5 was reconstructed using the initial STRING network as template. Colors indicate four enriched groups: yellow for non-membranous predominantly cytosolic proteins, red for nucleoproteins, blue for ribosomal proteins, and green for mRNA splicing. Node sizes indicate relative peptide abundances from mass spectrometry. (B) List of enriched gene ontology groups according to DAVID.

DISCUSSION AND CONCLUSIONS

In this study, we demonstrated a success in isolation of tagged NS5 and its interacting proteins from HuH-7 cells infected by etDENV. Our procedure for isolation of NS5 and data analysis provided superior performance compared with previous studies in all aspects such as lower background, high recovery rate of NS5 peptides, and high accuracy with peptide cut-off and weighted protein nodes. NS3 was found to be a major interactor of NS5. This is corroborated by a previous study showing the thumb domain of NS5 interacted with the C-terminal region in the RNA helicase domain of NS3 (14). Our NS5 interactome map was occupied by ribosomal proteins and translational factors. It is difficult to consider this result as contamination in our IP and data analysis. Conceivably, the NS5-ribosome interaction might enhance or inhibit translation according to a need for protein versus RNA. We also founded mRNA splicing factors including DHX15, ABCD3 and SH3PXD2A which are generally localized in the nucleus (15). A previous study reported that NS5 interacted with spliceosome to interfere with cellular splicing (12). Understanding functions and structures of NS5 complexes absolutely require further study such as sophisticated *in vitro* reconstitution and cryo-electron microscopy.

ACKNOWLEDGEMENTS

This work was supported by Grants-in-Aids for Research from Mahidol University, Thailand, and by Grants (RSA6080066) from the Thailand Research Fund (TRF) to SC. JJ was supported by the Molecular Genetics and Genetic Engineering Scholarship from the Institute of Molecular Biosciences, Mahidol University, and KH was supported by Rachadaphiseksompot Fund for Postdoctoral Fellowship, Chulalongkorn University, Thailand.

REFERENCES

1. Bhatt S, Gething PW, Brady OJ, Messina JP, Farlow AW, Moyes CL, et al. The global distribution and burden of dengue. *Nature*. 2013;496(7446):504-7.
2. Carabali M, Hernandez LM, Arauz MJ, Villar LA, Ridde V. Why are people with dengue dying? A scoping review of determinants for dengue mortality. *BMC Infect Dis*. 2015;15:301.
3. Gould EA, Solomon T. Pathogenic flaviviruses. *The Lancet*. 2008;371(9611):500-9.
4. Lim SP, Noble CG, Shi PY. The dengue virus NS5 protein as a target for drug discovery. *Antiviral Res*. 2015;119:57-67.
5. Ashour J, Laurent-Rolle M, Shi PY, Garcia-Sastre A. NS5 of dengue virus mediates STAT2 binding and degradation. *J Virol*. 2009;83(11):5408-18.
6. Dey L, Mukhopadhyay A. DenvInt: A database of protein-protein interactions between dengue virus and its hosts. *PLoS Negl Trop Dis*. 2017;11(10):e0005879.
7. Poyomtip T, Hodge K, Matangkasombut P, Sakuntabhai A, Pisitkun T, Jirawatnotai S, et al. Development of viable TAP-tagged dengue virus for investigation of host-virus interactions in viral replication. *J Gen Virol*. 2016;97(3):646-58.
8. Szklarczyk D, Morris JH, Cook H, Kuhn M, Wyder S, Simonovic M, et al. The STRING database in 2017: quality-controlled protein-protein association networks, made broadly accessible. *Nucleic Acids Res*. 2017;45(D1):D362-d8.

9. Shannon P, Markiel A, Ozier O, Baliga NS, Wang JT, Ramage D, et al. Cytoscape: a software environment for integrated models of biomolecular interaction networks. *Genome Res.* 2003;13(11):2498-504.
10. Hodge K, Tunghirun C, Kamkaew M, Limjindaporn T, Yenchitsomanus P-t, Chimnaronk S. Identification of a Conserved RNA-dependent RNA Polymerase (RdRp)-RNA Interface Required for Flaviviral Replication. *J Biol Chem.* 2016;291(33):17437-49.
11. Mairiang D, Zhang H, Sodja A, Murali T, Suriyaphol P, Malasit P, et al. Identification of New Protein Interactions between Dengue Fever Virus and Its Hosts, Human and Mosquito. *PloS One.* 2013;8(1):e53535.
12. De Maio FA, Risso G, Iglesias NG, Shah P, Pozzi B, Gebhard LG, et al. The Dengue Virus NS5 Protein Intrudes in the Cellular Spliceosome and Modulates Splicing. *PLoS Pathog.* 2016;12(8):e1005841.
13. Fischl W, Bartenschlager R. Exploitation of cellular pathways by Dengue virus. *Curr Opin Microbiol.* 2011;14(4):470-5.
14. Tay MYF, Saw WG, Zhao Y, Chan KWK, Singh D, Chong Y, et al. The C-terminal 50 Amino Acid Residues of Dengue NS3 Protein Are Important for NS3-NS5 Interaction and Viral Replication. *J Biol Chem.* 2015;290(4):2379-94.
15. Chen Y-IG, Moore RE, Ge HY, Young MK, Lee TD, Stevens SW. Proteomic analysis of in vivo-assembled pre-mRNA splicing complexes expands the catalog of participating factors. *Nucleic Acids Res.* 2007;35(12):3928-44.